

**UCSF**

**UC San Francisco Electronic Theses and Dissertations**

**Title**

Molecular mechanisms of nucleoside transport

**Permalink**

<https://escholarship.org/uc/item/7pp9x878>

**Author**

Wang, Juan,

**Publication Date**

1998

Peer reviewed|Thesis/dissertation

Molecular Mechanisms of Nucleoside Transport

by

Juan Wang

DISSERTATION

Submitted in partial satisfaction of the requirements for the degree of

DOCTOR OF PHILOSOPHY

in

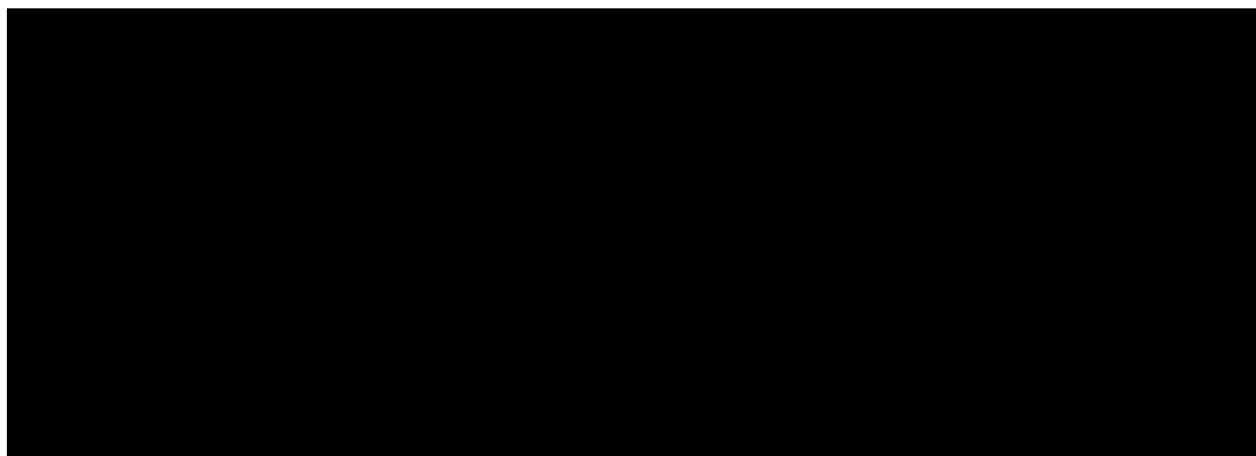
Pharmaceutical Chemistry

in the

GRADUATE DIVISION

of the

UNIVERSITY OF CALIFORNIA SAN FRANCISCO



Date

University Librarian

Degree Conferred: .....

*To my parents,  
and  
my husband, Tao*

## Acknowledgments

I would like to thank my advisor, Dr. Kathleen M. Giacomini, for her great mentorship, support, and friendship. Kathy is one of the few people who have made an important impact on me. Her mentorship will be a most valuable treasure from which I will benefit for years after. Her big view of science will always remind me not to get lost in things that I am doing; rather, to question why I am doing it and to think what I will do for the future. Being a caring mother of three outstanding children, Kathy is also a role model for me and many other women to look at for balancing career and family.

I would like to thank Dr. Leslie Benet and Wolfgang Sadeé, members of my thesis and orals committees, for their timely review of my dissertation and for their mentorship and support through the years. I am especially grateful to Dr. Leslie Benet, who chaired my oral examination and provided great suggestions to this dissertation. Many thanks to the other members of my oral committee: Drs. Lily Y. Jan, Martin D. Shetlar, and Susan M. Miller. Special thanks to Drs. Deanna L. Kroetz, Svein Øie and Ronald Siegel for their support in many areas. I also thank Drs. Robert Stroud, Charly Craik, Tom Ferrin, and Teri Klein for their excellent suggestions and advice on my research projects.

I thank all the past and present members of the Giacomini laboratory for their support through the years. Michelline Piquette-Miller, Joanne Chan, Carla Washington, Vikram Ramanathan, Marci Schaner, Sheng-Fang Su, Lei Zhang, Shigeyuki Terashita, Shoshana Zevin, Siljia Thomassen, Omar Perez, and Wenche Gorset were all great people to work with and learn from. Special thanks to Dr. Marci Schaner and Dr. Sheng-Fang Su, who were great friends and collaborators in the past and continue to provide me with encouragement and support from different places of the world. Thanks to the current KMG members: Mark Dresser, Karin Gerstin, Carlo Bello, Lara Magravite, and Maya Kaushal. Special thanks to Karin and Mark, for always being patient readers and

critical editors of my formal and informal writings. I would also like to thank Alan Lee and Sandra Ortiz for their assistance.

I thank Drs. Claire M. Brett, Patsy Babbitt, Betty-ann Hoener, and Jelveh Lemeh for their support and friendship. I also thank Vivian Tucker, Kim Bivens, Lisa Crosse, Judi Mozesson, Trinity Ordon, and Gloria Johnson for their help through the years. Many thanks to my classmates and friends on the 8th floor: Van Hoang, Herschel Wade, James Buckman, Dallas Connor, Rae Yuan, Caroline Mrejan, Mark Grillo, Mark Quillan, Dongyan Yang, Kedan Lin, Lingling Guan, Hongxia Li, Yongchang Qiu, Derek Zhang, Zhigang Yu, Ming Covitz, Lara Tolbert, Lisa Uyechi, Jay Tibbitts, Laurent Sulphati, Neil Burford, Marian Chang, Houhui Xia, Melinda Shockley, Danxin Wang, Philip Yook, Dolly Parasrampur, and many others. Special thanks to my friends, Ping Wang, Judy Fu, Lily Zheng, Liying Wang, Portland Coats, Shaobing Hua, Nancy Yu, Gary Strahan, D.C. Yu, and Mrs. Rose Bermudez, for sharing with me lots of wonderful things such as science, religion, music, arts, food, plants, etc.....

I would like to thank Professor Charles S.C. Lin at the University of Illinois at Chicago for introducing UCSF to me. Heartfelt thanks to Dr. Ching C. Wang, for providing me with the opportunity to work at UCSF and for his enthusiastic recommendation of me to the graduate program. Many thanks to Dr. Alice Wang, who first welcomed me to San Francisco.

I am indebted to all the members of my family. Without their love, support, and encouragement, I would have never made it to this point. I am grateful to my parents, who taught me to love life, people, and science. I sincerely thank my sister Helen, who cares about me so much and always tries to make sure that I made every right decision in my life. Dearest thanks to my sisters, Yan and Li, for their love and encouragement throughout the years. Special thanks to my parents-in-law, for being very supportive and understanding, and most of all, for granting me a wonderful husband that a person could hope for.

Finally, I would like to thank my husband, Tao (Terry) Ye, for his constant love, encouragement, and support, for always being there, and for always cheering me up.

Juan Wang

December, 1998

## ABSTRACT

### MOLECULAR MECHANISMS OF NUCLEOSIDE TRANSPORT

Juan Wang

In mammalian cells, transmembrane flux of nucleosides is mediated by equilibrative and Na<sup>+</sup>-dependent nucleoside transporters. These processes are essential for nucleotide synthesis by salvage pathways and are the route of cellular uptake of many therapeutic nucleoside analogs. The overall goal of this dissertation is to elucidate the molecular mechanisms involved in the membrane transport of nucleosides and nucleoside analogs. Research presented in this dissertation contributes significantly to the cloning, characterization, and structure-function analysis of Na<sup>+</sup>-nucleoside transporters.

Studies in the first part of this dissertation described the cloning and characterization of the human N1 subtype transporter, hSPNT1. Using homology cloning strategies, hSPNT1 was cloned from human kidney. The hSPNT1 protein is 81% identical to the previously cloned rat Na<sup>+</sup>-nucleoside transporter, SPNT, but differs markedly from SPNT in terms of its primary structure in the N-terminus. Functional expression in *Xenopus laevis* oocytes identified hSPNT1 as a Na<sup>+</sup>-dependent nucleoside transporter which selectively transports purine nucleosides and uridine. Northern analysis revealed that multiple transcripts of hSPNT1 are widely distributed in human kidney, heart, skeletal muscle, liver, intestine, and pancreas. The *hSPNT1* gene was localized to chromosome 15q13-14. This study demonstrated for the first time the molecular identity of a purine nucleoside transporter in human. Additional studies demonstrated that the pyrimidine-selective (N2 subtype) transporter, rCNT1, interacts with several clinically important nucleoside analogs and that the mRNA transcripts of rCNT1 are abundant in jejunum and also present at lower levels in duodenum and ileum, but not colon.

Studies in the second part focused on the determination of the substrate binding sites in the cloned N1 and N2 Na<sup>+</sup>-nucleoside transporters. A novel chimeric N1/N2

transporter approach was used to identify the structural elements contributing to substrate binding and selectivity. The data demonstrated that transmembrane domains 8-9 are the major sites for substrate binding and are responsible for the distinct substrate selectivity of N1 and N2. Transporters with novel substrate selectivities were engineered from the cloned transporters. Detailed functional and kinetic studies were carried out to determine the characteristics of an unusual chimeric transporter. Data from these studies provided interesting information on the molecular origins of N1, N2, and N3 nucleoside transport systems. Finally, site-directed mutagenesis was used to identify the critical amino acid residues responsible for the substrate selectivity of N2. The data demonstrated that a single residue, serine 318, in N2 is solely responsible for its transport selectivity for pyrimidine nucleosides. An adjacent residue, glutamine 319, was found to be important in influencing the apparent affinity of the transporter.

*Kathleen M. Giacomin*



## Table of Contents

<b>Acknowledgments</b> . . . . .	<b>.iv</b>
<b>Abstract</b> . . . . .	<b>.vii</b>
<b>List of Tables</b> . . . . .	<b>.xiv</b>
<b>List of Figures</b> . . . . .	<b>.xv</b>

### Chapter 1

#### **Introduction: an Overview of Membrane Transport and Nucleoside**

<b>Transporters</b> . . . . .	<b>.1</b>
Overall Goal . . . . .	1
General Mechanisms of Membrane Transport . . . . .	2
Transporters versus Channels . . . . .	2
Transport Kinetics . . . . .	3
Major Classes of Transporters . . . . .	5
Facilitated Transporters . . . . .	5
Primary Active Transporters . . . . .	5
Ion-coupled Transporters . . . . .	6
Uptake Sites and Roles of Transporters . . . . .	7
Mechanisms of Nucleoside Transport . . . . .	10
Background and General Mechanisms of Nucleoside Transport . . . . .	10
Equilibrative Systems . . . . .	13
Na <sup>+</sup> -dependent Systems . . . . .	15
Recent Advances and Molecular Characteristics of Cloned Nucleoside Transporters . . . . .	16

Cloning Strategies . . . . .	16
Cloned Equilibrative Nucleoside Transporters . . . . .	17
Cloned Na <sup>+</sup> -Nucleoside Transporters . . . . .	18
Other cloned Nucleoside Transporters . . . . .	20
Summary and Review of Chapters . . . . .	22
Chapter 2 . . . . .	22
Chapter 3 . . . . .	23
Chapter 4 . . . . .	23
Chapter 5 . . . . .	24
Chapter 6 . . . . .	25
References . . . . .	26

## **Chapter 2**

<b>Intestinal Distribution and Interaction of a Cloned Nucleoside Transporter (rCNT1) with Therapeutic Nucleoside Analogs . . . . .</b>	<b>37</b>
Introduction . . . . .	37
Materials and Methods . . . . .	40
Molecular Cloning of rCNT1 from Rat Intestine . . . . .	40
Preparation of Oocytes and Microinjection . . . . .	41
Transport Assays . . . . .	41
Localization in Intestine . . . . .	42
Data Analysis . . . . .	42
Results . . . . .	43
Molecular Cloning . . . . .	43
Inhibition Studies . . . . .	43

Uptake Studies . . . . .	47
Localization in Intestine . . . . .	47
Discussion . . . . .	47
References . . . . .	60

### **Chapter 3**

#### **Molecular Mechanism of Purine Nucleoside Transport in Human**

<b>Kidney . . . . .</b>	<b>63</b>
Introduction . . . . .	63
Materials and Methods . . . . .	64
cDNA Cloning and Analysis . . . . .	64
Expression in <i>Xenopus laevis</i> Oocytes and Nucleoside Uptake Assays . . . . .	65
Northern Blot Analysis . . . . .	66
Chromosome Localization . . . . .	66
Results . . . . .	67
Nucleotide and Deduced Amino Acid Sequences of hSPNT1 . . . . .	67
Functional Expression and Characterization of hSPNT1 . . . . .	70
Tissue Distribution of hSPNT1 mRNA . . . . .	77
Chromosomal Localization . . . . .	81
Discussion . . . . .	81
References . . . . .	84

### **Chapter 4**

#### **Identification of Substrate Recognition Domains in Na<sup>+</sup>-Dependent**

<b>Nucleoside Transporters . . . . .</b>	<b>.88</b>
--	------------

Introduction . . . . .	88
Materials and Methods . . . . .	90
Construction of Chimeric Transporters . . . . .	90
Transport Assays in <i>Xenopus laevis</i> Oocytes . . . . .	91
Results . . . . .	91
Construction and Functional Analysis of Chimeric Transporters . . . . .	91
Kinetic Analysis of Wild-Type and Chimeric Transporters . . . . .	99
Discussion . . . . .	99
References . . . . .	104

## **Chapter 5**

### **Characterization of a Bioengineered Chimeric Na<sup>+</sup>-Nucleoside**

<b>Transporter . . . . .</b>	<b>.108</b>
Introduction . . . . .	108
Materials and Methods . . . . .	111
Chimera T8 cDNA . . . . .	111
Expression in <i>Xenopus laevis</i> Oocytes . . . . .	111
Transport Assays . . . . .	112
Data Analysis . . . . .	113
Results . . . . .	113
Transport of Naturally Occurring Nucleosides . . . . .	113
Mechanism of Broad Selectivity . . . . .	114
Interaction with Nucleoside Analogs . . . . .	122
Na <sup>+</sup> Stoichiometry . . . . .	125
Discussion . . . . .	125

References . . . . .	131
----------------------	-----

## **Chapter 6**

### **Molecular Determinants of Pyrimidine Selectivity in N2 Na<sup>+</sup>-Nucleoside**

<b>Transporter . . . . .</b>	<b>.134</b>
Introduction . . . . .	134
Materials and Methods . . . . .	138
Site-directed Mutagenesis and Sequence Analysis . . . . .	138
Transport Assays in <i>Xenopus laevis</i> Oocytes . . . . .	138
Results . . . . .	139
Substrate Selectivity of Mutants . . . . .	139
Transport Kinetics of Mutants S318G and S318G/Q319M . . . . .	145
Helical Wheel Analysis of TM8 . . . . .	149
Discussion . . . . .	149
References . . . . .	153

## **Chapter 7**

<b>Summary and Conclusions . . . . .</b>	<b>156</b>
References . . . . .	162

UCSF LIBRARY  
REBERT ESON

## List of Tables

### Chapter 1

Table 1. Therapeutic Nucleoside Analogs . . . . .	12
Table 2. Characterized Nucleoside Transport Systems . . . . .	14
Table 3. Cloned Nucleoside Transporters . . . . .	21

### Chapter 2

Table 1. Bioavailability of Some Clinically Important Nucleoside Analogs. . . . .	38
Table 2. Inhibition of rCNT1-mediated <sup>3</sup> H-Thymidine Uptake in <i>X. laevis</i> oocytes . . . .	46
Table 3. Summary of IC <sub>50</sub> Values . . . . .	53

### Chapter 4

Table 1. Apparent K <sub>m</sub> Values of Wild-type and Chimeric Transporters . . . . .	100
--	-----

### Chapter 6

Table 1. Systematic Amino Acid Substitutions in Mutants and in Chimera T8. . . . .	137
--	-----

## List of Figures

### Chapter 1

- Figure 1. Kinetic characteristics and inhibition effect of carrier-mediated process . . . . . 4
- Figure 2. A model of transepithelial nucleoside flux . . . . . 8
- Figure 3. Structures of naturally occurring nucleosides . . . . . 11

### Chapter 2

- Figure 1. Uptake of <sup>3</sup>H-labeled pyrimidine and purine nucleosides by rCNT1 . . . . . 44
- Figure 2. Michaelis-Menten studies of thymidine uptake . . . . . 45
- Figure 3. Inhibition studies of <sup>3</sup>H-thymidine uptake in *X. laevis* oocytes injected with the cRNA of rCNT1 . . . . . 48
- Figure 4. Inhibition studies of <sup>3</sup>H-thymidine uptake in *X. laevis* oocytes injected with the cRNA of rCNT1 . . . . . 49
- Figure 5. Inhibition studies of <sup>3</sup>H-thymidine uptake in *X. laevis* oocytes injected with the cRNA of rCNT1 . . . . . 50
- Figure 6. Inhibition studies of <sup>3</sup>H-thymidine uptake in *X. laevis* oocytes injected with the cRNA of rCNT1 . . . . . 51
- Figure 7. Inhibition studies of <sup>3</sup>H-thymidine uptake in *X. laevis* oocytes injected with the cRNA of rCNT1 . . . . . 52
- Figure 8. Uptake of <sup>3</sup>H-labeled 2CdA in oocytes injected with rCNT1 cRNA or H<sub>2</sub>O . . 54
- Figure 9. Uptake of <sup>3</sup>H-labeled AraC in oocytes injected with rCNT1 cRNA or H<sub>2</sub>O . . 55
- Figure 10. RT-PCR analysis of rCNT1 mRNA transcripts in the various regions of rat intestine . . . . . 56

### Chapter 3

Figure 1. Nucleotide and deduced amino acid sequences of hSPNT1 . . . . .	68
Figure 2. Alignment of amino acid sequence of hSPNT1, SPNT, hCNT1 and rCNT1 . . . . .	69
Figure 3. cRNA dose-dependent uptake . . . . .	71
Figure 4. Time course of <sup>3</sup> H-inosine uptake . . . . .	72
Figure 5. Effects of nucleoside and nucleoside analogs on <sup>3</sup> H-inosine uptake in oocytes injected with hSPNT1 cRNA . . . . .	73
Figure 6. Uptake of <sup>3</sup> H-inosine, <sup>3</sup> H-uridine and <sup>3</sup> H-thymidine . . . . .	74
Figure 7. Michaelis-Menten studies of inosine uptake . . . . .	75
Figure 8. Michaelis-Menten studies of uridine uptake . . . . .	76
Figure 9. IC <sub>50</sub> studies of inosine uptake in the presence of adenosine at various concentration in hSPNT1 cRNA-injected oocytes . . . . .	78
Figure 10. IC <sub>50</sub> studies of inosine uptake in the presence of 2'-deoxyadenosine at various concentration in hSPNT1 cRNA-injected oocytes . . . . .	79
Figure 11. Northern blot analysis of hSPNT1 transcript in various human tissues . . . .	80

### Chapter 4

Figure 1. Structures and substrate selectivity of wild-type and chimeric transporters. . .	93
Figure 2. Uptake of <sup>3</sup> H-nucleosides by wild-type N1 and effects of naturally occurring nucleosides on <sup>3</sup> H-uridine uptake mediated by wild-type N1 . . . . .	94
Figure 3. Uptake of <sup>3</sup> H-nucleosides by wild-type N2 and effects of naturally occurring nucleosides on <sup>3</sup> H-uridine uptake mediated by wild-type N2 . . . . .	95



Figure 4. Uptake of <sup>3</sup> H-nucleosides by Chimera T8-9 and effects of naturally occurring nucleosides on <sup>3</sup> H-uridine uptake mediated by Chimera T8-9 . . . . .	97
Figure 5. Uptake of <sup>3</sup> H-nucleosides by Chimera T8 and effects of naturally occurring nucleosides on <sup>3</sup> H-uridine uptake mediated by Chimera T8 . . . . .	98
Figure 6. Sequence alignment of the TMD8-9 regions of cloned N1 and N2 transporter . . . . .	101

## **Chapter 5**

Figure 1. Secondary structures of chimera T8 and wild-type N1 and N2 transporters . . . . .	110
Figure 2. Uptake of <sup>3</sup> H-labeled naturally occurring purine nucleosides by Chimera T8 . . . . .	115
Figure 3. Uptake of <sup>3</sup> H-labeled naturally occurring pyrimidine nucleosides by Chimera T8 . . . . .	116
Figure 4. Effect of inosine on <sup>3</sup> H-thymidine uptake . . . . .	118
Figure 5. Effect of thymidine on <sup>3</sup> H-inosine uptake . . . . .	119
Figure 6. The inhibition mechanism of thymidine uptake by inosine. . . . .	120
Figure 7. The inhibition mechanism of inosine uptake by thymidine . . . . .	121
Figure 8. Effects of nucleoside and nucleoside analogs on <sup>3</sup> H-thymidine uptake in oocytes injected with T8 cRNA . . . . .	123
Figure 9. Uptake of <sup>3</sup> H-labeled L-thymidine and 2CdA by Chimera T8 . . . . .	124
Figure 10. Sodium dependency of T8-mediated uptake of thymidine . . . . .	126
Figure 11. Sodium dependency of T8-mediated uptake of inosine. . . . .	127

## **Chapter 6**

Figure 1. Secondary structures of chimera T8 and wild-type N1 and N2 transporters and the amino acid sequences of N2 and N1 in TM8 region . . . . .	136
Figure 2. Uptake of <sup>3</sup> H-labeled uridine by mutants, chimera T8, and wild-type N1 and N2 . . . . .	140
Figure 3. Uptake of <sup>3</sup> H-labeled inosine and thymidine by wild-type N2 and chimera T8 . . . . .	141
Figure 4. Uptake of <sup>3</sup> H-labeled inosine and thymidine by mutant S304T, mutant T306A, mutant S310A, and mutant Q319M . . . . .	142
Figure 5. Uptake of <sup>3</sup> H-labeled inosine and thymidine by mutant S318G and mutant S318G/Q319M . . . . .	143
Figure 6. Uptake of <sup>3</sup> H-labeled inosine and thymidine by mutant T8.G318S . . . . .	146
Figure 7. Michaelis-Menten studies of thymidine and inosine uptake mediated by mutant S318G . . . . .	147
Figure 8. Michaelis-Menten studies of thymidine and inosine uptake mediated by mutant S318G/Q319M . . . . .	148
Figure 9. Helical wheel analysis of the TM8 of N2 . . . . .	150

## CHAPTER 1

### INTRODUCTION: AN OVERVIEW OF MEMBRANE TRANSPORT AND NUCLEOSIDE TRANSPORTERS<sup>1</sup>

#### Overall Goal

To absorb essential nutrients, excrete metabolic wastes, and eliminate environmental toxins, living cells have evolved complex transport systems to transfer polar molecules across their membranes. In humans, transport systems are also the routes of entry and exit of numerous therapeutic agents into or out of the body, and therefore, are critical in the *in vivo* absorption, disposition, and elimination of a variety of drugs. The overall goal of the research presented in this dissertation is to elucidate the molecular mechanisms involved in the membrane transport of a special class of compounds, nucleosides and their analogs.

During the past decade, our understanding of membrane transport systems has progressed significantly. The development of cloning and expression strategies, in conjunction with advances in methods of measuring transport function (e.g. fluorescence and electrophysiological methods), has led to the identification and functional analysis of various membrane transporters, whose properties often, but not always, correspond to transport systems characterized in earlier studies. With the rapid growth of sequence

---

<sup>1</sup> Part of this chapter is being considered for publication in a chapter entitled "Uptake Sites and Transporters" in *Principles of Pharmacology and Drug Discovery* (M. Williams and N. Bowery, eds.). John Wiley, Chichester, 1999

UNIVERSITY LIBRARY

information and functional data, molecular mechanisms that govern the common design, specific substrate requirements, energy-coupling, regulation, subcellular targeting, and evolutionary origins of many transporters are being studied. This dissertation is focused on the molecular cloning, functional characterization, and structure-function relationship analysis of Na<sup>+</sup>-dependent nucleoside transporters.

This introductory chapter is divided into two major sections: I. General Mechanisms of Membrane Transport and II. Mechanisms of Nucleoside Transport. In the first section, the general characteristics of carrier-mediated membrane transport are reviewed. A summary of the major classes of mammalian transporters is presented. Finally, the physiological and pharmacological roles of several membrane transporters are addressed. The second section is focused on research in the field of nucleoside transport. Following a brief introduction to the therapeutic significance of nucleosides and nucleoside analogs, the general mechanisms of nucleoside transport in mammalian cells are discussed. Information on the functional and molecular properties of cloned nucleoside transporters is presented. Finally, a summary of the major findings in each chapter of this dissertation is presented.

## **I. GENERAL MECHANISMS OF MEMBRANE TRANSPORT**

The lipid bilayer of cell membranes functions as a barrier to the free passage of most ions and organic solutes. Transport systems are essential for cells to transfer ions and organic solutes across their membranes. These systems consist of numerous membrane channel and transporter proteins encoded by various gene families that have been conserved as well as diversified during evolution to perform various functions in prokaryote and eukaryote cells.

### **Transporters versus Channels**

Channels and transporters (or carriers) mediate transmembrane solute movement by fundamentally different mechanisms (1, 2). The transmembrane segments of channel proteins form narrow aqueous pores that span the lipid bilayer. Small ions such as  $\text{Na}^+$ ,  $\text{K}^+$ ,  $\text{Ca}^{2+}$ , or  $\text{Cl}^-$  move rapidly down their concentration gradients through these pores. The lumen of a channel is accessible from either side of the membrane simultaneously.

Transporters may also span the lipid bilayer, but their substrate binding sites are never accessible from both sides of the membrane simultaneously (1, 2). Transporters undergo three steps during a transporting event: binding to substrate, translocation of substrate, and release of substrate. Compounds transported by various carriers are highly diversified and include inorganic ions, heavy metals, and organic solutes such as sugars, amino acids, peptides, nucleosides, vitamins, organic cations or anions, neurotransmitters, and a variety of xenobiotics including drugs and environmental toxins. Furthermore, a transporter can couple to an energy source to catalyze active transport of substrates against their concentration gradients (1, 2).

### **Transport Kinetics**

The process mediated by a membrane transporter resembles an enzyme-substrate reaction which can be described with kinetic equations (1, 2). However, unlike an ordinary enzyme-substrate reaction, the transported substrate is not covalently modified by the transporter. Transporters with one substrate binding site (i.e. uniporters) exhibit simple Michaelis-Menten type kinetics. The rate of transport reaches a maximum ( $V_{max}$ ) when the transporter is saturated with the substrate (Figure 1A). The substrate concentration required to produce half maximal rate ( $K_m$ ) approximates the apparent binding constant for the substrate (Figure 1). The  $K_m$  generally reflects the substrate affinity for the binding site but is also influenced by rate constants of substrate translocation and dissociation. The kinetics of a coupled transport of two or more substrates are more complex but can be

WEST LIBRARY  
NOV 17 2007

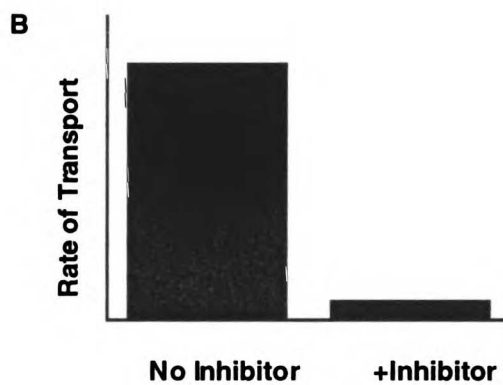
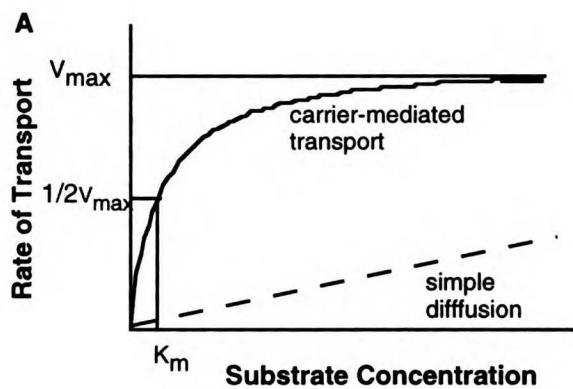


Figure 1. Kinetic characteristics (A) and inhibition effect (B) of carrier-mediated process.

studied in a basically similar way if the concentrations of all substrates but the one of interest are kept constant at saturating levels. As with enzymes, the transport activity can be blocked specifically by inhibitors which may or may not be transported (Figure 1B). In other words, an inhibitor of a transporter is not necessarily its substrate (permeant).

## **Major Classes of Transporters**

Based on energy requirements, mammalian transporters can be divided into three major classes: facilitated, primary active, and ion-coupled transporters (2-4). Facilitated transporters mediate passive (downhill) flux of solutes whereas primary active and ion-coupled transporters mediate active (uphill) transport of solutes (1-4).

### *Facilitated Transporters*

The facilitated transporters are not coupled to a free energy source. They usually mediate the passive flux of one substrate (uniport) down its electrochemical gradient. If the substrate is uncharged, it is the concentration gradient that drives the movement and determines the net direction of flux. If the substrate carries a net charge, its transport into the cell is then electrogenic, and is influenced by both the concentration gradient and the physiological membrane potential which generally favors the entry of positively charged substrates but opposes the entry of negatively charged substrates (1-4). Under physiological conditions, facilitated transporters function bidirectionally and the direction of substrate flux is determined by the electrochemical gradient of the substrates.

### *Primary Active Transporters*

Primary active transporters are coupled to energy supplied by chemical or photochemical reactions. Most mammalian primary active transporters are ATP-dependent transporters which couple the hydrolysis of ATP to the translocation of solutes across the

biological membrane. The P-type ATPase superfamily comprises a large number of primary active transporters which are involved in the active pumping of a variety of cations and heavy metals in eukaryotic and prokaryotic cells. They are characterized by the phosphorylation of the aspartic acid in the signature sequence DKTG following ATP hydrolysis (5, 6). A number of ion pumps, such as Na<sup>+</sup>, K<sup>+</sup>-ATPase and H<sup>+</sup>, K<sup>+</sup>-ATPase, are members of this family. They play important roles in the generation of ion concentration gradients across membranes, regulation of cellular volume and pH, and development of the membrane potential. The ABC (ATP Binding Cassette) transporters, also known as the traffic ATPases, are another large superfamily of ATP-dependent primary active transporters. They are characterized by their common modular organization and two conserved sequence motifs that constitute the ATP binding cassette (7-10). Prominent examples include the multidrug resistance protein (MDR or P-glycoprotein), the cystic fibrosis transmembrane conductance regulator (CFTR), and the multidrug resistance-associated protein (MRP).

### *Ion-coupled Transporters*

Ion-coupled transporters use energy stored in the ion gradients, established directly or indirectly by primary active transporters, to drive the active transport of solutes (3, 4, 11-13). They couple the translocation of substrates with the driving substrate (the driving ion) which always moves across the membrane in a direction that dissipates its electrochemical gradient. The second substrate (the driven substrate) moves against its electrochemical gradient. The direction of the transmembrane movement of the driven substrate can be either the same as (symport), or opposite to (counterport), that of the driving ion. Symport systems are often referred to as cotransporters or symporters, whereas counterport systems are often referred to as antiporters or exchangers. In mammalian cells, ion-coupled transporters are frequently coupled to the physiological inwardly directed Na<sup>+</sup> electrochemical gradient (3, 4, 11-13). Because the Na<sup>+</sup>



electrochemical gradient is established by the ubiquitous primary active  $\text{Na}^+$ ,  $\text{K}^+$ -ATPase,  $\text{Na}^+$ -coupled transporters are also referred to as secondary active transporters (3, 4, 11-13). A number of transporters are also coupled to the cotransport and/or to the counter-transport of  $\text{H}^+$ ,  $\text{Cl}^-$ ,  $\text{K}^+$ , and/or  $\text{OH}^-$ . Some  $\text{H}^+$ - or  $\text{Cl}^-$ -coupled antiporters may be referred to as tertiary active transporters because the  $\text{H}^+$  or  $\text{Cl}^-$  electrochemical gradient is generated from the secondary active  $\text{Na}^+$ - $\text{H}^+$  antiporter or  $\text{Na}^+$ - $\text{Cl}^-$  cotransporters. By coupling to ion gradients, secondary and tertiary active transporters can build up steep concentration gradients of substrates across biological membranes, particularly if the coupling ratio exceeds 1. This enables them to play important roles in the kidney, liver, intestine, or synaptic cleft to actively absorb nutrients, excrete metabolites, or terminate the action of neurotransmitters (4, 11-21).

### **Uptake Sites and Roles of Transporters**

Transporters play critical roles in the *in vivo* absorption, disposition, and elimination of a variety of compounds. In epithelial cells lining the lumen of the intestine, kidney tubules, and choroid plexus, vectorial flux of solutes often involves multiple transporters asymmetrically distributed in the brush border membrane (facing lumen) and the basolateral membrane (facing blood). Figure 2 demonstrates a transepithelial active absorption process of nucleosides in the lumen of the intestine. In other polarized cells such as hepatocytes and the endothelial cells in the brain capillary, asymmetric mechanisms also regulate transcellular solute flux. Since many transporters are the major routes for drug entry and exit from cells, they are important determinants of bioavailability, efficacy, and toxicity. Because of the pharmacological and pharmacokinetic importance of these drug transporters, it is anticipated that the study of transporters will provide a basis for evaluation and prediction of drug-drug interactions, adverse drug reactions, and will be valuable in the assessment of drug kinetics.

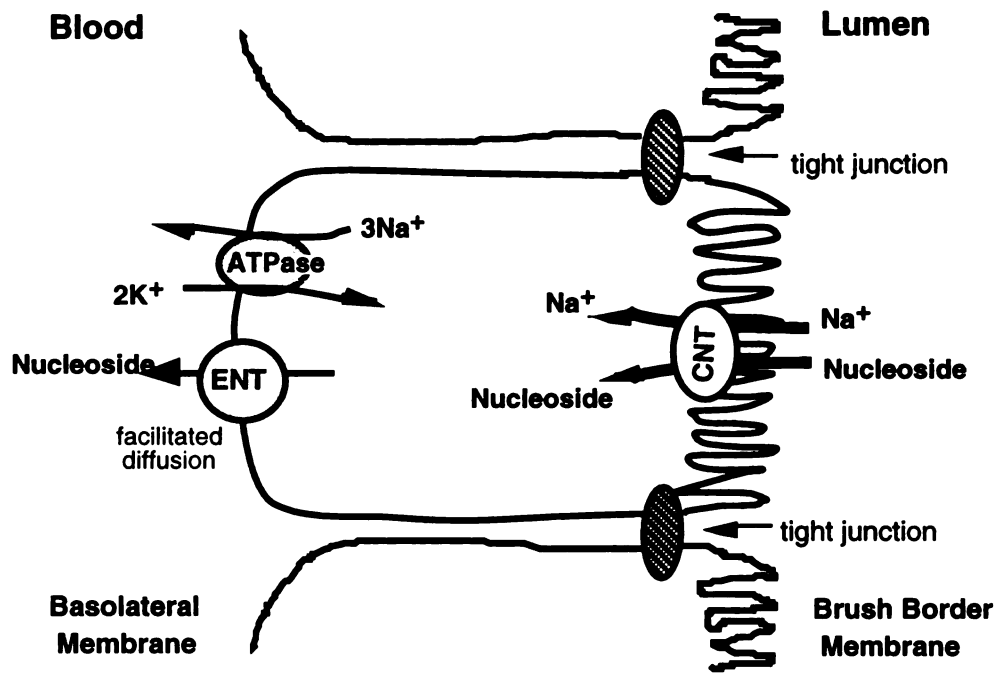


Figure 2. A model of transepithelial nucleoside flux mediated by a Na<sup>+</sup>-nucleoside cotransporter, CNT, and a facilitated nucleoside transporter, ENT in the lumen of the intestine.

In the intestine, ion-coupled transporters on the brush border membrane are actively involved in the absorption of many orally administered drugs (19). For example, a number of  $\beta$ -lactam antibiotics and peptide-mimetic drugs are absorbed by the proton-coupled oligopeptide transporter PepT1 (19, 22). To improve oral bioavailability, drugs can be designed or modified to be better substrates for these transporters. In contrast, the P-glycoprotein MDR1 limits the absorption of various lipophilic drugs by pumping these drugs into the gut lumen. Inhibition of MDR1 enhances the absorption of certain drugs (23). In the liver, transporters on the sinusoidal membrane (e.g. OCT, OATP) transport many drugs into the hepatocytes where they can be metabolized by various drug-metabolizing enzymes (18, 24, 25). Transporters (e.g. MRP2 and MDR1) on the canalicular membrane eliminate drugs and drug conjugates by secreting them into the bile (18, 25-27). Malfunction of the hepatobiliary transport systems may result in severe drug toxicity. Transporters in the kidney are critical in the body's defense against foreign substances including drugs, chemical carcinogens and other toxic agents. The renal epithelium functions to selectively reabsorb and eliminate endogenous compounds, nutrients, environmental toxins, and drugs. Transport in the renal tubule constitutes a major pathway of the disposition of many drugs and drug metabolites (28, 29). Transporters located in the blood-brain barrier and in the choroid plexus play important roles in maintaining cerebrospinal fluid homeostasis and in protecting the brain from various toxic compounds (30, 31). They may also represent promising routes for targeting therapeutic agents to the brain.

Many transporters themselves are important therapeutic targets. Among them are the neurotransmitter transporters and various transporters in the kidney. Diuretics such as bumetanide and furosemide act on  $\text{Na}^+ - \text{K}^+ - 2\text{Cl}^-$  transporters located in the renal tubules (32). Many psychostimulants and antidepressants are inhibitors of catecholamine transporters in the brain (14, 33, 34). In addition, the ABC transporters, MDR1 and MRP1, are responsible for multidrug resistance in many tumor cells (26, 27, 35). They

represent a major obstacle in cancer chemotherapy. Considerable effort is being devoted to the search for effective and non-toxic inhibitors of MDR transporters (36, 37).

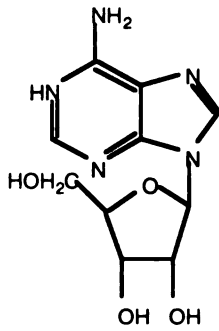
Genetic defects in transporter genes may lead to inherited diseases. For example, individuals with the inherited disease cystinuria, carrying a mutation in the amino acid transporter *rBAT* gene, are unable to reabsorb cystine in the kidney, leading to the accumulation of cystine and the formation of cystine stones in the kidney (17, 38). Similarly, polymorphisms in the genes of drug transporters may alter the pharmacokinetics in some individuals, contributing to the inter-individual variation in drug efficacy and toxicity observed in clinical therapy.

## **II. MECHANISMS OF NUCLEOSIDE TRANSPORT**

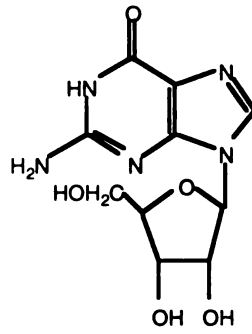
Natural and synthetic nucleosides play important physiological and pharmacological roles in mammals. Physiologic purine and pyrimidine nucleosides are precursors for DNA and RNA synthesis. The purine nucleoside, adenosine, is a neuromodulator that functions in the regulation of neurotransmitter release, platelet aggregation, coronary vasodilation, renal vasoconstriction, and lipolysis (39, 40). Due to its significant cardiac effects, adenosine is used clinically in the treatment of cardiac arrhythmias (41). Nucleoside analogs, including zidovudine (AZT) and didanosine (ddI) are currently being used in the treatment of patients with Human Immunodeficiency Virus (HIV) (42-44). Other nucleoside analogs, such as cladribine (2CdA), cytosine arabinoside (AraC), and 5-fluorouracil (5-FU), are important agents in cancer chemotherapy (45, 46). Structures of naturally occurring nucleosides are shown in Figure 3. Listed in Table 1 are various nucleoside analogs currently being used as therapeutic agents.

### **Background and General Mechanisms of Nucleoside Transport**

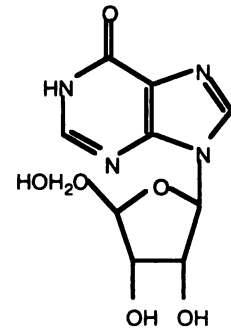
### Purine Nucleosides



**Adenosine**

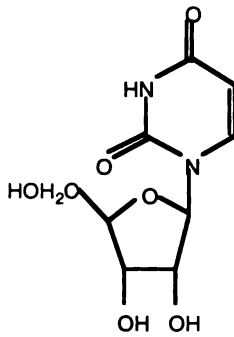


**Guanosine**

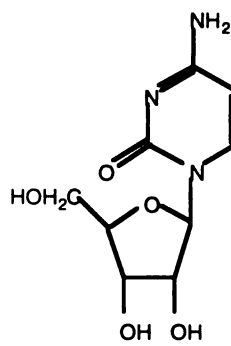


**Inosine**

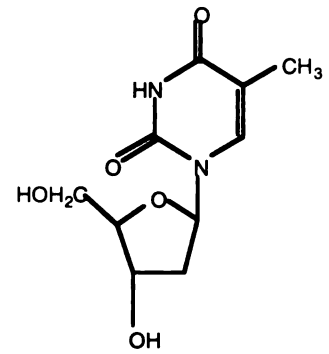
### Pyridine Nucleosides



**Uridine**



**Cytidine**



**Thymidine**

Figure 3. Structures of naturally occurring nucleosides

**Table 1. Therapeutic Nucleoside Analogs**

---

---

**Antiherpesvirus Agents**

Acyclovir	Valacyclovir (prodrug of acyclovir)
Famciclovir	Ganciclovir
Idoxuridine	Sorivudine
Trifluridine	Vidarabin (Ara-A)

**Antiretroviral Agents**

Didanosine (ddl)	Lamivudine
Stavudine	Zalcitabine (ddC)
Zidovudine (AZT)	

**Antineoplastic Agents**

Fluorouracil	Fluorodeoxyuridine
Cytarabine (AraC)	Mercaptopurine
Azathioprine	Thioguanine
Cladribine	Fludarabine Phosphate
Pentostatin (2'-Deoxyformycin)	

---

---

Most mammalian cells are capable of synthesizing nucleosides *de novo*. However, some animal cells, such as intestinal enterocytes, bone marrow, certain brain cells, erythrocytes, and leucocytes, are unable to synthesize nucleosides *de novo* (40), thus must take up nucleosides derived from dietary sources or from *de novo* synthesis by other cells. There is also evidence that salvage pathways are preferred over *de novo* pathways in cells that are capable of nucleoside synthesis (47). The transport of nucleosides across cell membranes is therefore essential in maintaining nucleoside homeostasis. Physiological nucleosides and most synthetic nucleoside analogs are hydrophilic and specific transport proteins, i.e. the nucleoside transporters, on the plasma membrane are required for their movement into or out of cells.

Earlier work in the field of nucleoside transport documented functional and kinetic studies of nucleoside flux in isolated cells and tissue preparations (40, 48, 49). These studies established that multiple nucleoside transport systems exist in mammalian cells (21, 40, 48, 49). Two major classes of nucleoside transporters have been identified: the equilibrative nucleoside transporters and the concentrative nucleoside transporters. The equilibrative nucleoside transporters are facilitated transport systems whereas the concentrative nucleoside transporters are Na<sup>+</sup>-dependent secondary active transport systems (21, 40, 48, 49). The characteristics of these transport systems are summarized in Table 2.

### *Equilibrative Systems*

Historically, the equilibrative transport systems were the first to be studied. The equilibrative nucleoside transporters mediate facilitated diffusion of nucleosides across plasma membranes and function bidirectionally in the transmembrane flux of nucleosides in accordance with the concentration gradient (40, 48, 49). Nitrobenzylthioinosine (NBMPR), a tight-binding and highly specific inhibitor, has been used successfully in the

**Table 2. Characterized Nucleoside Transport Systems**

<b>Transporter</b>	<b>Substrate Selectivity</b>	<b>Na<sup>+</sup>-dependency</b>	<b>NBMPR Sensitivity</b>
<b>Equilibrative</b>			
<i>es</i>	broad	No	Yes
<i>ei</i>	broad	No	No
<b>Concentrative</b>			
N1	purine nucleosides, uridine	Yes	No
N2	pyrimidine nucleosides, adenosine	Yes	No
N3	broad	Yes	No
N4	pyrimidine nucleosides, guanosine, adenosine	Yes	No
N5	formycin B, 2CdA	Yes	Yes



study of these transporters. Based on their sensitivity to inhibition by NBMPR, equilibrative nucleoside transporters have been classified into two subtypes (*es* and *ei*). The *es* subtype binds NBMPR with high affinity ( $K_d$  1-10 nM) as a result of a noncovalent interaction of NBMPR with a high affinity binding site located on the extracellular side of the plasma membrane (40, 48). Using NBMPR as a probe, the *es* transporter protein has been identified and purified from human erythrocytes (50). In contrast, the *ei* subtype is not affected by nanomolar concentrations of NBMPR, and is only inhibited by high (> 10  $\mu$ M) concentrations (40, 48). Both *es* and *ei* are inhibited by low concentrations (0.1-100 nM) of dipyrindamole and dilazep, although there are differences among cell types and species (40, 48). *Es* and *ei* exhibit broad substrate selectivity and transport all of the endogenous purine and pyrimidine nucleosides as well as a diverse group of structural analogs with various substituents in the base and/or sugar moieties (48). They are widely distributed in different cell types and tissues and many cells express both systems in varying proportions (40).

### *Na<sup>+</sup>-dependent Systems*

$\text{Na}^+$ -dependent systems mediate the active transport of nucleosides into cells by coupling the flux of substrates to the physiological  $\text{Na}^+$  gradient across the plasma membrane. Unlike the equilibrative systems, the  $\text{Na}^+$ -dependent nucleoside transporters exhibit distinct substrate selectivities for purine or pyrimidine nucleosides (21). Five  $\text{Na}^+$ -dependent nucleoside transport processes have been characterized functionally (21, 40, 48) (Table 2). These processes have been designated N1-N5 based on their substrate selectivity. The N1 process is considered purine-selective but also transports uridine. The N2 process is pyrimidine-selective but also transports adenosine. Both have been characterized in the epithelia of such tissues as intestine, kidney, liver, and several mammalian cell lines (40, 49, 51-58). The N3-N5 processes are all considered broadly-

selective, transporting both purines and pyrimidines (48, 53, 59-61). Each of these processes has been characterized in tissue or cell preparations or in mRNA expression studies. N3 has been characterized in rabbit choroid plexus and ileum and rat jejunum (54, 60-62). N4 which transports pyrimidines and the purine nucleosides adenosine and guanosine was characterized in brush border membrane vesicles isolated from human kidney (53). Limited functional data exists for the N5 process which has been characterized only in human leukemia cell lines (48). A  $\text{Na}^+$ :nucleoside coupling ratio of 1:1 has been reported for N1 and N2 transporters, indicating that the inward transport of each nucleoside molecule is driven by the interaction of one sodium ion (21, 40, 48). In contrast, a stoichiometry of 2:1 was observed for the N3 system, indicating two sodium ions are required for the translocation of one nucleoside molecule (60).

### **Recent Advances and Molecular Characteristics of Cloned Nucleoside Transporters**

In recent years, significant advances have been made in the field of nucleoside transport. The greatest progress is the cloning of various proteins responsible for the distinct nucleoside transport processes that have been characterized in cells or tissues in earlier functional and kinetic studies. In this section, the cloning strategies used for equilibrative and concentrative nucleoside transporters are reviewed. A summary of the molecular characteristics of various cloned nucleoside transporters is presented. Recent interests in the fields are discussed.

#### *Cloning Strategies*

The first cloned nucleoside transporter was the  $\text{Na}^+$ -dependent, N2 subtype transporter. Because the  $\text{Na}^+$ -nucleoside transport proteins are minor membrane components which have not been purified or sequenced, the immunologic and

oligonucleotide probes for conventional sequence-based cloning were not available. Functional expression in *Xenopus laevis* oocytes, an approach based on transport activity which had been used previously in cloning a number of membrane transporters (3), was employed by several laboratories to isolate cDNAs encoding the nucleoside transporters. Using this approach, Huang *et al.* first succeeded in cloning an N2 subtype transporter, rCNT1, in 1994 (63). A year later, using the same approach, Che *et al.* cloned an N1 subtype transporter, SPNT (64). Based on sequence information of rCNT1, its human homolog, hCNT1, was subsequently cloned by Ritzel *et al.* (65). The human N1 subtype transporter, hSPNT1, was cloned in our laboratory (Chapter 3) using homology cloning strategies and RT-PCR methods (66).

The *es* transporter protein was previously purified from human erythrocytes by immunoaffinity chromatography (50). Information obtained from the sequence of the N-terminal 21 residues was used to clone the *es* transporter, hENT1, from a human placental library (67). The *ei* transporter was cloned by two independent groups using different cloning strategies (68, 69). Using homology cloning based on the sequence of *es*, Yao *et al.* cloned the *ei* type transporter, rENT2, and the rat homolog of hENT1, rENT1, from rat tissue (69). By functional expression in a transport-deficient cell line, Crawford *et al.* cloned the *ei* type transporter, hENT2, from human (68). hENT2 was also cloned by Griffiths *et al.* from human placenta (70).

#### *Cloned Equilibrative Nucleoside Transporters*

The cloned ENT1 (456 residues for hENT1; 457 residues for rENT1) and ENT2 (456 residues for both hENT2 and rENT2) transporters share high sequence homology (> 46% identity) and belong to a new gene family designated ENT (67-70). All transporters are predicted to contain 11 membrane-spanning regions. When expressed in *Xenopus laevis* oocytes or in mammalian cells, the cloned transporters exhibited functional properties of classical *ei*- or *es*- type transport observed in earlier studies in intact cells or tissues (67-

70). Interestingly, notable species differences are observed between hENT1 and rENT1 in terms of post-translational glycosylation and sensitivity to inhibition by coronary vasoactive drugs such as dipyridamole, dilazep, and draflazine (71). hENT1 is sensitive whereas rENT1 is not. Using chimeric constructs of hENT1 and rENT1, Sundaram *et al.* showed that transmembrane domains 3-6 may form part of the vasoactive drug binding site in these transporters (71).

#### *Cloned Na<sup>+</sup>-Nucleoside Transporters*

To date, the N1 and N2 subtypes of Na<sup>+</sup>-dependent nucleoside transporters have been cloned from rat (rCNT1 and SPNT) and human (hCNT1 and hSPNT1) (63-66). Although the cloned N1 and N2 transporters have distinct substrate selectivity for purine and pyrimidine nucleosides, respectively, they share a high sequence homology (60-70%) and a similar predicted membrane topology (14 putative transmembrane domains). They belong to a *CNT* gene family that also includes the NupC proton-nucleoside symporter of *Escherichia coli* (63-66).

rCNT1 encodes a protein of 648 amino acid residues. When expressed in *Xenopus laevis* oocytes, the recombinant rCNT1 transporter exhibits a high level of nucleoside transport activity with a typical N2 substrate selectivity for pyrimidine nucleosides and adenosine (63). Nucleoside uptake is Na<sup>+</sup>-dependent and saturable with an apparent  $K_m$  of 37  $\mu$ M for uridine and 26  $\mu$ M for adenosine (63, 72). In the oocyte expression system as well as in a mammalian cell expression system, it has been shown that rCNT1 accepts the antiviral pyrimidine analogs, AZT and ddC, as permeants ( $K_m = 0.49$  and 0.51 mM, respectively) (73). Recently, studies from our laboratory revealed that the nucleoside analog 2CdA, a chemotherapeutic drug, also interacts with rCNT1 ( $IC_{50} = 61 \mu$ M) (21). These data suggest that N2 transporters may play an important role in the site-specific absorption/elimination of clinically used nucleoside analogs. The expression of the mRNA transcript of

rCNT1 was detected by Northern analysis in rat intestine and kidney but not in heart, brain, spleen, lung, liver or skeletal muscle (63). However, by more sensitive Reverse Transcriptase-PCR (RT-PCR) analysis, Anderson *et al.* found that the mRNA transcript of rCNT1 is also present in various regions of the brain including choroid plexus, posterior hypothalamus, hippocampus, cerebral cortex, cerebellum and brain stem (74). These data suggest that a small amount of the transporter is expressed in specific regions of the brain. The human homolog of rCNT1, hCNT1, was cloned from a human kidney cDNA library by hybridization cloning and RT-PCR strategies (65). hCNT1 is 83% identical to rCNT1 in amino acid sequence and exhibits similar transport characteristics. The transporter gene is localized to Chromosome 15.

The cDNA of the rat N1 transporter, SPNT, encodes a protein of 659 amino acid residues (64). There are five possible N-linked glycosylation sites, one ATP/GTP binding motif in the amino terminus, and several consensus sites for protein kinase A and C phosphorylation on both termini suggesting that SPNT may be regulated by mechanisms involving protein kinases, or intracellular ATP/GTP. Functionally, SPNT exhibits typical N1 transport characteristics with a substrate selectivity for purine nucleosides and uridine (64). SPNT mediated adenosine uptake is Na<sup>+</sup>-dependent and saturable with a  $K_m$  of 6  $\mu$ M (64). Recently, we developed a HeLa cell expression system to study the functional characteristics of SPNT (75). The nucleoside analogs, 2CdA and ddI, significantly inhibited <sup>3</sup>H-inosine uptake. The IC<sub>50</sub> of 2CdA was 13  $\mu$ M and that of ddI was 46  $\mu$ M. 2CdA was also found to be a permeant of SPNT. In contrast, ddI was not a permeant of SPNT (75). These data suggest that SPNT may play an important role in the cellular transport of nucleoside drugs. Northern analysis revealed that multi-transcripts of SPNT are expressed in liver, intestine, spleen, and heart (64). The relatively wide tissue distribution of SPNT may suggest that SPNT is involved in regulation of purinergic receptor-mediated nucleoside effects in addition to salvaging nucleosides.

Recently, using homology cloning strategies and reverse transcriptase polymerase reactions, we cloned the human N1 homolog, hSPNT1, from kidney (66). At the amino acid level, hSPNT1 is 81% identical to rat SPNT with the most divergent region at the N-terminus. The ATP/GTP binding motif at the N-terminus of SPNT is absent in hSPNT1. hSPNT1 and SPNT have the same substrate selectivity, transporting both purine nucleosides and uridine. Northern analysis revealed that multiple transcripts of hSPNT1 are widely distributed in human tissues including kidney, heart, liver, intestine, skeletal muscle, and pancreas (66). Interestingly, the rat SPNT transcript is absent in the kidney (64). The wide tissue distribution of hSPNT1 suggest that this transporter may play a critical role in the specific uptake and salvage of purine nucleosides in a variety of human tissues. The hSPNT1 gene is localized to Chromosome 15.

Some molecular properties of the cloned transporters in the ENT and CNT families are summarized in Table 3.

#### *Other cloned Nucleoside Transporters*

A putative Na<sup>+</sup>-dependent nucleoside transporter, SNST1, was cloned (76) in addition to rCNT1, SPNT, hCNT1 and hSPNT1. The sequence of SNST1 is homologous to the transporters in the Na<sup>+</sup>-glucose transporter family but not to the CNT gene family (76). Although SNST1 exhibits a substrate selectivity similar to the N3 subtype, its low transport activity, absence of mRNA transcripts in rabbit intestine (on Northern analysis), and sequence divergence from the recently cloned N1 and N2 transporters suggest that this transporter may not represent the well characterized N3 system reported in rabbit choroid plexus and ileum (21, 76). Efforts to elucidate the physiologic role of SNST1 and cloning of nucleoside transporters from rabbit ileum or choroid plexus will provide us with a better understanding of other Na<sup>+</sup>-dependent nucleoside transporters.

**Table 3. Cloned Nucleoside Transporters**

<b>Transporter</b>	<b>Species</b>	<b>Subtype</b>	<b>Amino Acid</b>	<b>Reference</b>
rCNT1	rat	N2	648	(63)
hCNT1	human	N2	650	(65)
SPNT	rat	N1	659	(64)
hSPNT1	human	N1	658	(66)
hENT1	human	<i>es</i>	456	(67)
rENT1	rat	<i>es</i>	457	(69)
hENT2	human	<i>ei</i>	456	(68, 70)
rENT2	rat	<i>ei</i>	456	(69)

## Summary and Review of Chapters

With the cloning of nucleoside transporters, functional and kinetic properties of individual transporter subtypes were obtained by studying the transporters in heterologous expression systems. The roles of each subtype in the absorption and disposition of specific nucleoside drugs were investigated by studying the interactions of nucleoside drugs with cloned transporter overexpressed in mammalian cells or in *X. laevis* oocytes. However, little is known about the structural elements and molecular mechanisms that underlie the functional properties of Na<sup>+</sup>-dependent nucleoside transporters.

The overall goal of the research presented in this dissertation is to elucidate the molecular mechanisms involved in the membrane transport of nucleosides and their analogs. Specifically, research presented in this dissertation is focused on the molecular cloning, functional characterization, and structure-function relationship analysis of Na<sup>+</sup>-dependent nucleoside transporters. A brief summary of the work presented in each chapter is presented below.

### Chapter 2

The goal of the study presented in this chapter was to investigate the interaction of the cloned N2 subtype transporter (rCNT1) with clinically important nucleoside analogs, and to determine the distribution of rCNT1 in the different segments of intestine (i.e. duodenum, jejunum, ileum, and colon). Using an RT-PCR based method, rCNT1 was cloned from rat intestine and was expressed in *X. laevis* oocytes. The interaction of rCNT1 with various nucleoside drugs was determined in inhibition studies as well as in uptake studies. The data suggest that rCNT1 interacts with several clinically important nucleoside analogs and accepts the anticancer drugs 2CdA and AraC as permeants. To determine the distribution of rCNT1 along the intestine, mRNA from rat duodenum,



jejunum, ileum and colon was isolated and subjected to specific RT-PCR analysis. The mRNA transcript of rCNT1 is detected in duodenum, jejunum, ileum, but not in colon. These results suggest that rCNT1 plays a role in the intestinal absorption of some clinically important nucleoside analogs and the absorption may occur largely in jejunum as well as in duodenum and ileum.

### Chapter 3

Many purine nucleosides and their analogs are actively transported in the kidney. The goal of this study was to investigate the molecular mechanism of purine nucleoside transport in human kidney. Using homology cloning strategies and reverse transcriptase polymerase chain reactions, we isolated a cDNA encoding a Na<sup>+</sup>-dependent nucleoside transporter, hSPNT1, from human kidney. Functional expression in *Xenopus laevis* oocytes identified hSPNT1 as a Na<sup>+</sup>-dependent nucleoside transporter which selectively transports purine nucleosides but also transports uridine. The  $K_m$  of uridine (80  $\mu$ M) in interacting with hSPNT1 was substantially higher than that of inosine (4.5  $\mu$ M). hSPNT1 (658 amino acids) is 81% identical to the previously cloned rat Na<sup>+</sup>-nucleoside transporter, SPNT, but differs markedly from SPNT in terms of its primary structure in the N-terminus. In addition, an *Alu* repetitive element (~ 282 bp) is present in the 3' untranslated region (UTR) of the hSPNT1 cDNA. Northern analysis revealed that multiple transcripts of hSPNT1 are widely distributed in human tissues including human kidney. In contrast, rat SPNT transcripts are absent in kidney and highly localized to liver and intestine. The hSPNT1 gene was localized to chromosome 15. This is the first demonstration of a purine nucleoside transporter in human tissues.

### Chapter 4

The goal of this study was to identify structural domains involved in substrate binding and molecular determinants responsible for distinct transport selectivity. Chimeric

transporters were constructed from the cloned rat N1 and N2 transporters and the substrate selectivity of each chimera was analyzed in oocyte expression system. Of the 14 transmembrane domains (TM) of N1 and N2, transplanting TM8-9 of N1 into N2 converted N2 from a pyrimidine- to a purine- selective transporter. Transplanting only TM8 generated a chimera with characteristics similar to the N3 transporter that has yet to be cloned. These data suggest that TM8-9 confer substrate selectivity and may form at least part of a substrate binding site in Na<sup>+</sup>-dependent nucleoside transporters.

### Chapter 5

In studies described in Chapter 4, we created a chimeric N1/N2 transporter, T8, which seemed to exhibit a novel substrate selectivity. Limited studies suggested that T8 may possess characteristics of the N3 transporter that has not been cloned. The purpose of this study was to determine the substrate profile, transport mechanism, and Na<sup>+</sup>-coupling stoichiometry of T8, and compare with wild-type N1, N2, and N3. In *Xenopus laevis* oocytes expressing T8, Na<sup>+</sup>-dependent uptake of <sup>3</sup>H-labeled purine (adenosine, inosine, and guanosine) and pyrimidine nucleosides (uridine, thymidine, and cytidine) was significantly enhanced (3.5-18.6 fold), suggesting that T8 is a broadly-selective transporter that accepts both purine and pyrimidine nucleosides as permeants. T8-mediated uptake of <sup>3</sup>H-thymidine, was competitively inhibited by inosine; and T8-mediated uptake of <sup>3</sup>H-inosine was competitively inhibited by thymidine, suggesting that purine and pyrimidine nucleosides may share a common binding site. Base-modified ribo- and 2'-deoxyribo-nucleosides were potent inhibitors of T8. In contrast, 2', 3'-dideoxyinosine, 2', 3'-dideoxycytidine and 3'-azidothymidine, which are known inhibitors of N1 or N2, did not inhibit T8-mediated uptake. These data suggest that the substrate profile of T8 is not a combination of those of N1 and N2; rather, it is similar to that of N3. However, the

Na<sup>+</sup>:nucleoside stoichiometric ratio of T8 was determined to be 1, consistent with both N1 and N2 but different from N3.

### *Chapter 6*

Using chimeric rat N2/N1 transporters, we demonstrated that transmembrane domains (TM) 8 and 9 are the major sites for substrate binding and discrimination (Chapter 4). Interestingly, when TM8 of N2 was replaced by that of N1, the resulting chimera, T8, lost the pyrimidine selectivity of N2 and accepted both purine and pyrimidine nucleosides (Chapter 5). Five residues differ between rat N2 and N1 in TM8. To identify the critical residues responsible for transport selectivity, the five residues in N2 were systematically changed to their equivalents in N1. Replacing the serine residue at position 318 to its equivalent N1 residue, glycine, caused N2 to lose its selectivity for pyrimidine nucleosides and accept purine nucleosides as substrates. In contrast, replacing the other four residues did not change the pyrimidine selectivity of N2. Furthermore, when glycine 318 in chimera T8 was changed back to serine, the chimeric transporter regained pyrimidine-selectivity. These observations suggest that serine 318 is located in the nucleoside permeation pathway and is responsible for the substrate selectivity of N2. An adjacent residue, glutamine 319, was found to be important in modulating the apparent affinity for nucleosides.

## References

1. Alberts, B., D. Bray, J. Lewis, M. Raff, K. Roberts, and J. D. Watson. Membrane transport of small molecules and the ionic basis of membrane excitability, in *Molecular Biology of the Cell* pp507-522, Garland Publishing, Inc, New York (1994).
2. Wolfersberger, M. G. Uniporters, symporters and antiporters. *J Exp Biol* **196**:5-6 (1994).
3. Hediger, M. A. Structure, function and evolution of solute transporters in prokaryotes and eukaryotes. *J Exp Biol* **196**:15-49 (1994).
4. Sadee, W., V. Drubbisch, and G. L. Amidon. Biology of membrane transport proteins. *Pharm Res* **12**:1823-37 (1995).
5. Lutsenko, S., and J. H. Kaplan. Organization of P-type ATPases: significance of structural diversity. *Biochemistry* **34**:15607-13 (1995).
6. Moller, J. V., B. Juul, and M. le Maire. Structural organization, ion transport, and energy transduction of P-type ATPases. *Biochim Biophys Acta* **1286**:1-51 (1996).
7. Higgins, C. F. The multidrug resistance P-glycoprotein. *Curr Opin Cell Biol* **5**:684-7 (1993).
8. Higgins, C. F., R. Callaghan, K. J. Linton, M. F. Rosenberg, and R. C. Ford. Structure of the multidrug resistance P-glycoprotein. *Semin Cancer Biol* **8**:135-42 (1997).

9. Tusnady, G. E., E. Bakos, A. Varadi, and B. Sarkadi. Membrane topology distinguishes a subfamily of the ATP-binding cassette (ABC) transporters. *FEBS Lett* **402**:1-3 (1997).
10. van Veen, H. W., and W. N. Konings. Multidrug transporters from bacteria to man: similarities in structure and function. *Semin Cancer Biol* **8**:183-91 (1997).
11. Hediger, M. A., Y. Kanai, G. You, and S. Nussberger. Mammalian ion-coupled solute transporters. *J Physiol (Lond)* **482**:7S-17S (1995).
12. Vandenberg, R. J. Molecular pharmacology and physiology of glutamate transporters in the central nervous system. *Clin Exp Pharmacol Physiol* **25**:393-400 (1998).
13. Wright, E. M., D. D. Loo, E. Turk, and B. A. Hirayama. Sodium cotransporters. *Curr Opin Cell Biol* **8**:468-73 (1996).
14. Bonisch, H., and L. Eiden. Catecholamine reuptake and storage. Overview. *Adv Pharmacol* **42**:149-64 (1998).
15. Jursky, F., S. Tamura, A. Tamura, S. Mandiyan, H. Nelson, and N. Nelson. Structure, function and brain localization of neurotransmitter transporters. *J Exp Biol* **196**:283-95 (1994).
16. Kanner, B. I. Sodium-coupled neurotransmitter transport: structure, function and regulation. *J Exp Biol* **196**:237-49 (1994).

17. Malandro, M. S., and M. S. Kilberg. Molecular biology of mammalian amino acid transporters. *Annu Rev Biochem* **65**:305-36 (1996).
18. Muller, M., and P. L. Jansen. Molecular aspects of hepatobiliary transport. *Am J Physiol* **272**:G1285-303 (1997).
19. Tsuji, A., and I. Tamai. Carrier-mediated intestinal transport of drugs. *Pharm Res* **13**:963-77 (1996).
20. Uhl, G. R., and P. S. Johnson. Neurotransmitter transporters: three important gene families for neuronal function. *J Exp Biol* **196**:229-36 (1994).
21. Wang, J., M. E. Schaner, S. Thomassen, S. F. Su, M. Piquette-Miller, and K. M. Giacomini. Functional and molecular characteristics of Na(+)-dependent nucleoside transporters. *Pharm Res* **14**:1524-32 (1997).
22. Fei, Y. J., V. Ganapathy, and F. H. Leibach. Molecular and structural features of the proton-coupled oligopeptide transporter superfamily. *Prog Nucleic Acid Res Mol Biol* **58**:239-61 (1998).
23. Salphati, L., and L. Z. Benet. Effects of ketoconazole on digoxin absorption and disposition in rat. *Pharmacology* **56**:308-13 (1998).
24. Zhang, L., C. M. Brett, and K. M. Giacomini. Role of organic cation transporters in drug absorption and elimination. *Annu Rev Pharmacol Toxicol* **38**:431-60 (1998).

25. Koepsell, H. Organic cation transporters in intestine, kidney, liver, and brain. *Annu Rev Physiol* **60**:243-66 (1998).
26. Kavallaris, M. The role of multidrug resistance-associated protein (MRP) expression in multidrug resistance. *Anticancer Drugs* **8**:17-25 (1997).
27. Barrand, M. A., T. Bagrij, and S. Y. Neo. Multidrug resistance-associated protein: a protein distinct from P-glycoprotein involved in cytotoxic drug expulsion. *Gen Pharmacol* **28**:639-45 (1997).
28. Giacomini, K. M. Membrane transporters in drug disposition. *J Pharmacokinet Biopharm* **25**:731-41 (1997).
29. Somogyi, A. Renal transport of drugs: specificity and molecular mechanisms. *Clin Exp Pharmacol Physiol* **23**:986-9 (1996).
30. Angeletti, R. H., P. M. Novikoff, S. R. Juvvadi, J. M. Fritschy, P. J. Meier, and A. W. Wolkoff. The choroid plexus epithelium is the site of the organic anion transport protein in the brain. *Proc Natl Acad Sci U S A* **94**:283-6 (1997).
31. Preiss, R. P-glycoprotein and related transporters. *Int J Clin Pharmacol Ther* **36**:3-8 (1998).
32. Mount, D. B., E. Delpire, G. Gamba, A. E. Hall, E. Poch, R. S. Hoover, and S. C. Hebert. The electroneutral cation-chloride cotransporters. *J Exp Biol* **201**:2091-102 (1998).

33. Amara, S. G., and J. L. Arriza. Neurotransmitter transporters: three distinct gene families. *Curr Opin Neurobiol* **3**:337-44 (1993).
34. Blakely, R. D., L. J. De Felice, and H. C. Hartzell. Molecular physiology of norepinephrine and serotonin transporters. *J Exp Biol* **196**:263-81 (1994).
35. Gottesman, M. M., I. Pastan, and S. V. Ambudkar. P-glycoprotein and multidrug resistance. *Curr Opin Genet Dev* **6**:610-7 (1996).
36. Sarkadi, B., and M. Muller. Search for specific inhibitors of multidrug resistance in cancer. *Semin Cancer Biol* **8**:171-82 (1997).
37. Stein, W. D. Kinetics of the multidrug transporter (P-glycoprotein) and its reversal. *Physiol Rev* **77**:545-90 (1997).
38. Palacin, M. A new family of proteins (rBAT and 4F2hc) involved in cationic and zwitterionic amino acid transport: a tale of two proteins in search of a transport function. *J Exp Biol* **196**:123-37 (1994).
39. Thorn, J. A., and S. M. Jarvis. Adenosine transporters. *Gen Pharmacol* **27**:613-20 (1996).
40. Griffith, D. A., and S. M. Jarvis. Nucleoside and nucleobase transport systems of mammalian cells. *Biochim Biophys Acta* **1286**:153-81 (1996).
41. Lerman, B. B., and L. Belardinelli. Cardiac electrophysiology of adenosine. Basic and clinical concepts. *Circulation* **83**:1499-509 (1991).



42. Portegies, P. Review of antiretroviral therapy in the prevention of HIV-related AIDS dementia complex (ADC). *Drugs* 1:25-31; discussion 38-40 (1995).
43. Whitley, R. J. The past as prelude to the future: history, status, and future of antiviral drugs [see comments]. *Ann Pharmacother* 30:967-71 (1996).
44. Mayers, D. Rational approaches to resistance: nucleoside analogues. *Aids* S9-13 (1996).
45. Saven, A., and L. D. Piro. The newer purine analogs. Significant therapeutic advance in the management of lymphoid malignancies. *Cancer* 72:3470-83 (1993).
46. Saven, A., M. L. Figueroa, L. D. Piro, and J. D. Rosenblatt. 2-Chlorodeoxyadenosine to treat refractory histiocytosis X [letter]. *N Engl J Med* 329:734-5 (1993).
47. Karle, J. M., L. W. Anderson, and R. L. Csyk. Effect of plasma concentrations of uridine on pyrimidine biosynthesis in cultured L1210 cells. *J Biol Chem* 259:67-72 (1984).
48. Cass, C. E. Nucleoside transport, in *Drug Transport in Antimicrobial and Anticancer Chemotherapy*. (N. H. Georgopapadaku, ed.) pp.403-451, Marcel Dekker, New York (1995).
49. Belt, J. A., N. M. Marina, D. A. Phelps, and C. R. Crawford. Nucleoside transport in normal and neoplastic cells. *Adv Enzyme Regul* 33:235-52 (1993).

50. Kwong, F. Y., A. Davies, C. M. Tse, J. D. Young, P. J. Henderson, and S. A. Baldwin. Purification of the human erythrocyte nucleoside transporter by immunoaffinity chromatography. *Biochem J* **255**:243-9 (1988).
51. Chandrasena, G., R. Giltay, S. D. Patil, A. Bakken, and J. D. Unadkat. Functional expression of human intestinal Na<sup>+</sup>-dependent and Na<sup>+</sup>-independent nucleoside transporters in *Xenopus laevis* oocytes. *Biochem Pharmacol* **53**:1909-18 (1997).
52. Che, M., Z. Gatmaitan, and I. M. Arias. Ectonucleotidases, purine nucleoside transporter, and function of the bile canalicular plasma membrane of the hepatocyte. *FASEB J* **11**:101-8 (1997).
53. Gutierrez, M. M., and K. M. Giacomini. Substrate selectivity, potential sensitivity and stoichiometry of Na<sup>(+)</sup>-nucleoside transport in brush border membrane vesicles from human kidney. *Biochim Biophys Acta* **1149**:202-8 (1993).
54. Huang, Q. Q., C. M. Harvey, A. R. Paterson, C. E. Cass, and J. D. Young. Functional expression of Na<sup>(+)</sup>-dependent nucleoside transport systems of rat intestine in isolated oocytes of *Xenopus laevis*. Demonstration that rat jejunum expresses the purine-selective system N1 (cif) and a second, novel system N3 having broad specificity for purine and pyrimidine nucleosides. *J Biol Chem* **268**:20613-9 (1993).
55. Lee, C. W., C. I. Cheeseman, and S. M. Jarvis. Transport characteristics of renal brush border Na<sup>(+)</sup>- and K<sup>(+)</sup>-dependent uridine carriers. *Am J Physiol* **258**:F1203-10 (1990).

56. Patil, S. D., and J. D. Unadkat. Sodium-dependent nucleoside transport in the human intestinal brush-border membrane. *Am J Physiol* **272**:G1314-20 (1997).
57. Plagemann, P. G., and J. M. Aran. Characterization of Na(+)-dependent, active nucleoside transport in rat and mouse peritoneal macrophages, a mouse macrophage cell line and normal rat kidney cells. *Biochim Biophys Acta* **1028**:289-98 (1990).
58. Roovers, K. I., and G. K. Meckling. Characterization of equilibrative and concentrative Na+-dependent (cif) nucleoside transport in acute promyelocytic leukemia NB4 cells. *J Cell Physiol* **166**:593-600 (1996).
59. Wu, X., and K. M. Giacomini. Expression of the choroid plexus sodium-nucleoside cotransporter (N3) in *Xenopus laevis* oocytes. *Biochem Pharmacol* **48**:432-4 (1994).
60. Wu, X., G. Yuan, C. M. Brett, A. C. Hui, and K. M. Giacomini. Sodium-dependent nucleoside transport in choroid plexus from rabbit. Evidence for a single transporter for purine and pyrimidine nucleosides. *J Biol Chem* **267**:8813-8 (1992).
61. Redlak, M. J., Z. E. Zehner, and S. L. Betcher. Expression of rabbit ileal N3 Na+/nucleoside cotransport activity in *Xenopus laevis* oocytes. *Biochem Biophys Res Commun* **225**:106-11 (1996).
62. Wu, X., M. M. Gutierrez, and K. M. Giacomini. Further characterization of the sodium-dependent nucleoside transporter (N3) in choroid plexus from rabbit. *Biochim Biophys Acta* **1191**:190-6 (1994).

63. Huang, Q. Q., S. Y. Yao, M. W. Ritzel, A. R. Paterson, C. E. Cass, and J. D. Young. Cloning and functional expression of a complementary DNA encoding a mammalian nucleoside transport protein. *J Biol Chem* **269**:17757-60 (1994).
64. Che, M., D. F. Ortiz, and I. M. Arias. Primary structure and functional expression of a cDNA encoding the bile canalicular, purine-specific Na(+)-nucleoside cotransporter. *J Biol Chem* **270**:13596-9 (1995).
65. Ritzel, M. W., S. Y. Yao, M. Y. Huang, J. F. Elliott, C. E. Cass, and J. D. Young. Molecular cloning and functional expression of cDNAs encoding a human Na<sup>+</sup>-nucleoside cotransporter (hCNT1). *Am J Physiol* **272**:C707-14 (1997).
66. Wang, J., S. F. Su, M. J. Dresser, M. E. Schaner, C. B. Washington, and K. M. Giacomini. Na(+)-dependent purine nucleoside transporter from human kidney: cloning and functional characterization. *Am J Physiol* **273**:F1058-65 (1997).
67. Griffiths, M., N. Beaumont, S. Y. Yao, M. Sundaram, C. E. Boumah, A. Davies, F. Y. Kwong, I. Coe, C. E. Cass, J. D. Young, and S. A. Baldwin. Cloning of a human nucleoside transporter implicated in the cellular uptake of adenosine and chemotherapeutic drugs [see comments]. *Nat Med* **3**:89-93 (1997).
68. Crawford, C. R., D. H. Patel, C. Naeve, and J. A. Belt. Cloning of the human equilibrative, nitrobenzylmercaptapurine riboside (NBMPR)-insensitive nucleoside transporter ei by functional expression in a transport-deficient cell line. *J Biol Chem* **273**:5288-93 (1998).

69. Yao, S. Y., A. M. Ng, W. R. Muzyka, M. Griffiths, C. E. Cass, S. A. Baldwin, and J. D. Young. Molecular cloning and functional characterization of nitrobenzylthioinosine (NBMPR)-sensitive (es) and NBMPR-insensitive (ei) equilibrative nucleoside transporter proteins (rENT1 and rENT2) from rat tissues. *J Biol Chem* **272**:28423-30 (1997).

70. Griffiths, M., S. Y. Yao, F. Abidi, S. E. Phillips, C. E. Cass, J. D. Young, and S. A. Baldwin. Molecular cloning and characterization of a nitrobenzylthioinosine-insensitive (ei) equilibrative nucleoside transporter from human placenta. *Biochem J* **328**:739-43 (1997).

71. Sundaram, M., S. Y. Yao, A. M. Ng, M. Griffiths, C. E. Cass, S. A. Baldwin, and J. D. Young. Chimeric constructs between human and rat equilibrative nucleoside transporters (hENT1 and rENT1) reveal hENT1 structural domains interacting with coronary vasoactive drugs. *J Biol Chem* **273**:21519-25 (1998).

72. Yao, S. Y., A. M. Ng, M. W. Ritzel, W. P. Gati, C. E. Cass, and J. D. Young. Transport of adenosine by recombinant purine- and pyrimidine-selective sodium/nucleoside cotransporters from rat jejunum expressed in *Xenopus laevis* oocytes. *Mol Pharmacol* **50**:1529-35 (1996).

73. Yao, S. Y., C. E. Cass, and J. D. Young. Transport of the antiviral nucleoside analogs 3'-azido-3'-deoxythymidine and 2',3'-dideoxycytidine by a recombinant nucleoside transporter (rCNT) expressed in *Xenopus laevis* oocytes. *Mol Pharmacol* **50**:388-93 (1996).

74. Anderson, C. M., W. Xiong, J. D. Young, C. E. Cass, and F. E. Parkinson. Demonstration of the existence of mRNAs encoding N1/cif and N2/cit sodium/nucleoside cotransporters in rat brain. *Brain Res Mol Brain Res* **42**:358-61 (1996).
75. Schaner, M. E., J. Wang, S. Zevin, K. M. Gerstin, and K. M. Giacomini. Transient expression of a purine-selective nucleoside transporter (SPNTint) in a human cell line (HeLa). *Pharm Res* **14**:1316-21 (1997).
76. Pajor, A. M., and E. M. Wright. Cloning and functional expression of a mammalian Na<sup>+</sup>/nucleoside cotransporter. A member of the SGLT family. *J Biol Chem* **267**:3557-60 (1992).

## CHAPTER 2

### INTESTINAL DISTRIBUTION AND INTERACTION OF A CLONED NUCLEOSIDE TRANSPORTER (rCNT1) WITH THERAPEUTIC NUCLEOSIDE ANALOGS<sup>1</sup>

Pyrimidine and purine nucleoside analogs are currently being developed and used as antineoplastic, antiviral, antiarrhythmic, and antiparasitic agents. Understanding the mechanism by which the intestine transports nucleosides and nucleoside analogs is of importance since many nucleoside drugs are used orally (Table 1).

A problem with some orally-used nucleoside analogs is that they have low bioavailability and require high doses to achieve a therapeutic effect (1-3). Even for nucleoside drugs which are generally absorbed well in the intestine, dramatic decreases in bioavailability may occur if the drug is coadministered with other nucleoside analogs during combination therapy (4). Furthermore, low bioavailability may be associated with large inter- and intra- individual variations in plasma concentrations (2, 3). Because of these reasons, rational and safe oral administration of nucleoside analogs is difficult. Knowledge of the mechanisms by which the intestine transports nucleoside and nucleoside analogs may help to enhance rational therapeutic use of these agents.

---

<sup>1</sup> Part of this chapter was published in a review article entitled: "Functional and molecular characteristics of Na<sup>+</sup>-dependent nucleoside transporters" Wang, J., Schaner, M. E., Thomassen, S., Su, S. F., Piquette-Miller, M., and Giacomini, K. M. *Pharmaceutical Research* 14: 1524-32, 1997.

**Table 1. Bioavailability of Some Clinically Important Nucleoside Analogs**

<b>Nucleoside Analog</b>	<b><i>F</i> (%)</b>
Stavudine	70-86
Azidothymidine (AZT)	60-70
Dideoxyinosine (ddl)	38
Dideoxycytidine (ddC)	80
Ganciclovir	3
Acyclovir	10-20
2-Chloro-2'-deoxyadenosine (2CdA)	37-51



Intestinal absorption of nucleosides and their analogs requires a Na<sup>+</sup>-linked secondary active transporting system (4-7). Based upon functional studies in tissue preparations, three major classes of Na<sup>+</sup>-nucleoside transporters, selective for purine (N1), pyrimidine (N2), and both purine and pyrimidine (N3) nucleosides, have been characterized in the intestinal epithelia of human, rat and rabbit (8-10). Using functional expression in *Xenopus laevis* oocytes, Huang and coworkers first succeeded in cloning the N2 subtype transporter, rCNT1, in 1994. rCNT1 cDNA was cloned from a rat jejunum library (11). The 2.4 kb cDNA predicts a protein of 648 amino acids (71 kDa) with 14 putative transmembrane domains. There are three potential N-linked and four potential O-linked glycosylation sites, and four protein kinase C-dependent phosphorylation sites. When expressed in *X. laevis* oocytes, the recombinant rCNT1 transporter exhibits a high level of nucleoside transport activity with a typical N2 substrate selectivity for pyrimidine nucleosides and adenosine (11). rCNT1-mediated nucleoside uptake is Na<sup>+</sup>-dependent and saturable with an apparent  $K_m$  of 37  $\mu$ M for uridine and 26  $\mu$ M for adenosine (11, 12). These data suggest that rCNT1 is important in the absorption of endogenous pyrimidine nucleosides and adenosine. However, the role of rCNT1 in the intestinal absorption of nucleoside drugs and its distribution along the intestine are poorly understood.

The goal of this study was to investigate the interaction of rCNT1 with clinically important nucleoside analogs, and to determine the distribution of rCNT1 in the different segments of intestine (i.e. duodenum, jejunum, ileum, and colon). Using an RT-PCR based method, rCNT1 was cloned from rat intestine and was expressed in *X. laevis* oocytes. The interaction of rCNT1 with various nucleoside drugs was determined in inhibition studies as well as in uptake studies. To determine the distribution of rCNT1 along the intestine, mRNA from rat duodenum, jejunum, ileum and colon was isolated and subjected to specific RT-PCR analysis. The results suggest that rCNT1 plays a role

in the intestinal absorption of some clinically important nucleoside analogs and the absorption may occur largely in jejunum as well as in duodenum and ileum.

## **Materials and Methods**

*Molecular Cloning of rCNT1 from Rat Intestine.* Mucosal scrapings from the small intestine were obtained from non-fasting adult male Sprague-Dawley rats. Poly (A<sup>+</sup>) RNA (mRNA) was immediately isolated from the scrapings by homogenization with TRIzol Reagent (GibcoBRL) and selection on Maxi-Oligo(dT) Cellulose Spin Columns (5' Prime 3', Boulder, CO). Standard manufacturer's protocols were employed. Reverse transcription of mRNA was then performed using the Superscript Preamplification System for First Strand cDNA Synthesis (GibcoBRL) following the manufacturer's protocol. Ten percent (2  $\mu$ l) of the first strand product was used for PCR amplification.

The two amplification oligonucleotide primers (forward, 5' -CTGAAGAGCCAA GCACATGGCAGACAACAC-3'; reverse, 5' -TCTAGAGACAGCTTTTGGGGGG ATAC-3') were derived from the positions 141-170 and 2376-2401 of the published sequence of rCNT1 (GenBank #U25055). Amplification was carried out using a Perkin-Elmer/thermal cycler (Model 2400) for 30 cycles involving denaturation at 94°C for 30 s, annealing at 55°C for 1 min, and extension at 72°C for 3 min. PCR products were analyzed by 1% agarose gel electrophoresis. A single 2.3 kb PCR product was obtained, and was then ligated into pGEM-T vector (Promega, Madison, WI) followed by transformation into DH5 $\alpha$  competent cells (GibcoBRL). The Wizard Minipreps DNA Purification System (Promega, Madison, WI) was used to extract the plasmid DNA from overnight culture of the transformed bacteria. Isolated plasmids were screened by Pst I restriction enzyme analysis and were sequenced using an automated Model 373A DNA Sequencer (Applied Biosystems Inc.).

*Preparation of Oocytes and Microinjection.* *X. laevis* frogs (*Xenopus*, Ann Arbor, MI) were anesthetized in 0.3% tricaine solution. A small incision was made on the abdomine and portions of the ovarian lobes were removed and maintained in OR II solution (82.5 mM NaCl, 2 mM KCl, 1 mM MgCl<sub>2</sub>, 10 mM Hepes/Tris pH 7.4). The ovarian lobes were cut into small clumps and a 2% solution of collagenase D (Boehringer Mannheim, Indianapolis, In) in OR II was used to remove the follicular layers. The oocytes were then washed 10 times with OR II and 10 times with modified Barth's solution (1 mM KCl, 0.82 mM MgSO<sub>4</sub>, 0.41 mM CaCl<sub>2</sub>, 0.33 mM Ca(NO<sub>3</sub>)<sub>2</sub>, 2.4 mM NaHCO<sub>3</sub>, 10 mM Hepes/Tris pH 7.4, 88 mM NaCl, 20 µg/ml Gentamycin, and 100 U Penicillin/Streptomycin). Healthy stage V or VI oocytes were sorted and incubated in Barth's Solution at 18°C overnight prior to injection. Plasmid containing rCNT1 was linearized with Xba I and transcribed *in vitro* using T7 polymerase (Promega). 50 nl of water or 20 mg of cRNA in a total volume of 50 nl was injected into each oocyte using a semi-automatic injector (PL1-188, Nikon, Melville, NY). Injected oocytes were incubated for 2 to 4 days in Barth's solution at 18°C. Uptake experiments were carried out 48-56 hours post-injection.

*Transport Assays.* Uptake of nucleosides by oocytes was traced with the respective <sup>3</sup>H-labeled nucleosides (Moravek Biochemicals, Brea, CA). Assays were performed at 25 °C on groups of 10 oocytes in 150 µl of transport buffer containing 100 mM NaCl or 100 mM choline chloride and 2 mM KCl, 1 mM CaCl<sub>2</sub>, 1 mM MgCl<sub>2</sub>, 10 mM HEPES, pH 7.4. At the end of the incubation, uptake was terminated by removing the incubation medium followed by six rapid washes in ice-cold choline chloride buffer. Individual oocytes were dissolved in 10% SDS and the radioactive content of each oocytes was assayed by liquid scintillation counting. For inhibition studies, non-radioactive compounds (Sigma Chemicals, St. Louis, MO) were also included in the reaction mixture at concentrations indicated in Table 2.

*Localization in Intestine.* Non-fasting adult male Sprague-Dawley rats were used in this study (Simonson, Gilroy, CA). The rats were anesthetized with diethyl ether before decapitation. The duodenum was cut from the stomach and approximately 8 centimeters down the intestine. The ileum was cut from where the small intestine emptied into the cecum and 2 centimeters up the intestine. The remaining section left after the duodenum and the ileum were excised, was the jejunum. As this section would also contain the overlapping regions of duodenum/jejunum and jejunum/ileum, these overlapping regions, approximately 5-10 centimeters from both ends of the jejunum, were cut off and discarded. The colon was easily identified and isolated, starting from the cecum and ending at the rectum. Segments were kept separately in an ice-cold 0.9% NaCl solution. Intestinal content was then emptied and the epithelia was scraped. mRNA was immediately isolated using TRIZOL Reagent (GibcoBRL) followed by selection on Oligo(dT) columns (5' Prime 3', Boulder, CO). To ascertain the localization of the mRNA transcript of rCNT1 along the intestine, 0.5 mg of mRNA isolated from segments of the duodenum, jejunum, ileum and colon was subjected to RT-PCR. The amplification primers (forward, 5'-GGGGACATGGTGGATAT CCAGGGACTCAGC-3'; reverse, 5'-CTATGTGCAGACTGTGTGGTTGTA AAAATCG ACAGCA-3'), designed to amplify a 0.6 kb fragment of rCNT1, were derived from nucleotide sequence of rCNT1. Amplification was carried out using a Perkin-Elmer/thermal cycler (Model 2400) for 30 cycles under the following conditions: 94°C for 1 min, 50°C for 1.5 min, 72°C for 1.5 min. The PCR products were analyzed by 1% agarose gel electrophoresis.

*Data Analysis.* Uptake values are presented as mean  $\pm$  standard error for 8-10 individual oocytes. In kinetic studies, the apparent  $K_m$  and  $V_{max}$  values were determined by fitting the data to the Michaelis-Menten equation by non-linear regression. The  $IC_{50}$  was determined by fitting the data to the equation  $V = V_o / (1 + (I / IC_{50}))^n$ , where  $V$  is the uptake of thymidine in the presence of the inhibitor,  $V_o$  is the uptake of thymidine in the absence of inhibitor,  $I$  is the inhibitor concentration and  $n$  is the slope. Because of the

substantial variability in expression obtained in oocytes harvested from different frogs, the uptake values in the presence of inhibitors are reported as a percentage of the control values. The significance of difference ( $p < 0.05$ ) was determined using the unpaired Student's t-test.

## Results

*Molecular Cloning.* Using primers derived from the sequence published by Huang *et al.* (11), a single 2.3 kb fragment encoding rCNT1 was isolated by RT-PCR from rat intestine. The predicted amino acid sequence is identical to that of the published sequence of rCNT1. This fragment was then subcloned into the pGEM-T vector and expressed in *X. laevis* oocytes. Significant Na<sup>+</sup>-dependent thymidine (a model pyrimidine nucleoside) uptake was observed in cRNA injected oocytes (Figure 1). In contrast, there was no significant Na<sup>+</sup>-dependent inosine (a model purine nucleoside) uptake (Figure 1). These data suggest that we have obtained a functional rCNT1 clone from rat intestine which exhibits characteristics of the pyrimidine-selective N2 Na<sup>+</sup>-nucleoside transporter. rCNT1-mediated thymidine uptake was saturable with a  $K_m$  of  $24 \pm 6.7 \mu\text{M}$  and a  $V_{max}$  of  $15 \pm 1.1 \text{ pmol/oocyte/30 min}$  (Figure 2).

*Inhibition Studies.* The interactions of various nucleoside analogs with rCNT1 were investigated by measuring rCNT1-mediated <sup>3</sup>H-thymidine uptake in the presence of unlabeled compounds (Table 2). At the concentration of 1 mM, thymidine, 2-chloroadenosine, 2-chloro-2'-deoxyadenosine (2CdA), and 5-fluorouridine, significantly inhibited greater than 80% of <sup>3</sup>H-thymidine uptake. Cytosine arabinoside (AraC), at 10 mM inhibited 82% of [<sup>3</sup>H]thymidine uptake. Dideoxycytidine (ddC), at 10 mM also inhibited the uptake (Table 2). In contrast, synthetic dideoxynucleoside analogs (at 1 mM) including dideoxyinosine (ddI) and dideoxyadenosine (ddA), azidothymidine (AZT) at 4 mM, and acycloguanosine (5 mM) did not significantly inhibit rCNT1-mediated

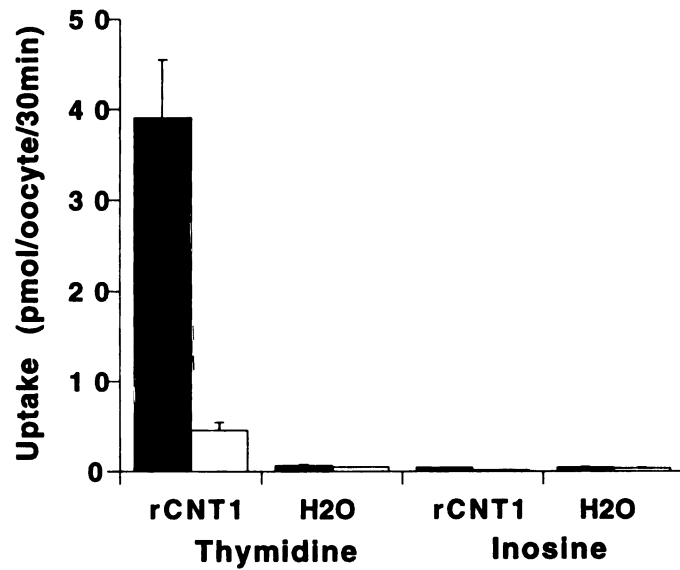


Figure 1. Uptake of <sup>3</sup>H-labeled pyrimidine and purine nucleosides by rCNT1. Uptake was measured at 25°C in the presence (solid bars) or absence of Na<sup>+</sup> (open bars). Each value represents the mean ± S.E. (n = 8-10).

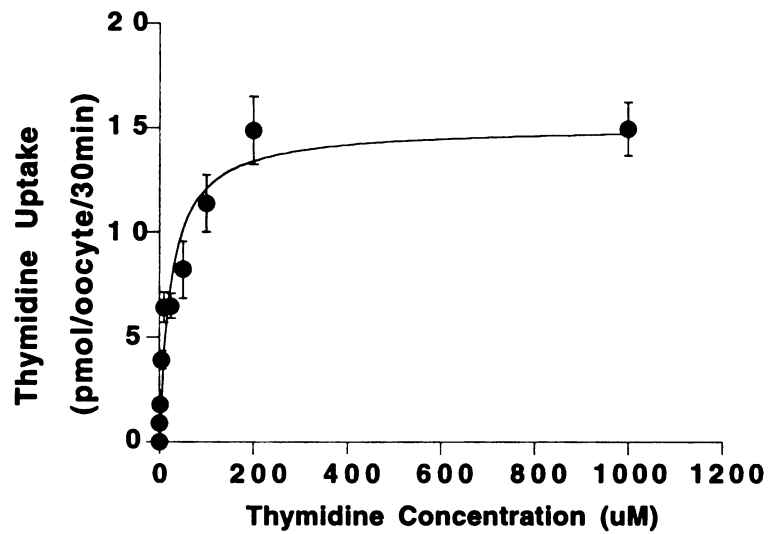


Figure 2. Michaelis-Menten studies of thymidine uptake. Each point represents the mean  $\pm$  S.E. (n=8-10). Apparent  $K_m$  and  $V_{max}$  values were determined by fitting the data to a Michaelis-Menten equation.

**Table 2. Inhibition of rCNT1-mediated <sup>3</sup>H-Thymidine Uptake in *X. laevis* oocytes.**

<b>Nucleoside Analog</b>	<b>% Uptake of Control</b>
Control	100 ± 7.9
1 mM thymidine	6.8 ± 0.6*
1 mM 2-chloroadenosine	10.9 ± 0.7*
1 mM 2CdA	8.1 ± 0.5*
1 mM 5-fluorouridine	5.6 ± 0.5*
10 mM AraC	17.5 ± 2.6*
4 mM AZT	78.1 ± 5.4
10 mM ddC	71.9 ± 7.4*
1 mM ddi	107.5 ± 16.0
1 mM ddA	96.1 ± 15.2
5 mM acyclovir	88.8 ± 11.0

\* Values significantly different from the control (p<0.05).



thymidine uptake. The effect of concentration with thymidine, 2-chloroadenosine, 2CdA, 5-fluorouridine, and AraC on rCNT1-mediated thymidine uptake was examined (Figures 3-7). The  $IC_{50}$  values are summarized in Table 3.

*Uptake Studies*. Data from inhibition studies suggest that the clinically important nucleoside analogs 2CdA and AraC interact with rCNT1. However, an inhibitor of a transporter is not necessarily a substrate (or permeant). To investigate whether 2CdA and AraC are true substrates of rCNT1, we studied the uptake of radio-labeled 2CdA and AraC (Figures 8-9). Compared to the uptake in water-injected oocytes, significant  $Na^+$ -dependent uptake of [ $^3H$ ]2CdA (Figure 8) and [ $^3H$ ]AraC (Figure 9) were observed in rCNT1 cRNA-injected oocytes. These data suggest that in addition to being inhibitors of rCNT1, 2CdA and AraC are also true permeants of this transporter.

*Localization in Intestine*. The localization of rCNT1 in the various regions of the intestine was investigated by analyzing the expression of rCNT1 mRNA transcripts in these regions. The presence and abundance of rCNT1 transcripts in the duodenum, jejunum, ileum and colon were characterized by the presence and the intensity of the 0.6 kb RT-PCR product from mRNA isolated from these regions. The most prominent band in the small intestine was from the jejunum, but clear bands were also obtained from the PCR products of the duodenum and jejunum (Figure 10). No band was obtained from the PCR products of colon. These data correspond to a strong expression of rCNT1 mRNA in rat jejunum, a moderate expression in duodenum and ileum, and no expression in colon.

## **Discussion**

Many nucleoside drugs are used orally. Understanding the mechanism by which the intestine transports nucleosides and nucleoside analogs is important for rational drug

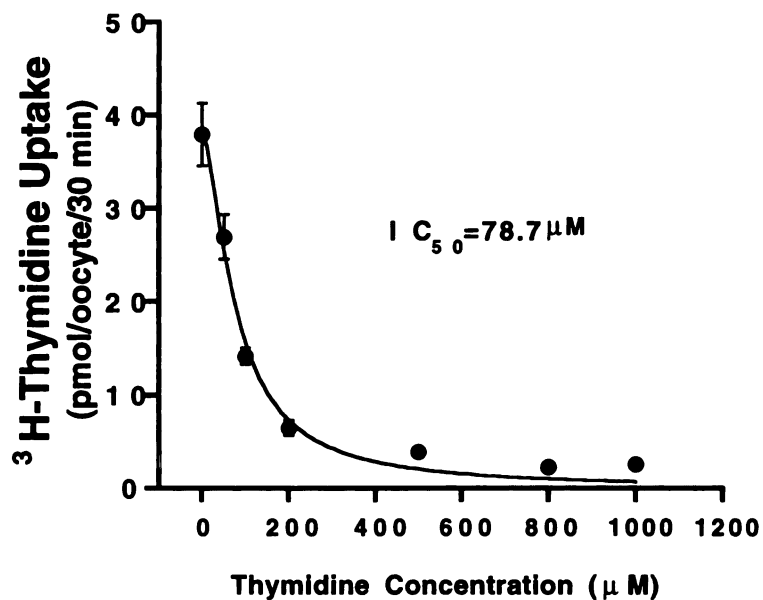


Figure 3. Inhibition studies of <sup>3</sup>H-thymidine uptake in *X. laevis* oocytes injected with the cRNA of rCNT1. Inhibition of <sup>3</sup>H-thymidine uptake was determined in the presence of unlabeled thymidine at various concentrations. Each point represents the mean  $\pm$  S.E. (n=8-10). The apparent IC<sub>50</sub> value was obtained by fitting the data to the equation  $V=V_0/(1+(I/IC_{50})^n)$ .

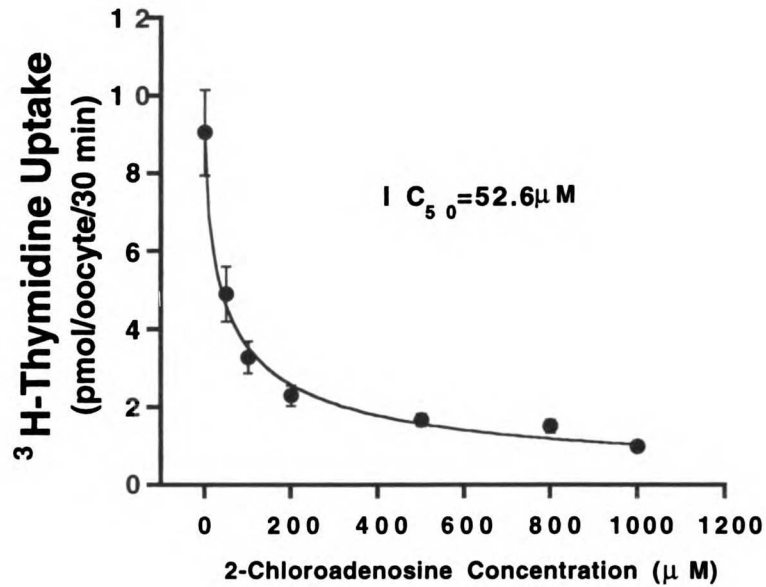


Figure 4. Inhibition studies of <sup>3</sup>H-thymidine uptake in *X. laevis* oocytes injected with the cRNA of rCNT1. Inhibition of <sup>3</sup>H-thymidine uptake was determined in the presence of unlabeled 2-chloroadenosine at various concentrations. Each point represents the mean  $\pm$  S.E. (n=8-10). The apparent IC<sub>50</sub> value was obtained by fitting the data to the equation  $V=V_0/(1+(I/IC_{50}))^n$ .

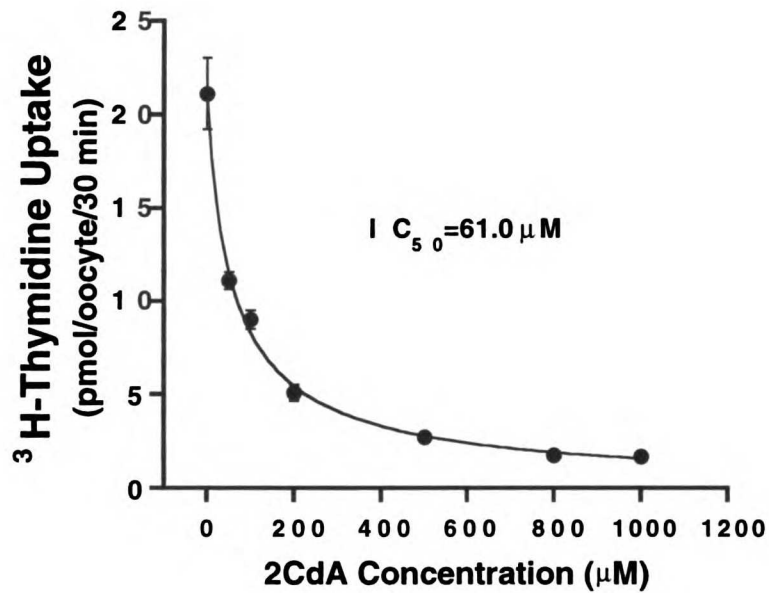


Figure 5. Inhibition studies of <sup>3</sup>H-thymidine uptake in *X. laevis* oocytes injected with the cRNA of rCNT1. Inhibition of <sup>3</sup>H-thymidine uptake was determined in the presence of unlabeled 2CdA at various concentrations. Each point represents the mean  $\pm$  S.E. (n=8-10). The apparent IC<sub>50</sub> value was obtained by fitting the data to the equation  $V=V_0/(1+(I/IC_{50})^n)$ .

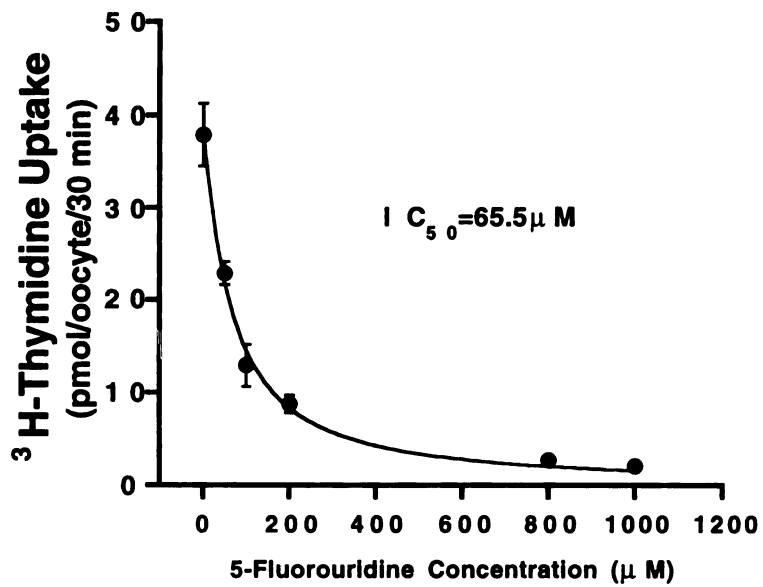


Figure 6. Inhibition studies of <sup>3</sup>H-thymidine uptake in *X. laevis* oocytes injected with the cRNA of rCNT1. Inhibition of <sup>3</sup>H-thymidine uptake was determined in the presence of unlabeled 5-fluorouridine at various concentrations. Each point represents the mean  $\pm$  S.E. (n=8-10). The apparent IC<sub>50</sub> value was obtained by fitting the data to the equation  $V=V_0/(1+(I/IC_{50}))^n$ .

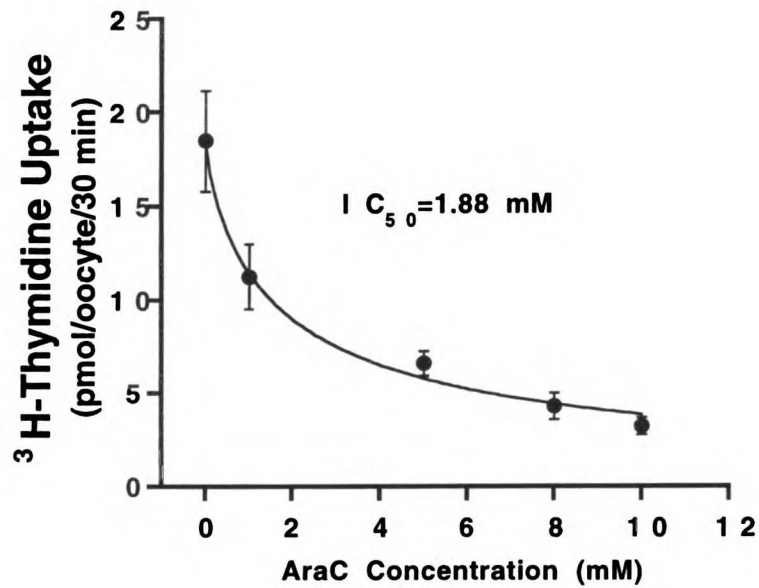


Figure 7. Inhibition studies of <sup>3</sup>H-thymidine uptake in *X. laevis* oocytes injected with the cRNA of rCNT1. Inhibition of <sup>3</sup>H-thymidine uptake was determined in the presence of unlabeled AraC at various concentrations. Each point represents the mean  $\pm$  S.E. (n=8-10). The apparent IC<sub>50</sub> value was obtained by fitting the data to the equation  $V=V_0/(1+(I/IC_{50})^n)$ .

**Table 3. Summary of IC<sub>50</sub> Values**

<b>Nucleoside Analog</b>	<b>IC<sub>50</sub> Value</b>
Thymidine	78.7 ± 8.7 μM
2-Chloroadenosine	52.6 ± 9.0 μM
2CdA	61.0 ± 5.3 μM
5-Fluorouridine	65.5 ± 6.6 μM
AraC	1.88 ± 0.36 mM

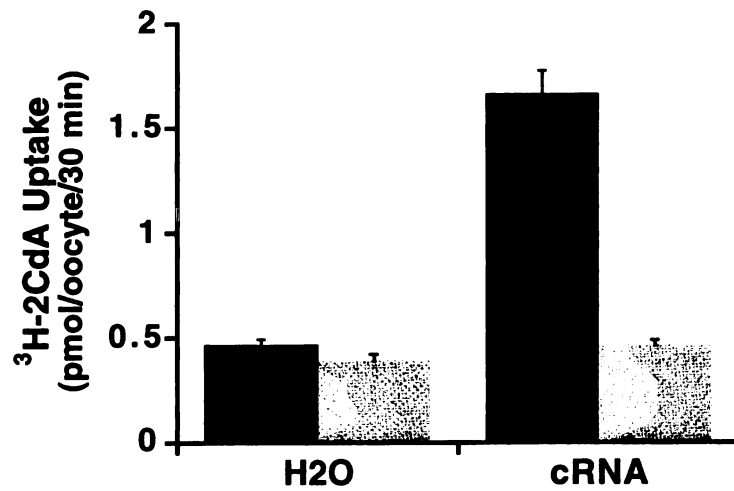


Figure 8. Uptake of <sup>3</sup>H-labeled 2CdA in oocytes injected with rCNT1 cRNA or H<sub>2</sub>O. Uptake was measured at 25°C in the presence (solid bars) and absence of Na<sup>+</sup> (gray bars). Data represent the mean ± S.E. of results from 8-10 oocytes.



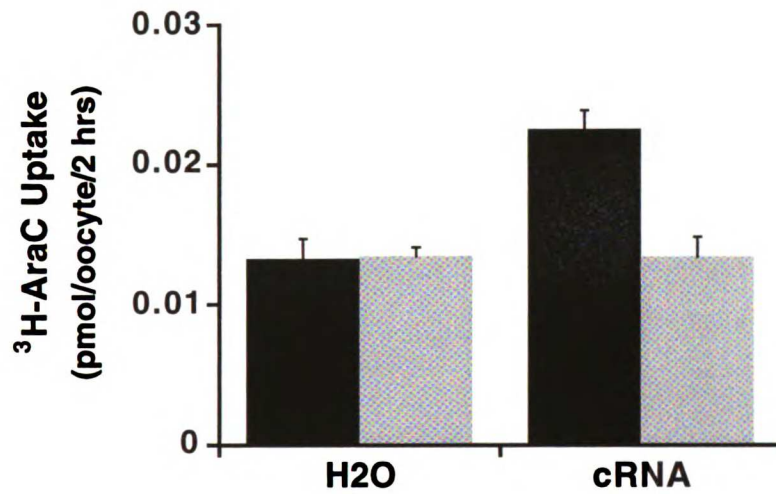


Figure 9. Uptake of <sup>3</sup>H-labeled AraC in oocytes injected with rCNT1 cRNA or H<sub>2</sub>O. Uptake was measured at 25°C in the presence (solid bars) and absence of Na<sup>+</sup> (gray bars). Data represent the mean ± S.E. of results from 8-10 oocytes.

WOLF LIBRARY  
11/18/17 10:30

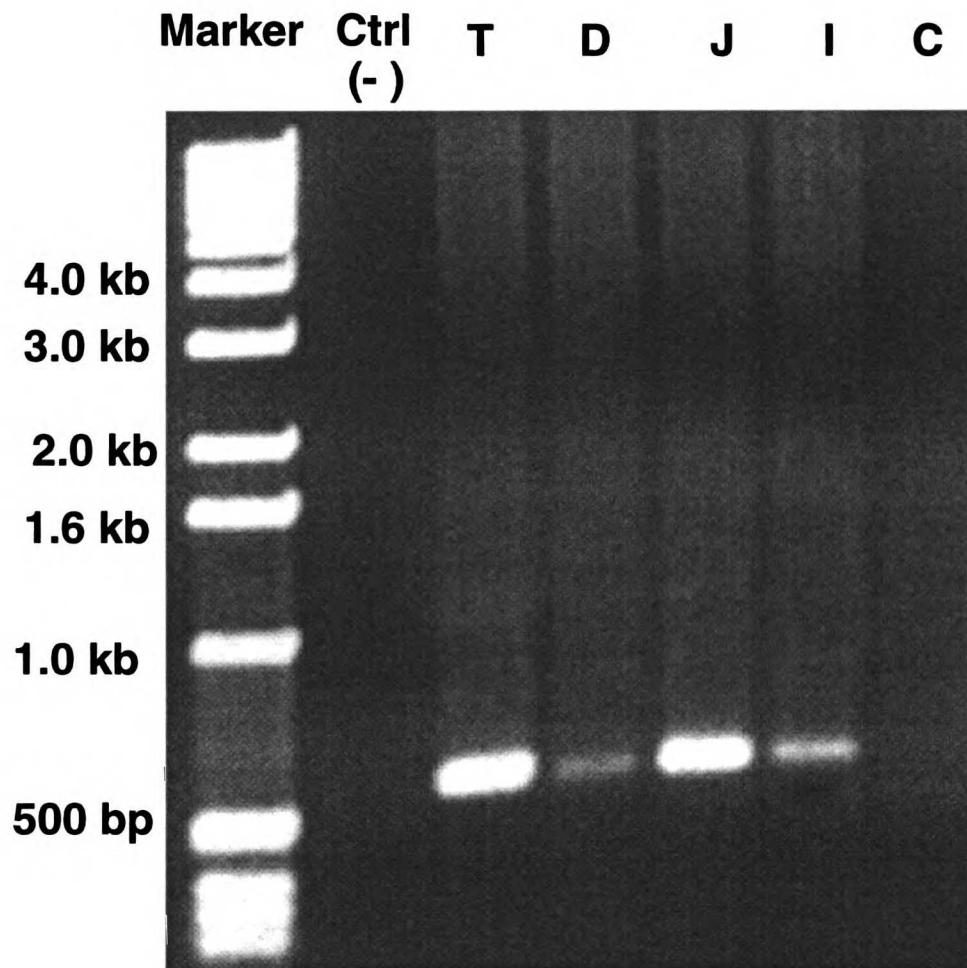


Figure 10. RT-PCR analysis of rCNT1 mRNA transcripts in the various regions of rat intestine. The RT-PCR product was separated by electrophoresis on a 1% agarose gel. Each lane represents a DNA product resulting from RT-PCR amplification of 10 ng mRNA isolated from total rat intestine (T), duodenum (D), jejunum (J), ileum (I), and colon (C). Ctrl (-) represents negative control in which no cDNA template was added to the PCR reaction mixture.

therapy since many nucleoside drugs are associated with low bioavailability and large inter- and intra- individual variations (Table 1). The epithelial cells in the intestine express several subtypes of nucleoside transporters (13-15) which precludes definitive identification of specific substrate selectivity due to substrate overlap within the system being studied. With the cloning of the rCNT1 transporter, it is now possible to gain a more detailed knowledge of the role of rCNT1 in intestinal nucleoside drug absorption by studying the cloned nucleoside transporter in heterologous expression systems. In addition, it is now possible to study the regional expression of this nucleoside transporter along the intestine.

In this study, we first investigated the role of rCNT1 in the absorption of clinically important nucleoside analogs. Using an RT-PCR based method, rCNT1 was cloned from rat intestine and was expressed in *X. laevis* oocytes (Figures 1-2). The interaction of rCNT1 with various nucleoside drugs was first determined by inhibition studies. Our data suggest that 2-chloroadenosine, 2CdA, and 5-fluorouridine may interact with rCNT1 potently *in vivo* (Tables 2 and 3). AraC interacts with rCNT1 less potently ( $IC_{50} = 1.88$  mM). However, millimolar luminal concentrations of drugs may be achieved in the intestine after oral doses. This is clinically important in combination therapy with nucleoside analogs because co-administration of several nucleoside analogs may alter the bioavailability of each individual drug. The data suggested that rCNT1 does not play a role in the absorption of ddC, ddI, ddA, AZT, and acyclovir (Table 2).

Recently, Fang *et al.* demonstrated that AraC significantly inhibited  $^3H$ -uridine uptake in COS-1 cells transiently transfected with the cDNA of rCNT1 (16). Their data are in agreement with our observation that AraC significantly inhibited rCNT1-mediated  $^3H$ -thymidine uptake. However, they also observed significant inhibition of  $^3H$ -uridine uptake by AZT and ddC. Yao *et al.* also demonstrated that rCNT1 accepts the antiviral pyrimidine analogs, AZT and ddC, as permeants in the oocyte expression system ( $K_m = 0.49$  and  $0.51$  mM, respectively) (17). In contrast, in our system, we observed negligible

inhibition of thymidine uptake by these two compounds. The reasons for these discrepancies are unknown, but may be due to the difference of permeants used in the inhibition studies (thymidine versus uridine) and other differences in the experimental conditions. Therefore, whether ddC and AZT interact with rCNT1 needs further investigation.

The inhibition studies revealed that 2CdA and AraC produced a concentration-dependent inhibition of Na<sup>+</sup>-dependent thymidine uptake in the oocytes (Figures 5 and 7). 2CdA has been used effectively in the treatment of hairy cell leukemia, chronic lymphocytic leukemia, and cutaneous T-cell lymphoma. AraC has long been used as a successful antineoplastic agent. Because of their clinical importance, we further investigated whether 2CdA and AraC are true substrates of rCNT1 using radio-labeled 2CdA and AraC (Figures 8-9). Significant Na<sup>+</sup>-dependent uptake of [<sup>3</sup>H]2CdA (Figure 8) and [<sup>3</sup>H]AraC (Figure 9) was observed, suggesting that 2CdA and AraC are true permeants of rCNT1. These data suggest that rCNT1 transporters in the intestine may play an important role in the absorption of some clinically used base- and ribose-modified nucleoside analogs.

Although rCNT1 was cloned from rat intestine, the distribution of this transporter along the intestine was unclear. To address this question, our laboratory employed an RT-PCR based method to detect the regional distribution of the rCNT1 mRNA. Using this method, we detected strong expression of rCNT1 mRNA in rat jejunum, moderate expression in duodenum and ileum, and no expression in colon (Fig. 5). These data suggest that rCNT1 mediated intestinal transport may occur primarily in the jejunum but also in duodenum and ileum. Interestingly, our results are consistent with functional studies in brush border membrane vesicles prepared from different regions of human intestine (18). The direct analysis of the regional distribution and membrane location of the rCNT1 transport protein (rather than the mRNA transcript) awaits the use of rCNT1 specific antibodies.

In summary, a functional N2 clone, rCNT1, was isolated from rat intestine. The mRNA transcript of rCNT1 is detected in duodenum, jejunum, ileum, but not in colon. rCNT1 interacts with several clinically important nucleoside analogs and accepts the anticancer drugs 2CdA and AraC as permeants. rCNT1 may play an important role in the intestinal absorption of some therapeutic nucleoside analogs, and the absorption may occur largely in jejunum and to a lesser extent in duodenum and ileum.

## References

1. Drusano, G. L., G. J. Yuen, G. Morse, T. P. Cooley, M. Seidlin, J. S. Lambert, H. A. Liebman, F. T. Valentine, and R. Dolin. Impact of bioavailability on determination of the maximal tolerated dose of 2',3'-dideoxyinosine in phase I trials. *Antimicrob Agents Chemother* **36**:1280-3 (1992).
2. Boudinot, F. D., R. F. Schinazi, K. J. Doshi, H. M. McClure, and C. K. Chu. Pharmacokinetics and metabolism of 3'-azido-2',3'-dideoxy-5-methylcytidine in rhesus monkeys. *Drug Metab Dispos* **21**:855-60 (1993).
3. Schinazi, R. F., F. D. Boudinot, K. J. Doshi, and H. M. McClure. Pharmacokinetics of 3'-fluoro-3'-deoxythymidine and 3'-deoxy-2',3'-didehydrothymidine in rhesus monkeys. *Antimicrob Agents Chemother* **34**:1214-9 (1990).
4. Waclawski, A. P., and P. J. Sinko. Oral absorption of anti-acquired immune deficiency syndrome nucleoside analogues. 2. Carrier-mediated intestinal transport of stavudine in rat and rabbit preparations. *J Pharm Sci* **85**:478-85 (1996).
5. Cass, C. E. Nucleoside transport, in *Drug Transport in Antimicrobial and Anticancer Chemotherapy*. (N. H. Georgopapadakou, ed.) pp.403-451, Marcel Dekker, New York (1995).
6. Griffith, D. A., and S. M. Jarvis. Nucleoside and nucleobase transport systems of mammalian cells. *Biochim Biophys Acta* **1286**:153-81 (1996).

7. Wang, J., M. E. Schaner, S. Thomassen, S. F. Su, M. Piquette-Miller, and K. M. Giacomini. Functional and molecular characteristics of Na(+)-dependent nucleoside transporters. *Pharm Res* **14**:1524-32 (1997).
8. Patil, S. D., and J. D. Unadkat. Sodium-dependent nucleoside transport in the human intestinal brush-border membrane. *Am J Physiol* **272**:G1314-20 (1997).
9. Huang, Q. Q., C. M. Harvey, A. R. Paterson, C. E. Cass, and J. D. Young. Functional expression of Na(+)-dependent nucleoside transport systems of rat intestine in isolated oocytes of *Xenopus laevis*. Demonstration that rat jejunum expresses the purine-selective system N1 (cif) and a second, novel system N3 having broad specificity for purine and pyrimidine nucleosides. *J Biol Chem* **268**:20613-9 (1993).
10. Jarvis, S. M. Characterization of sodium-dependent nucleoside transport in rabbit intestinal brush-border membrane vesicles. *Biochim Biophys Acta* **979**:132-8 (1989).
11. Huang, Q. Q., S. Y. Yao, M. W. Ritzel, A. R. Paterson, C. E. Cass, and J. D. Young. Cloning and functional expression of a complementary DNA encoding a mammalian nucleoside transport protein. *J Biol Chem* **269**:17757-60 (1994).
12. Yao, S. Y., A. M. Ng, M. W. Ritzel, W. P. Gati, C. E. Cass, and J. D. Young. Transport of adenosine by recombinant purine- and pyrimidine-selective sodium/nucleoside cotransporters from rat jejunum expressed in *Xenopus laevis* oocytes. *Mol Pharmacol* **50**:1529-35 (1996).
13. Plagemann, P. G., and J. M. Aran. Na(+)-dependent, active nucleoside transport in mouse spleen lymphocytes, leukemia cells, fibroblasts and macrophages, but not in

equivalent human or pig cells; dipyridamole enhances nucleoside salvage by cells with both active and facilitated transport. *Biochim Biophys Acta* **1025**:32-42 (1990).

14. Roovers, K. I., and K. A. Meckling-Gill. Characterization of equilibrative and concentrative Na<sup>+</sup>-dependent (cif) nucleoside transport in acute promyelocytic leukemia NB4 cells. *J Cell Physiol* **166**:593-600 (1996).

15. Belt, J. A., N. M. Marina, D. A. Phelps, and C. R. Crawford. Nucleoside transport in normal and neoplastic cells. *Adv Enzyme Regul* **33**:235-52 (1993).

16. Fang, X., F. E. Parkinson, D. A. Mowles, J. D. Young, and C. E. Cass. Functional characterization of a recombinant sodium-dependent nucleoside transporter with selectivity for pyrimidine nucleosides (cNT1rat) by transient expression in cultured mammalian cells. *Biochem J* **317**:457-65 (1996).

17. Yao, S. Y., C. E. Cass, and J. D. Young. Transport of the antiviral nucleoside analogs 3'-azido-3'-deoxythymidine and 2',3'-dideoxycytidine by a recombinant nucleoside transporter (rCNT) expressed in *Xenopus laevis* oocytes. *Mol Pharmacol* **50**:388-93 (1996).

18. Chandrasena, G., S. Patil, R. Giltay, A. Bakken, and J. D. Unadkat. Functional characterization of Na<sup>+</sup>-dependent and Na<sup>+</sup>-independent human intestinal nucleoside transporters expressed in *Xenopus laevis* oocytes. *Pharm. Res.* **13**:S-410 (Abstr.) (1996).



## CHAPTER 3

### MOLECULAR MECHANISM OF PURINE NUCLEOSIDE TRANSPORT IN HUMAN KIDNEY<sup>1</sup>

Purine nucleosides and their analogs are widely being used and developed for the treatment of cardiac disease, cancer and viral infections. Despite extensive studies of the therapeutic activity of purine nucleosides, little is known about the renal handling of these compounds. Nephrotoxicity is one of the limiting toxicities of some purine nucleoside analogs and has been observed in deoxycoformycin and tubercidin therapy in humans (1, 2). Thus, understanding the mechanisms by which the kidney transports purine nucleosides is essential in rational drug therapy and development.

Previous clinical studies indicate that purine nucleosides are actively transported in the human kidney (3). In mammalian cells, several subtypes of Na<sup>+</sup>-dependent secondary active nucleoside transporters have been described including a purine selective nucleoside transporter, N1 (4), a pyrimidine selective nucleoside transporter, N2 (4, 5), and several broadly-selective nucleoside transporters (N3 and N4) (6, 7). Recently, an N1-type transporter, SPNT, was cloned from a rat liver cDNA library (8), and an N2-type transporter, rCNT1, was cloned from a rat intestine cDNA library (9). Interestingly, Northern analysis (8) and RT-PCR studies in our laboratory demonstrated that the mRNA transcript of SPNT was not expressed in the rat kidney indicating that this transporter does not play a role in the renal transport of purine nucleosides in the rat.

---

<sup>1</sup> Most of this chapter was published in a manuscript entitled: Na<sup>+</sup>-dependent purine nucleoside transporter from human kidney: cloning and functional characterization. *American Journal of Physiology* 273(6 Pt 2): F1058-65, 1997.

Recently, a human homolog of rCNT1, termed hCNT1, was cloned from human kidney providing the first evidence that pyrimidine selective transporters are present in human kidney (10). However, it is not known whether the purine selective transporters are present in human kidney. In this study, we cloned and functional characterized a Na<sup>+</sup>-dependent purine-selective transporter hSPNT1 in human kidney. The many unique features of hSPNT1 suggest that this transporter may play a critical role in the specific uptake and salvage of purine nucleosides in human kidney and other human tissues. This study provides the first molecular evidence of a Na<sup>+</sup>-purine nucleoside transporter in humans .

## **Materials and Methods**

*cDNA Cloning and Analysis.* Two nondegenerate primers, spnt1 (5'-GTGAT GTCTATTCTCTACTACCTGGGCCTTGTG-3') and spnt2 (5'-CCCTATGGAAGTAG ATTGGCAAATCC ACAGAG -3' ), derived from rat SPNT corresponding to conserved regions VMSILYYLGLV and LCGFANLTSIGITLG (8) were used in PCR to amplify sequences of nucleoside transporters from human kidney cDNA under the following conditions: 94°C for 1 min, 50°C for 1.5 min, 72°C for 2 min , 30 cycles followed by a final 15 min incubation at 72°C. A PCR product of 0.8 kb (hNT1) was obtained and DNA sequencing of hNT1 showed 88% identity to rat SPNT cDNA. To obtain the 5' and 3' portions of the full length cDNA, 5' RACE and 3' RACE System for Rapid Amplification of cDNA Ends (RACE) (Gibco-BRL) was used according to the manufacture's protocol. A 1.6 kb 3' RACE product was obtained after two rounds of amplification with the adapter primer and nested primers derived from hNT1. The sequence of this 1.6 kb fragment overlapped with hNT1 and contained a 15-bp poly (A)<sup>+</sup> tail. A 1.0 kb 5' RACE product was obtained after two rounds of amplification with the anchor primer and nested primers. This 1.0 kb fragment overlapped with hNT1 and

contained a 5' untranslated sequence as indicated by alignment with rat SPNT cDNA. The full clone was obtained by RT-PCR using a primer spanning nucleotides (nt) 10-33 of the 5' RACE product and a primer before the poly (A)<sup>+</sup> tail of the 3' RACE product. The full-length cDNA fragment, termed hSPNT1, was subcloned into pGEM-T vectors (Promega) and oriented under the control of the T7 promoter. At least three clones from independent PCR reactions were sequenced. The open reading frames of all sequenced clones were identical except for a T to C change at position 124 in one clone which corresponded to a change of Pro22 to Leu22. Either Ex-Taq (TaKaRa Shuzo Co Japan) or Pfu (Stratagene) DNA polymerase was used in PCR to increase the fidelity of the reactions. DNA was sequenced at the Biochemical Resource Center at the University of California, San Francisco, using an automated DNA sequencer (Applied Biosystems). BLAST network at the NCBI was used in data base searching, and the Genetics Computer Group software package (Wisconsin Package) was used to analyze nucleotides and the deduced amino acid sequences.

*Expression in Xenopus laevis oocytes and nucleoside uptake assays.* hSPNT1 cRNA was synthesized and injected into defolliculated oocytes. Uptake activity reached a maximum after a two day incubation at 18°C. All uptake experiments were carried out with the respective <sup>3</sup>H-labeled nucleoside (Moravek Biochemicals) 48-56 hour post-injection at 25°C in transport buffer containing 100 mM NaCl or 100 mM choline chloride. In kinetic studies, the apparent K<sub>m</sub> and V<sub>max</sub> values were determined by fitting the data to the Michaelis-Menten equation by non-linear regression. The IC<sub>50</sub> was determined by fitting the data to the equation  $V=V_o/(1+(I/IC_{50}))^n$ , where V is the uptake of inosine in the presence of the inhibitor, V<sub>o</sub> is the uptake of inosine in the absence of inhibitor, I is the inhibitor concentration and n is the slope. Assuming a competitive mechanism of inhibition, the K<sub>i</sub> was determined by the equation  $K_i = IC_{50}/(1+C/K_m)$ ,

where  $C$  represents the concentration of inosine,  $K_m$  represents the apparent  $K_m$  of inosine uptake.

*Northern Blot Analysis.* A biotin-labeled antisense RNA probe of hSPNT1 corresponding to amino acid residues 27-300 was synthesized and hybridized to a commercial human multiple tissue blot (Clontech) at 68°C overnight and detected using the BrightStar Nonisotopic Detection System (Ambion) followed by membrane exposure to Hyperfilm-ECL film. In addition, 3 µg of human small intestine poly(A)<sup>+</sup> RNA was fractionated on a formaldehyde-agarose gel, transferred to nylon membrane (Ambion) and hybridized to the probe. The quality and quantity of the poly (A)<sup>+</sup> RNA of each tissue loaded on the blot was checked by stripping the membrane and re-probing with a human β-actin cDNA probe.

*Chromosome localization.* Chromosome localization was performed by Research Genetics using radiation hybrid mapping methods (12, 13). A GeneBridge 4 Panel containing 93 radiation hybrid clones of human and hamster cells was screened by PCR in a 96-well cycle plate under standard screening conditions. The primers (sense, 5'-GAGGAGCCAGAGGGAATCAA TTCC-3' ; antisense, 5'-CTCCTCCTCTGGTAAG TGGAAGGGCCCAGTCCATC-3') used in the reaction were derived from the 5' region of the hSPNT1 cDNA. A single hSPNT1 gene-specific PCR product, which was further confirmed by DNA sequencing, was generated when using human genomic DNA as a template, whereas no product was detected when using hamster genomic DNA as the template. The presence or absence of this gene marker in each hybrid cell line was scored by the presence or absence of the PCR product from three independent PCR reactions. The scores were then linked to the data base of Whitehead radiation hybrid framework map at the MIT Center for Genome Research, and the position of the gene marker was localized on the framework map.

## Results

*Nucleotide and Deduced Amino Acid Sequences of hSPNT1.* Excluding the poly (A)<sup>+</sup> tail, the exact length of the hSPNT1 cDNA is 2,459 bp with an open reading frame of 1,977 bp. The open reading frame encodes a protein of 658 amino acids, and is flanked by 59 bp 5' UTR and 423 bp 3' UTR (Fig. 1). The predicted initiation codon is preceded by a Kozak consensus sequence (A/GXXATG) (14). Two in-frame upstream stop codons further suggest that the ATG at position 60 is the translation initiation site. The encoded protein has a calculated molecular mass of 72 kDa and an isoelectric point of 7.93. Hydropathy analysis of the primary amino acid sequence suggested the presence of 14 putative membrane spanning segments. The N- and C- termini were predicted to be intracellular and the 14 putative transmembrane domains were assigned by a combination of Kyte-Doolittle hydropathy analysis (15), application of the positive-inside rule (16) and multiple sequence alignment analysis of hSPNT1 and its related rat transporters rCNT1 and SPNT. There are six possible N-linked glycosylation sites (Asn-238, -538, -600, -605, -624, -and 653). However, none of these sites is predicted to be extracellular, therefore none will be glycosylated if the membrane topology prediction of hSPNT1 is correct. There are six potential protein kinase C phosphorylation sites (Ser-5, -36, -198, -376, -522, and Thr-604). Except Ser-376, all of the other sites are predicted to be intracellular, and therefore may be substrates of protein kinase C. The 3' UTR of hSPNT1 contains an *Alu* repetitive element (nt 2177-2458) (Fig. 1). Alignment with *Alu* consensus sequences shows it shares the highest identity (92%) with the *Alu*-Sb subfamily, one of the several subfamilies of human *Alu* genes.

hSPNT1 is one amino acid shorter than rat SPNT, and shares 81% identity with the rat liver SPNT. The most divergent region between hSPNT1 and rat SPNT resides in the N-terminal region. Less than 50% identity was observed in the first 63 amino acids located in



```

1 50
hcNT1a MENDPSRRRE SISLTPVAKG LENMGADFLE SLEGGQLPRS DLSPAEIRS.
rCNT1a MADNTQRQRE SISLTPMAHG LENMGAEPLE SMEEGR LPHS HSSLPEGEG.
hSPNT1a .MEKASGRQ SIALSTVETG TVNPG...LE LME.KEVEPE GSKRRTDAQGH
SPNT .MAKSEGRK SASQDTSSENG MENPG...LE LMEVGNLEGGKTLEEVTDQGH

51 100
hcNT1a SWSEAAPKPF SRWRNLQPAL RARSFCREHM QLFRWIGTGL LCTGLS AFLL
rCNT1a GLNKAERKAF SRWRSLQPTV QARSFCREHR QLPGWICKGL LSTACLGFLLM
hSPNT1a SLGDGLGPST YQRRSRWPFK KARSFCKTHA RLFKKILLGL LCLAYAAAYLL
SPNT SLKDGGLGHSS LWRRILQPFT KARSFYQRHA GLFKKILLGL LCLAYAAAYLL

101 150
hcNT1a VACLLDFQRA LALFVLTVCV LTFLGHRLLK RLLGPKLRRF LVKPPQGHPRL
rCNT1a VACLLDLQRA LALLIITCVV LVFLAYDLLK RLLGSKLRRC .VKFQGHSC
hSPNT1a AACILNFQRA LALFVITCLV IFVLVHVSFLK KLLGKLLTRC .LKPFFENSRL
SPNT AACILNFRRA LALFVITCLV IFILACHFLK KFFAKKSIRC .LKPLKNTRL

151 200
hcNT1a LLWFKRGLAL AAFLGLVLWL SLDTSORPEQ LVSFAGICVF VALLFACSKH
rCNT1a SLWLKRGLAL AAGVGLLWL SLDTAQRPEQ LVSFAGICVF LVLLFAGSKH
hSPNT1a RLWTKWFVAG VSLVGLLWL ALDTAQRPEQ LIPFAGICMF ILILFACSKH
SPNT RLWLRKRVFMG AAVVGLLWL ALDTAQRPEQ LISFAGICMF ILILFACSKH

201 250
hcNT1a HCAVSWRAVS WGLGLQFVLG LLVIRTEPGF IAPEWLGEQI RIFLSYTKAG
rCNT1a HRAVSWRAVS WGLGLQFVLG LRVIRTEPGF IAPQWLGDQI QVPLSYTEAG
hSPNT1a HSAVSWRTVF SGLGLQFVFG ILVIRTDLGY TVFQWLGEQV QIFLNYTVAG
SPNT HSAVSWRTVF WGLGLQFVFG ILVIRTEPGF NAFQWLGDQI QIFLAYTVEG

251 300
hcNT1a SSFVFGAALV KDVFAFQVLP IIVFFSCVIS VLYHVGLMQW VILKIAWLMQ
rCNT1a SSFVFGAALV KDVFAFQVLP IIVFFSCVMS VLYYLGLMQW VILKIAWLMQ
hSPNT1a SSFVFGDTLV KDVFAFQALP IIVFFGCVVS ILYYLGLVQW VVQKVAWFLQ
SPNT SSFVFGDTLV QSVFAFQSLP IIVFFGCVMS ILYYLGLVQW VIQKIAWFLQ

301 350
hcNT1a VTMGTATATET LSVAGNIFVS QTEAPLLIRP YLADMTLSEV HVVMTGGYAT
rCNT1a VTMGTSATET LSVAGNIFVS QTEAPLLIRP YLADMTLSEV HVVMTGGYAT
hSPNT1a ITMGTATATET LAVAGNIFVG MTEAPLLIRP YLADMTLSEI HAVMTGGFAT
SPNT ITMGTAAET LAVAGNIFVG MTEAPLLIRP YLADMTLSEI HAVMTGGFAT

351 400
hcNT1a IAGSLLGAYI SFGIDATSLI AASVMAAPCA LALSCLVYPE VEESKFRREE
rCNT1a IAGSLLGAYI SFGIDAASLI AASVMAAPCA LALSCLVYPE VEESKFRSEN
hSPNT1a ISGTVLGAFI AFGVDASSLI SASVMAAPCA LASSKLAYPE VEESKFKSEE
SPNT IAGTVLGAFI SFGIDASSLI SASVMAAPCA LALSCLVYPE VEESKFKSKE

401 450
hcNT1a GVKLTYGDAQ NLIEAASGA AISVKVANI AANLIAFLAV LDFINAALSW
rCNT1a GVKLTYGDAQ NLLEAASAGA AISVKVANI AANLIAFLAV LAFVNAALSW
hSPNT1a GVKLPRGKER NVLEAASNGA VDAIGLATNV AANLIAFLAV LAFINAALSW
SPNT GVKLPRGEER NILEAASNGA TDAIALVANV AANLIAFLAV LAFINSTLSW

451 500
hcNT1a LGDMVDIQGL SFQLICSYIL RPVAFMLGVA WEDCPVVAEL LGIKLFLNEF
rCNT1a LGDMVDIQGL SFQLICSYVL RPVAFMLGVA WEDCPVVAEL LGIKFPLNEF
hSPNT1a LGELVDIQGL TFQVICSYLL RPMVFMGVE WDCPMVAEM VGIRKFFINEF
SPNT LGEMVDIHGL TFQVICSYVL RPMVFMGQV WADCPVAEI VGVKFFINEF

501 550
hcNT1a VAYQDLSKYK QRRLAGAEW VGDRKQWISV RAEVLTTFAL CGFANFSSIG
rCNT1a VAYQELSQYK QRRLAGAEW LGDKKQWISV RAEILTYAL CGFANFSSIG
hSPNT1a VAYQDLSQYK NKRLSGMEW IEGEKQWISV RAEIITFSL CGFANLSSIG
SPNT VAYQDLSQYK NKRLSGVEW INGEKQWISV RAEIATFSL CGFANLTSIG

551 600
hcNT1a IMLGGLTSMV PQRKSDFSQI VLRALFTGAC VSLVNACMAG ILYMPRGAEV
rCNT1a IMLGGLTSLV PQRKSDFSQI VLRALITGAF VSLLNACVAG ILYVPRGVEV
hSPNT1a ITLGGTSLV PHRKSDDLK VVRALFTGAC VSLISACMAG ILYVPRGAEV
SPNT ITLGGTSMV PQRKSDLCKL VVRALFTGAC VSFISACMAG ILYVPRGAET

601 650
hcNT1a DCMSLLNNTL SSSSFEIYQC CREAQSV... .NPEFSPE
rCNT1a DCVSLLNQTV SSSSFEVYLC CRQVFQST... .SSEFSQV
hSPNT1a DCVSPNTSF TNRTYETVMC CRGLFQSTSL NGTNPPSFSG PWEDKEFSAM
SPNT DCVSFLNTNF TNRTYETVVC CRELFQSTLL NGTNMPSFSG PWQDKESSLR

651 666
hcNT1a ALDNCCRFYN HTICAQ
rCNT1a ALDNCCRFYN HTVCT.
hSPNT1a ALTNCCGFYN NTVCA.
SPNT NLAACCDLYT STVCA.

```

Figure 2. Alignment of amino acid sequence of hSPNT1, SPNT, hcNT1 and rCNT1. Amino acids are presented in their single letter codes. Periods indicate the gaps introduced to generate the alignment. The ATP/GTP binding motif (GXXXXGKT) in rat SPNT is indicated in bold.

the predicted N-terminal intracellular region, whereas more than 84% identity was observed in the remaining regions (amino acids 64-658). An important difference in the N-terminus is that the rat SPNT possesses an ATP/GTP binding motif (GXXXXGKT) whereas hSPNT1 does not (Fig. 2). Comparison with protein sequences in the data base shows that hSPNT1, similar to SPNT, shares significant homology with the pyrimidine selective transporter hCNT1 and its rat homolog rCNT1 (Fig. 2) (8-10).

*Functional Expression and Characterization of hSPNT1.* The uptake of inosine, a model purine, in *Xenopus laevis* oocytes two days after injection was dependent on the injected dose of cRNA in a saturable manner (Fig. 3). Because maximal expression was obtained at cRNA doses of 10-40 ng, a 20 ng dose of cRNA was used in all subsequent studies to ensure maximum expression. Compared to water injected oocytes, a 35-fold increase in the uptake of <sup>3</sup>H-inosine (at 30 min) was observed in cRNA-injected oocytes. <sup>3</sup>H-inosine uptake driven by the Na<sup>+</sup> gradient (extracellular concentration kept constant at 100 mM) was linear up to 3 hours (Fig. 4).

Inhibition studies with various purine and pyrimidine nucleosides demonstrated that <sup>3</sup>H-inosine (12 μM) uptake was almost completely inhibited by (1 mM) adenosine, guanosine, and uridine but only slightly by cytidine and thymidine (Fig. 5). Formycin B, a purine derivative, also significantly inhibited the uptake activity, however it appeared to have a lower inhibition potency than the other purines. Hypoxanthine, a nucleobase, did not inhibit the uptake (Fig. 5). Uptake studies with <sup>3</sup>H-thymidine demonstrated that hSPNT1 did not transport thymidine to a significant extent (Fig. 6). These data suggest that hSPNT1 is a functional human Na<sup>+</sup>-dependent purine selective nucleoside transporter that belongs to the N1 subtype, and differs from the previously characterized brush border membrane transporter, N4, and the recently cloned N2 subtype, hCNT1, in human kidney (7, 10).

Although hSPNT1 exhibits purine selectivity, it also transports the pyrimidine,



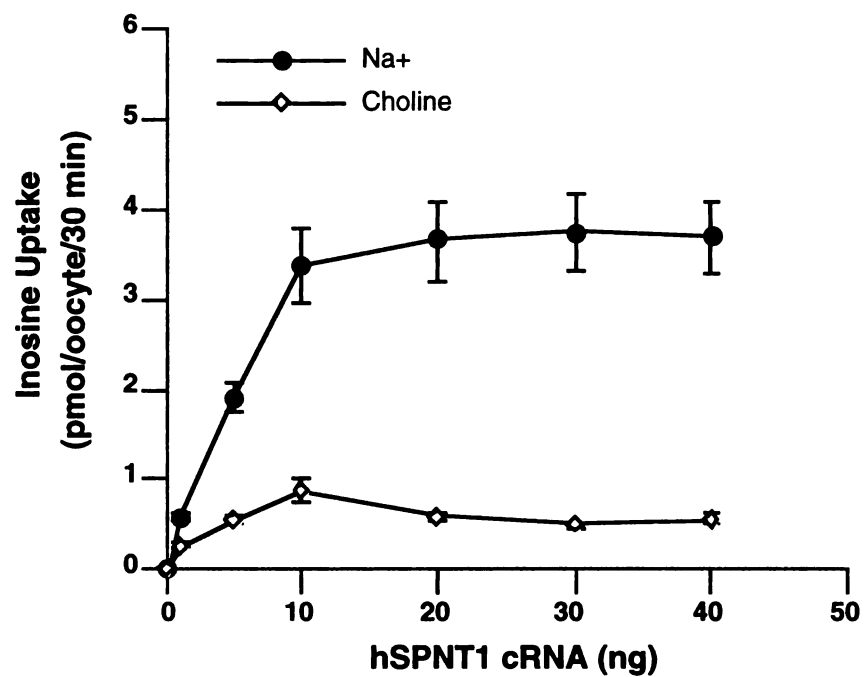


Figure 3. cRNA dose-dependent uptake. Oocytes were injected with 1, 5, 10, 20, 30, 40 ng of hSPNT1 cRNA. Uptake of 10 mM of  $^3\text{H}$ -inosine was measured at 25°C in the presence of sodium or choline. Each value represents the mean  $\pm$  S.E. from 8-10 oocytes.

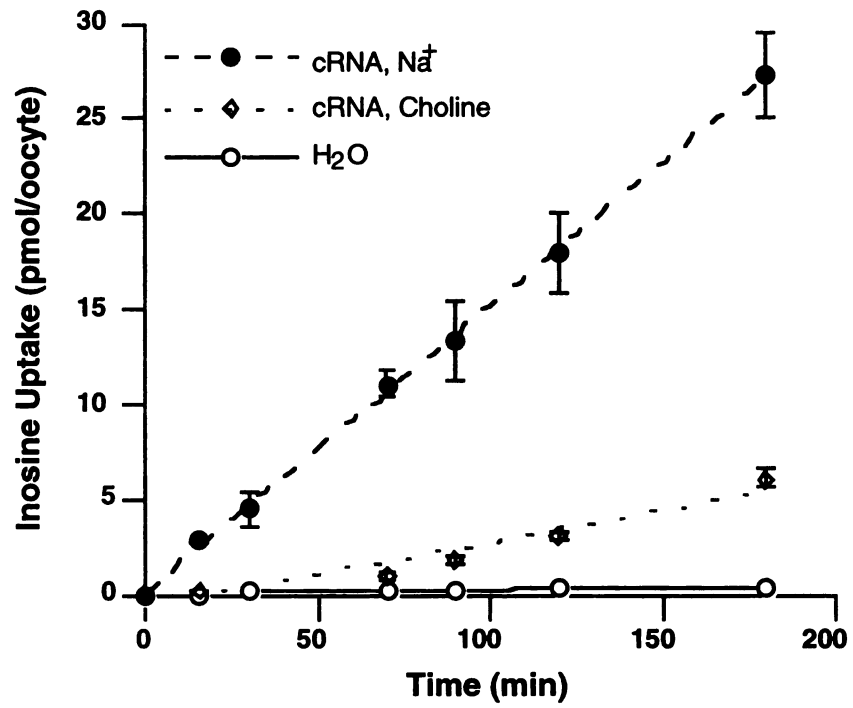
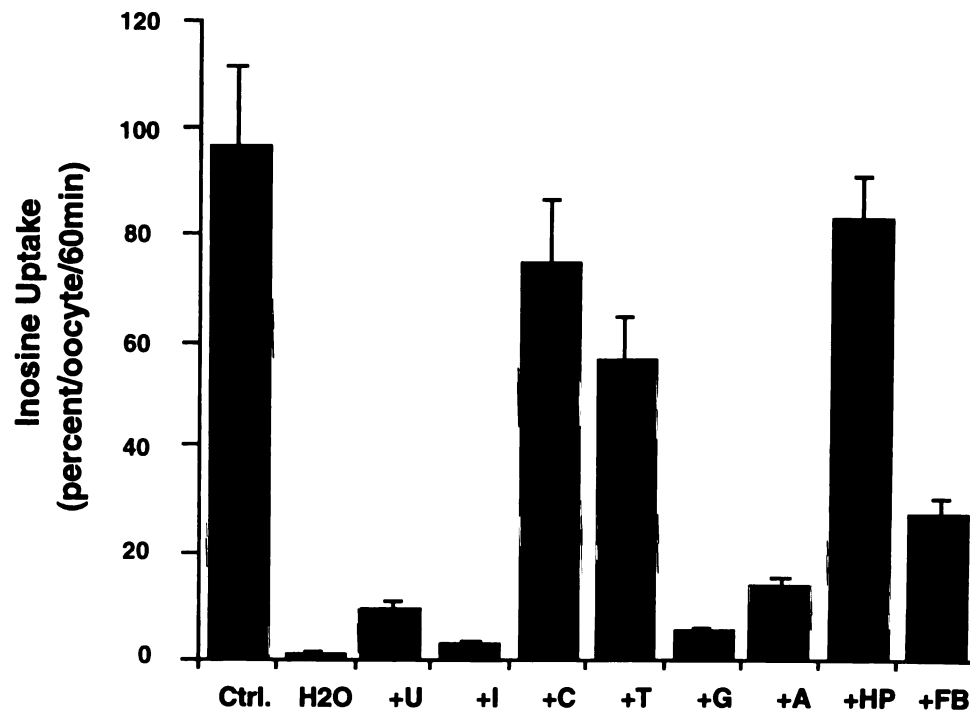
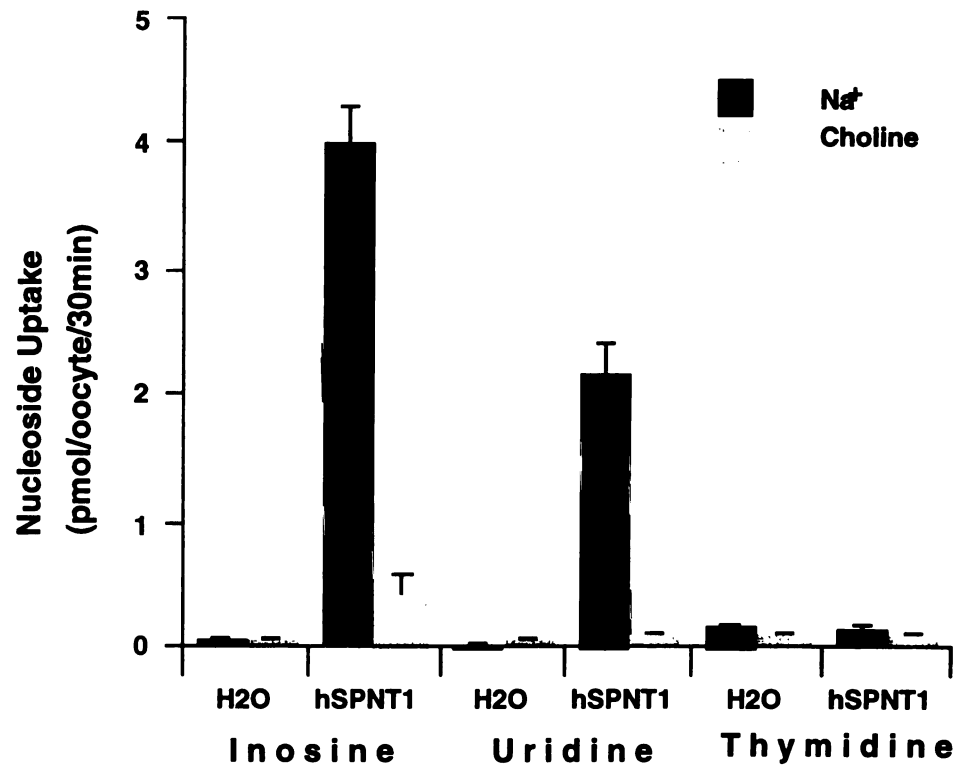


Figure 4. Time course of <sup>3</sup>H-inosine uptake. Each value represents the mean ± S.E. from 8-10 oocytes.



**Figure 5.** Effects of nucleoside and nucleoside analogs on  $^3\text{H}$ -inosine uptake in oocytes injected with hSPNT1 cRNA. Uptake was determined in sodium buffer in the presence and the absence (ctrl., as control) of 1 mM of various compounds (U, uridine; I, inosine; C, cytidine; T, thymidine; G, guanosine; A, adenosine; HP, hypoxanthine; FB, formycin B). Each value represents the mean  $\pm$  S.E. from 8-10 oocytes.



**Figure 6.** Uptake of <sup>3</sup>H-inosine, <sup>3</sup>H-uridine and <sup>3</sup>H-thymidine. Each value represents the mean ± S.E. from 8-10 oocytes.

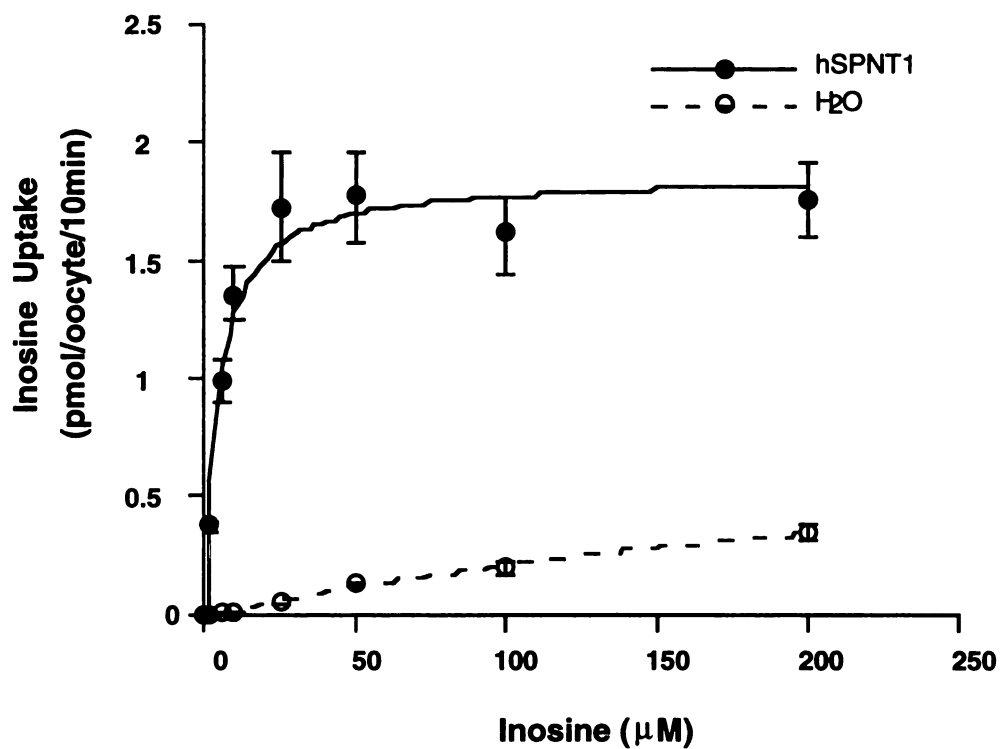


Figure 7. Michaelis-Menten studies of inosine uptake. Each point represents the mean  $\pm$  S.E. (n=8-10) from one representative experiment. Apparent  $K_m$  and  $V_{max}$  values were determined by fitting the data to the Michaelis-Menten equation.

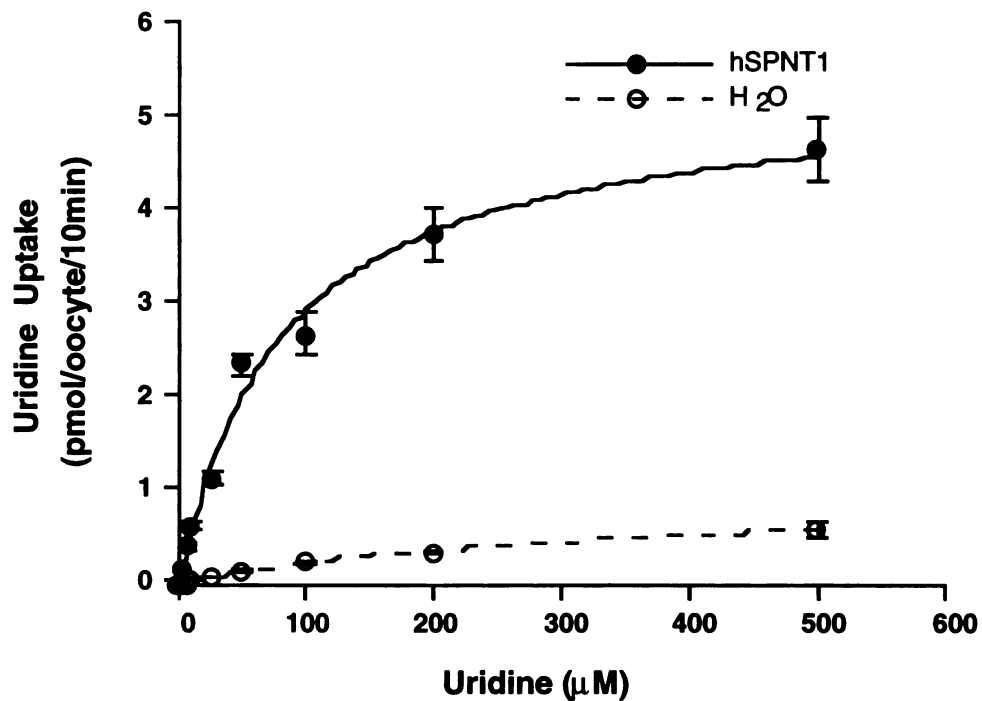


Figure 8. Michaelis-Menten studies of uridine uptake. Each point represents the mean  $\pm$  S.E. (n=8-10) from one representative experiment. Apparent  $K_m$  and  $V_{max}$  values were determined by fitting the data to the Michaelis-Menten equation.

uridine (Fig. 6). To investigate whether there was a kinetic difference between the purine and pyrimidine transport processes, the initial rates of uptake of inosine and uridine were examined. Uptake of both nucleosides was saturable (Figs. 7, 8). The  $K_m$  of inosine was  $4.5 \pm 1.0 \mu\text{M}$  whereas the  $K_m$  of uridine was  $80 \pm 10 \mu\text{M}$ . The  $V_{\text{max}}$  of inosine was  $1.9 \pm 0.1 \text{ pmol/oocyte/10 min}$  whereas that of uridine was  $5.3 \pm 0.2 \text{ pmol/oocyte/10 min}$  (Figs. 7, 8). These data suggest, for the first time, that the N1 transporters have a higher affinity (18-fold) for inosine than for uridine, and therefore may primarily transport purines under physiological conditions in which low concentrations of nucleosides (i.e. less than micromolar concentrations) are found.

The inhibition potency of adenosine and 2'-deoxyadenosine was determined by  $\text{IC}_{50}$  studies. At an inosine concentration of  $12 \mu\text{M}$ , an  $\text{IC}_{50}$  of  $23 \pm 3 \mu\text{M}$  and a  $K_i$  of  $6 \pm 1 \mu\text{M}$  were obtained for adenosine (Fig. 9). Under identical conditions, an  $\text{IC}_{50}$  of  $110 \pm 26 \mu\text{M}$  and a  $K_i$  of  $30 \pm 7 \mu\text{M}$  were obtained for 2'-deoxyadenosine (Fig. 10). In addition, we observed that the  $\text{Na}^+$ -dependent uptake of the analog of 2'-deoxyadenosine,  $^3\text{H}$ -2-chloro-2'-deoxyadenosine, was enhanced approximately two-fold over that in water injected oocytes (data not shown) suggesting that 2'-deoxyribo-purine nucleosides may be permeants of hSPNT1.

*Tissue Distribution of hSPNT1 mRNA.* Transcripts of 4.4, 2.6, 2.4 and 1.6 kb were identified in Northern Blotting studies (Fig. 11). The 4.4 kb transcript was present in all tissues tested (heart, liver, skeletal muscle, kidney, intestine, pancreas, placenta, brain, lung) with the strongest signal in the heart and the weakest in the lung. The 2.6 and 2.4 kb bands were relatively weaker than the 4.4 kb band and were observed in heart, liver, skeletal muscle, kidney and pancreas. The 2.6 kb, but not the 2.4 kb, band was seen in the intestine. In addition, a strong 1.6 kb transcript was detected in heart and skeletal muscle. Excluding the poly (A) tail, the exact length of the hSPNT1 cDNA is 2,459 bp. The 3' RACE product in the cloning process contained a 15-bp poly (A) tail, suggesting

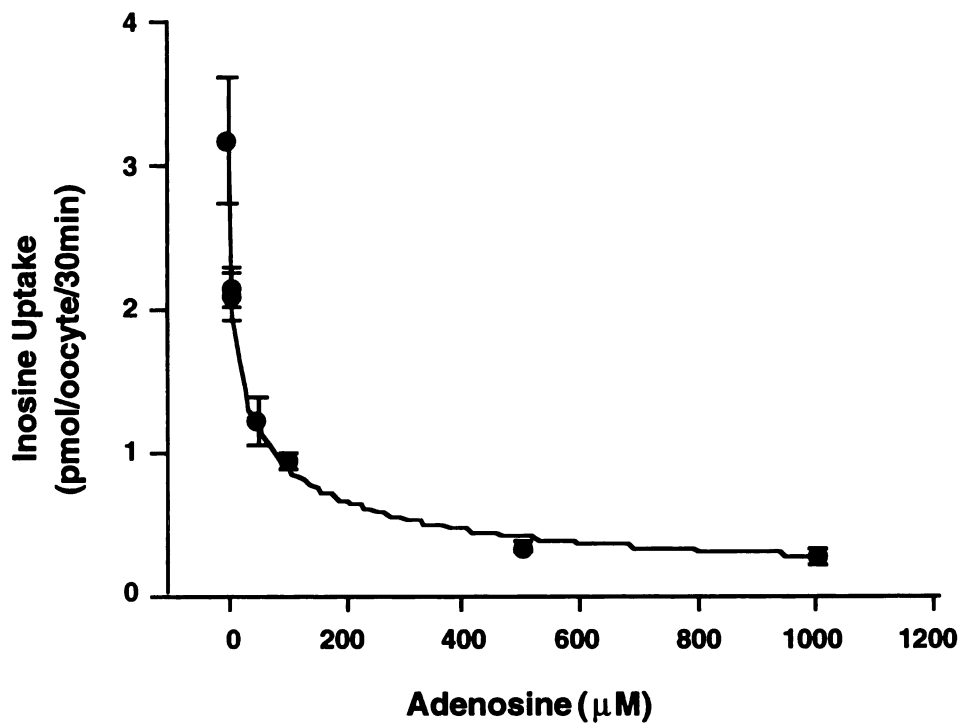


Figure 9.  $IC_{50}$  studies of inosine uptake in the presence of adenosine at various concentration in hSPNT1 cRNA-injected oocytes. Each point represents the mean  $\pm$  S.E. (n=8-10) from one representative experiment. Apparent  $IC_{50}$  and  $K_i$  values were obtained by fitting the data to the equations  $V=V_0/(1+(I/IC_{50})^n)$  and  $K_i=IC_{50}/(1+C/K_m)$ , respectively.



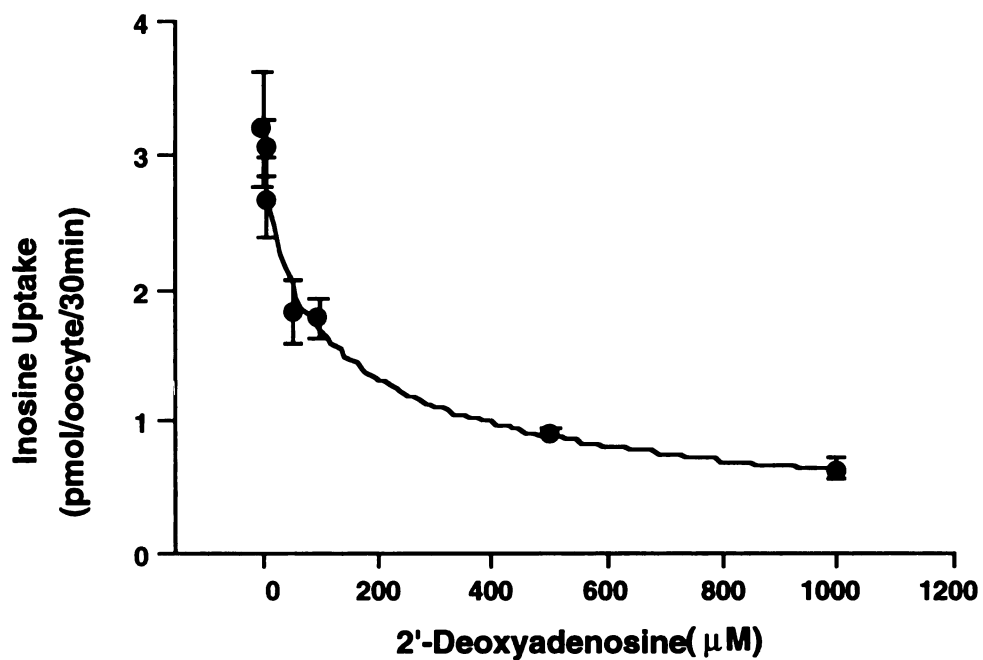


Figure 10.  $IC_{50}$  studies of inosine uptake in the presence of 2'-deoxyadenosine at various concentration in hSPNT1 cRNA-injected oocytes. Each point represents the mean  $\pm$  S.E. (n=8-10) from one representative experiment. Apparent  $IC_{50}$  and  $K_i$  values were obtained by fitting the data to the equations  $V=V_0/(1+(I/IC_{50}))^n$  and  $K_i=IC_{50}/(1+C/K_m)$ , respectively.

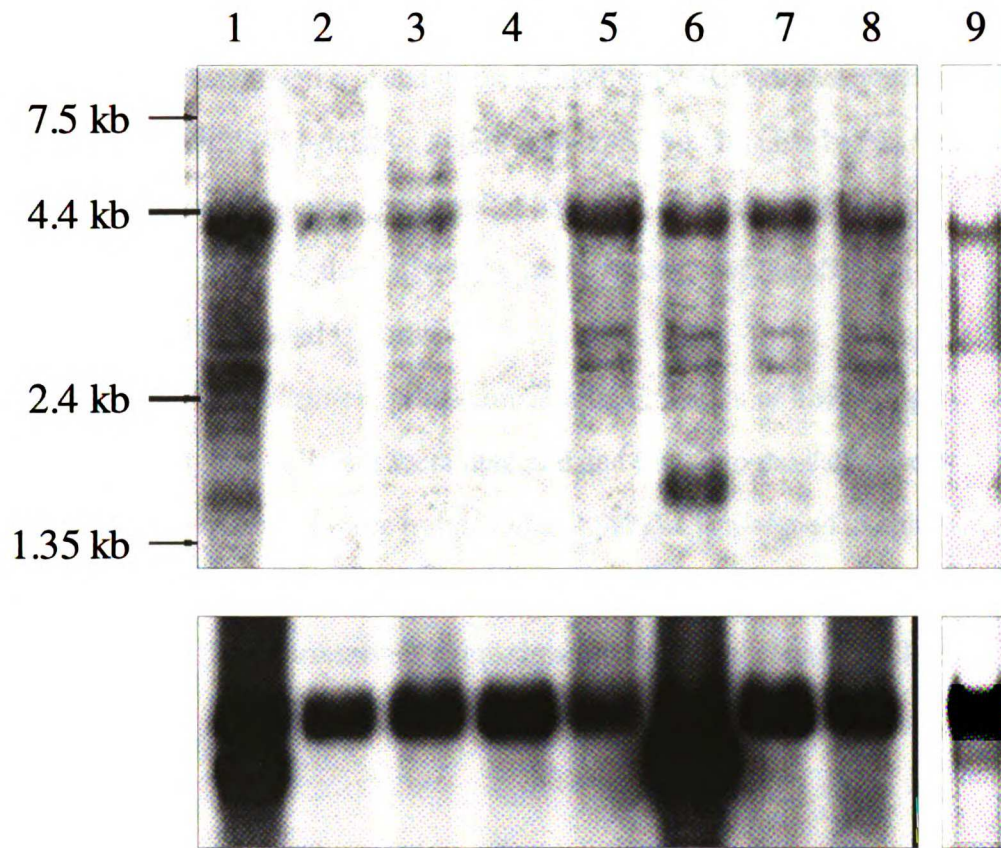


Figure 11. Northern blot analysis of hSPNT1 transcript in various human tissues. Lanes 1-8 represent mRNA samples (2  $\mu\text{g}/\text{lane}$ ) from heart (lane 1), brain (lane 2), placenta (lane 3), lung (lane 4), liver (lane 5), skeletal muscle (lane 6), kidney (lane 7), pancreas (lane 8), and intestine (lane 9). The same blots were stripped and reprobed with a human  $\beta$ -actin cDNA probe (lower panel).

that the 3' UTR sequence of hSPNT1 cDNA is complete. However, the poly (A) tail in the mRNA transcript of the hSPNT1 can be much longer. In addition, the sequence of the 5' UTR may be incomplete due to limitations of the 5' RACE method, and additional sequences may be present at the 5' end of the hSPNT1 cDNA. For these reasons, the mRNA transcript of hSPNT1 must be longer than 2,459 bp. It is likely that the mRNA transcript at 2.6 kb represents the transcript of hSPNT1. The presence of multiple transcripts may be a result of alternatively spliced transcripts of the hSPNT1 gene or the co-existence of closely related isoforms.

*Chromosomal localization.* The scores for the presence of hSPNT1 gene marker in the 93 radiation hybrid cell lines were obtained and linked to the data base of Whitehead framework map of these hybrid cells. hSPNT1 is assigned to chromosome 15, 3.25 centiRays (about 880 kb) from the framework marker WI-4772 (linkage odds  $\geq 1000:1$ ,  $P < 0.05$ ). This corresponds approximately to chromosome 15q13-14 on the cytogenetic map.

## **Discussion**

Previous clinical studies indicate that purine nucleosides are actively transported in the human kidney. In particular, the active tubular transport of adenosine and 2'-deoxyadenosine in humans has been described by Kuttesch and Nelson (3). However, little is known about the molecular mechanisms involved in the active transport of purines in the human kidney.

Using consensus sequences from known cloned transporters, we isolated a cDNA encoding a  $\text{Na}^+$ -dependent purine-selective nucleoside transporter, hSPNT1, from human kidney. Functional studies suggest that hSPNT1 transports purines selectively (Figs. 5, 3d) and interacts with both ribo- and deoxyribo- purine nucleosides (Figs. 9, 10). In addition, hSPNT1 transports the pyrimidine, uridine with a lower affinity than that of

inosine (Figs. 7, 8). Consistent with our findings, Che and coworkers reported an adenosine  $K_m$  of 6 mM for the rat liver SPNT (8), identical to the  $K_i$  of adenosine (6  $\mu$ M) for hSPNT1. They also reported a minor SPNT-mediated transport of thymidine with a  $K_m$  of 13 mM (8). In contrast, no detectable hSPNT1-mediated thymidine transport was observed (Fig. 6). Since  $V_{max}$  varies between batches of oocytes and is dependent upon the level of expression, it is difficult to compare transport capacities between human and rat clones. Nonetheless, the data suggest that there may be some functional differences between the rat and the human transporters.

Several unique structural features markedly distinguish hSPNT1 from rat SPNT. First, the deduced N-terminal amino acid sequence of hSPNT1 is considerably different (less than 50% identity) from that of rat SPNT despite the overall high sequence homology (81% identical). An important difference in this region is that the rat SPNT possesses an ATP/GTP binding motif whereas hSPNT1 does not (Fig. 2). These data suggest that it is possible that different mechanisms may be involved in the regulation, targeting and activation of these proteins. Second, an *Alu* repetitive element is found in the 3' UTR of the hSPNT1 cDNA. *Alu* repetitive elements are short interspersed DNA sequences which are unique to primates and comprise 5% of human genomic DNA. Recently, *Alu* sequences have been found to function as estrogen receptor-dependent transcriptional enhancers and as a silencer in the Wilm's tumor 1 gene (17, 18). Proteins that bind to the *Alu* element and *Alu* RNA have been identified in human cells (19, 20). Thus, it is possible that hSPNT1 can be regulated through an *Alu*-dependent pathway.

Strong signals of multiple hSPNT1 transcripts of different sizes (4.4, 2.6, 2.4 and 1.6 kb) were detected in human kidney as well as in heart, skeletal muscle, liver, intestine, and pancreas. In contrast, a single 3.4 kb transcript of hCNT1 was detected in human kidney mRNA (10). Because our high stringency hybridization methods did not detect the 3.4 kb transcript, these data suggest that other more closely hSPNT1-related transporters may exist. Interestingly, the distribution of the hSPNT1 transcripts

correlates well with the sites of action of purinergic effects. In the kidney, adenosine is locally produced and exerts various purinergic effects that include reducing the glomerular filtration rate by altering the resistance of the glomerular arterioles and inhibiting renin release as well as neurotransmission (21, 22). Adenosine also has profound cardiac effects and has been shown to prevent muscle skeleton ischemic necrosis (23-25). The findings that multi-transcripts of hSPNT1 exist in these organs suggest that hSPNT1 and related transporters may be actively involved in adenosine induced effects in humans. A possible role may be the removal of adenosine from the extracellular fluids surrounding its receptors resulting in the attenuation of its site-specific action.

In summary, we cloned and functionally characterized the first Na<sup>+</sup>-dependent purine-selective transporter hSPNT1 in human. hSPNT1 is functionally distinct from the recently cloned pyrimidine selective Na<sup>+</sup>-nucleoside transporter in human kidney and also differs from the rat purine selective Na<sup>+</sup>-nucleoside transporter, SPNT, in terms of its structure and tissue distribution. The existence of multiple transcripts and the broad tissue distribution of hSPNT1 suggests that this transporter may play a critical role in the uptake and salvage of nucleosides in the kidney as well as in a variety of human tissues.

## References

1. Grever, M. R., M. F. Siaw, W. F. Jacob, J. A. Neidhart, J. S. Miser, M. S. Coleman, J. J. Hutton, and S. P. Balcerzak. The biochemical and clinical consequences of 2'-deoxycoformycin in refractory lymphoproliferative malignancy. *Blood* **57**:406-17 (1981).
2. Grage, T. B., D. B. Rochlin, A. J. Weiss, and W. L. Wilson. Clinical studies with tubercidin administered after absorption into human erythrocytes. *Cancer Res.* **30**:79-81 (1970).
3. Kuttesch, J. J., and J. A. Nelson. Renal handling of 2'-deoxyadenosine and adenosine in humans and mice. *Cancer Chemother Pharmacol* **8**:221-9 (1982).
4. Vijayalakshmi, D., and J. A. Belt. Sodium-dependent nucleoside transport in mouse intestinal epithelial cells. Two transport systems with differing substrate specificities. *J Biol Chem* **263**:19419-23 (1988).
5. Williams, T. C., and S. M. Jarvis. Multiple sodium-dependent nucleoside transport systems in bovine renal brush-border membrane vesicles. *Biochem J* **27**:27-33 (1991).
6. Wu, X., G. Yuan, C. M. Brett, A. C. Hui, and K. M. Giacomini. Sodium-dependent nucleoside transport in choroid plexus from rabbit. Evidence for a single transporter for purine and pyrimidine nucleosides. *J Biol Chem* **267**:8813-8 (1992).

7. Gutierrez, M. M., and K. M. Giacomini. Substrate selectivity, potential sensitivity and stoichiometry of Na(+)-nucleoside transport in brush border membrane vesicles from human kidney. *Biochim Biophys Acta* **1149**:202-8 (1993).
8. Che, M., D. F. Ortiz, and I. M. Arias. Primary structure and functional expression of a cDNA encoding the bile canalicular, purine-specific Na(+)-nucleoside cotransporter. *J Biol Chem* **270**:13596-9 (1995).
9. Huang, Q. Q., S. Y. Yao, M. W. Ritzel, A. R. Paterson, C. E. Cass, and J. D. Young. Cloning and functional expression of a complementary DNA encoding a mammalian nucleoside transport protein. *J Biol Chem* **269**:17757-60 (1994).
10. Ritzel, M. W., S. Y. Yao, M. Y. Huang, J. F. Elliott, C. E. Cass, and J. D. Young. Molecular cloning and functional expression of cDNAs encoding a human Na<sup>+</sup>-nucleoside cotransporter (hCNT1). *Am J Physiol* **272**:C707-14 (1997).
11. Zhang, L., M. J. Dresser, A. T. Gray, S. C. Yost, T. S., and G. K. M. Cloning and functional expression of a human liver organic cation transporter. *Mol Pharmacol* **51**:913-21 (1997).
12. Cox, D. R., M. Burmeister, E. R. Price, S. Kim, and R. M. Myers. Radiation hybrid mapping: a somatic cell genetic method for constructing high-resolution maps of mammalian chromosomes. *Science* **250**:245-50 (1990).
13. Walter, M. A., D. J. Spillett, P. Thomas, J. Weissenbach, and P. N. Goodfellow. A method for constructing radiation hybrid maps of whole genomes. *Nat Genet* **7**:22-8 (1994).

14. Kozak, M. Point mutations define a sequence flanking the AUG initiator codon that modulates translation by eukaryotic ribosomes. *Cell* **44**:283-92 (1986).
15. Kyte, J., and R. F. Doolittle. A simple method for displaying the hydropathic character of a protein. *J Mol Biol* **157**:105-32 (1982).
16. Von, H. G. Membrane protein structure prediction. Hydrophobicity analysis and the positive-inside rule. *J Mol Biol* **225**:487-94 (1992).
17. Britten, R. J. DNA sequence insertion and evolutionary variation in gene regulation. *Proc Natl Acad Sci U S A* **93**:9374-7 (1996).
18. Hewitt, S. M., G. C. Fraizer, and G. F. Saunders. Transcriptional silencer of the Wilms' tumor gene WT1 contains an Alu repeat. *J Biol Chem* **270**:17908-12 (1995).
19. Chiang, Y., and J. K. Vishwanatha. Characterization of the HeLa cell 35 kDa Alu-element binding protein. *Mol Cell Biochem* **155**:131-8 (1996).
20. Hsu, K., D. Y. Chang, and R. J. Maraia. Human signal recognition particle (SRP) Alu-associated protein also binds Alu interspersed repeat sequence RNAs. Characterization of human SRP9. *J Biol Chem* **270**:10179-86 (1995).
21. Le, H. M., and B. Kaissling. Distribution and regulation of renal ecto-5'-nucleotidase: implications for physiological functions of adenosine [editorial]. *Am J Physiol* **F377-87** (1993).



22. Siragy, H. M., and J. Linden. Sodium intake markedly alters renal interstitial fluid adenosine. *Hypertension* 404-7 (1996).
23. Belardinelli, L., J. Linden, and R. M. Berne. The cardiac effects of adenosine. *Prog Cardiovasc Dis* 32:73-97 (1989).
24. Tucker, A. L., and J. Linden. Cloned receptors and cardiovascular responses to adenosine. *Cardiovasc Res* 27:62-7 (1993).
25. Pang, C. Y., and C. R. Forrester. Acute pharmacologic preconditioning as a new concept and alternative approach for prevention of skeletal muscle ischemic necrosis. *Biochem Pharmacol* 49:1023-34 (1995).

## CHAPTER 4

### IDENTIFICATION OF SUBSTRATE RECOGNITION DOMAINS IN Na<sup>+</sup>-DEPENDENT NUCLEOSIDE TRANSPORTERS<sup>1</sup>

Nucleosides and nucleoside analogs are increasingly being developed and used in the treatment of cancer, viral infections, and cardiac arrhythmias (1-3). Notable examples of therapeutic nucleoside analogs include cytosine arabinoside (Ara-C), cladribine, azidothymidine (AZT), and 2',3'-dideoxyinosine (ddI) used in the treatment of cancer and human immunodeficiency virus (HIV) infection. The endogenous nucleoside, adenosine, exerts profound cardiac effects, and is used in the treatment of cardiac arrhythmias (3). In mammalian cells, transmembrane flux of nucleosides and nucleoside analogs are mediated by both equilibrative and Na<sup>+</sup>-dependent nucleoside transporters (4-7). Consequently the distribution and functional characteristics of these transporters play important roles in determining the absorption, disposition, and elimination of nucleoside drugs (5, 6). Nucleoside transporters presented in tumor cells and in the vicinity of purinergic receptors may also represent important gene targets for drug therapy (3, 7).

The equilibrative nucleoside transporters mediate passive downhill transport of nucleosides and function bidirectionally in accordance with the concentration gradient of the substrate. Equilibrative nucleoside transporters exhibit a broad substrate selectivity for both purine and pyrimidine nucleosides and appear to be ubiquitous in mammalian cells.

---

<sup>1</sup> Most of this chapter was published in a manuscript entitled: Molecular determinants of substrate selectivity in Na<sup>+</sup>-dependent nucleoside transporters. *Journal of Biological Chemistry* 272(46): 28845-8, 1997.

They have been further classified into two subtypes (*es* and *ei*) according to their sensitivity to inhibition by nitrobenzylthioinosine (5-7). The human *es* type transporter, hENT1, is recently cloned and has been implicated in the cellular uptake of some chemotherapeutic drugs (8).

Na<sup>+</sup>-dependent nucleoside transporters mediate active uphill transport of nucleosides into cells by coupling to the inwardly directed Na<sup>+</sup> gradient across the plasma membrane. These transporters have been demonstrated in a variety of tissues including intestinal and renal epithelia, hepatocytes, choroid plexus, and cultured leukemia cells (9-14). Na<sup>+</sup>-dependent nucleoside transporters exhibit distinct transport selectivity for purine and pyrimidine nucleosides and have been classified into several subtypes based on their substrate selectivity. The N1 (or *cif*) Na<sup>+</sup>-dependent nucleoside transport system is purine-selective; the N2 (or *cit*) system is pyrimidine-selective; and the N3 (or *cib*) system is broadly-selective (or non-selective). Uridine and adenosine are transported by all known Na<sup>+</sup>-dependent nucleoside transport systems. The unique features of Na<sup>+</sup>-dependent nucleoside transporters such as their ability to mediate uphill nucleoside transport, their distinct transport selectivity for purine and pyrimidine nucleosides, and their presence in many critical organs suggest that they may play special physiological and pharmacological roles in mammalian cells.

Recently, a purine-selective (N1 subtype) nucleoside transporter, SPNT, and a pyrimidine-selective (N2 subtype) transporter, rCNT1 were cloned from rat by expression cloning in *Xenopus laevis* oocytes (9, 10). The cloned N1 (659 amino acids) and N2 (648 amino acids) transporters share 64% identity and are both predicted to possess 14 putative transmembrane domains. These two cloned transporters are shown to be involved in the cellular uptake of nucleoside drugs including adenosine, cladribine, AZT and ddC (9, 15-17). More recently, the human N1 and N2 homologs (hSPNT1 and hCNT1) have been cloned (18, 19). The human homologs show high sequence homology to their rat analogs

(81% identity for N1 and 83% identity for N2) and display no functional differences from the rat clones (18, 19).

Despite the extensive studies on the kinetic properties of these transporters and their interactions with nucleoside drugs, little is known about the structural elements and molecular mechanisms that underlie the functional properties of Na<sup>+</sup>-dependent nucleoside transporters. In this study, I focus on delineating the structural domains involved in substrate binding and the molecular determinants responsible for the distinct substrate selectivity of N1 and N2 nucleoside transporters. By constructing a series of chimeric N1/N2 transporters and analyzing their transport selectivity for purine or pyrimidine nucleosides, structural elements contributing to substrate binding and selectivity are revealed. Knowledge about the substrate binding domains of Na<sup>+</sup>-dependent nucleoside transporters and the determinants of their substrate selectivity should benefit the design of nucleoside drugs with improved membrane permeability and the development of nucleoside transporter inhibitors with improved potency and specificity.

## **Materials and Methods**

*Construction of Chimeric Transporters.* The cDNAs of wild-type N1 and N2 transporters were isolated by reverse transcriptase polymerase chain reaction (RT-PCR) from mRNA prepared from rat IEC-6 cells and rat intestine respectively. The cDNAs were then subcloned into pGEM-T vector (Promega) under the control of T7 promoter. The predicted amino acid sequence of N2 is identical to the published sequence of rCNT1. The predicted amino acid sequence of N1 is identical to the published sequence of SPNT except for an Ala to Gly substitution at residue 419. The A419G substitution was also observed by other workers and was attributed to polymorphism in rats (16).

The Genetics Computer Group software (Wisconsin Package, Version 8 ) was used to align the nucleotides and the deduced amino acid sequences of N1 and N2. Chimeras

were constructed by using both native restriction enzyme sites and engineered sites introduced through site-directed mutagenesis (Sculptor™ *in vitro* mutagenesis system, Amersham). Junctions were made within homologous regions, generally in stretches of identical amino acid sequences between the wild-type transporters. No foreign amino acid was introduced in any chimera construct. The sequence of each chimera was confirmed by automated DNA sequencing in the Biochemical Resource Center at the University of California, San Francisco.

*Transport Assays in Xenopus laevis Oocytes.* cRNA of each chimera was synthesized and injected into defolliculated oocytes. Uptake was measured on groups of 10 oocytes 48-56 hour post-injection at 25°C in 150 µl of transport buffer (2 mM KCl, 1 mM CaCl<sub>2</sub>, 1 mM MgCl<sub>2</sub>, 10 mM HEPES, pH 7.4) containing either 100 mM NaCl or 100 mM choline chloride, and the respective <sup>3</sup>H-labeled nucleoside (Moravek Biochemicals). The kinetic parameter (apparent K<sub>m</sub> values) were determined by non-linear least-squares fits of substrate/velocity profiles to the Michaelis-Menten equation using Kaleidagraph (Version 3.0, Synergy Software). Because of the intrinsic variability in the expression level of the transporters between batches of oocytes, the data are generally expressed as the mean ± S.E. from a representative experiment performed in the same batch of oocytes. However, experiments were repeated at least twice in separated batches of oocytes.

## Results

*Construction and Functional Analysis of Chimeric Transporters.* The cDNAs of rat N1 transporter (SPNT) and rat N2 transporter (rCNT1) were cloned by RT-PCR. The 14 putative transmembrane domains of N1 and N2 were assigned according to the published model of rCNT1 (10). A series of chimeras were constructed and expressed in *Xenopus laevis* oocytes. Since uridine and adenosine are transported by all known Na<sup>+</sup>-dependent nucleoside transporters, chimeras were first screened with the common substrate <sup>3</sup>H-

uridine for activity. Purine- or pyrimidine-selectivity, was then tested with both  $^3\text{H}$ -inosine (a model purine nucleoside) and  $^3\text{H}$ -thymidine (a model pyrimidine nucleoside). Inhibition studies with naturally occurring nucleosides were performed to further confirm purine or pyrimidine selectivity. The structures and selectivity of wild-type N1 and N2 transporters and chimeric transporters are shown in Figure 1.

The first chimera produced (Figure 1), Chimera T8-14, consisting of TM1-7 of N2 and TM8-14 of N1 maintained the transport selectivity of N1, suggesting that domains responsible for substrate discrimination reside in the C-terminal half of the transporter. Subsequent smaller replacements narrowed down this region to TM8-9. Replacing TM8-9 of N2 with that of N1 generated Chimera T8-9; replacing only TM8 generated Chimera T8; and replacing only TM9 generated Chimera T9 (Figure 1). The uptake of  $^3\text{H}$ -inosine and  $^3\text{H}$ -thymidine by N1, N2, Chimera T8-9 and Chimera T8 and the effect of various naturally occurring purine and pyrimidine nucleosides on  $^3\text{H}$ -uridine uptake by these transporters are shown in Figures 2-5. All of these chimeras were functional suggesting that all were expressed, folded and inserted into the oocyte plasma membrane.

Wild-type N1 transports inosine, but not thymidine (Figure 2A). The N1-mediated  $\text{Na}^+$ -dependent uridine uptake is fully inhibited (i.e. to the uptake level in the water-injected oocytes) by the common substrates, uridine and adenosine, as well as by the model purine nucleosides, inosine and guanosine. The model pyrimidine nucleosides, cytidine and thymidine, only partially inhibit the uptake (Figure 2B). In contrast, wild-type N2 transports thymidine, but not inosine (Figure 3A). N2-mediated  $\text{Na}^+$ -dependent uridine uptake is fully inhibitable by the model pyrimidine nucleosides and the common substrates, but not by the model purine nucleosides (Figure 3B). Chimera T8-9, exhibited both a substrate selectivity and an inhibition profile similar to those of the wild-type N1 (Figure 4), suggesting that TM8-9 contain domains responsible for the distinct purine-selectivity. Interestingly, the requirement of  $\text{Na}^+$  in the transport process seemed less stringent in

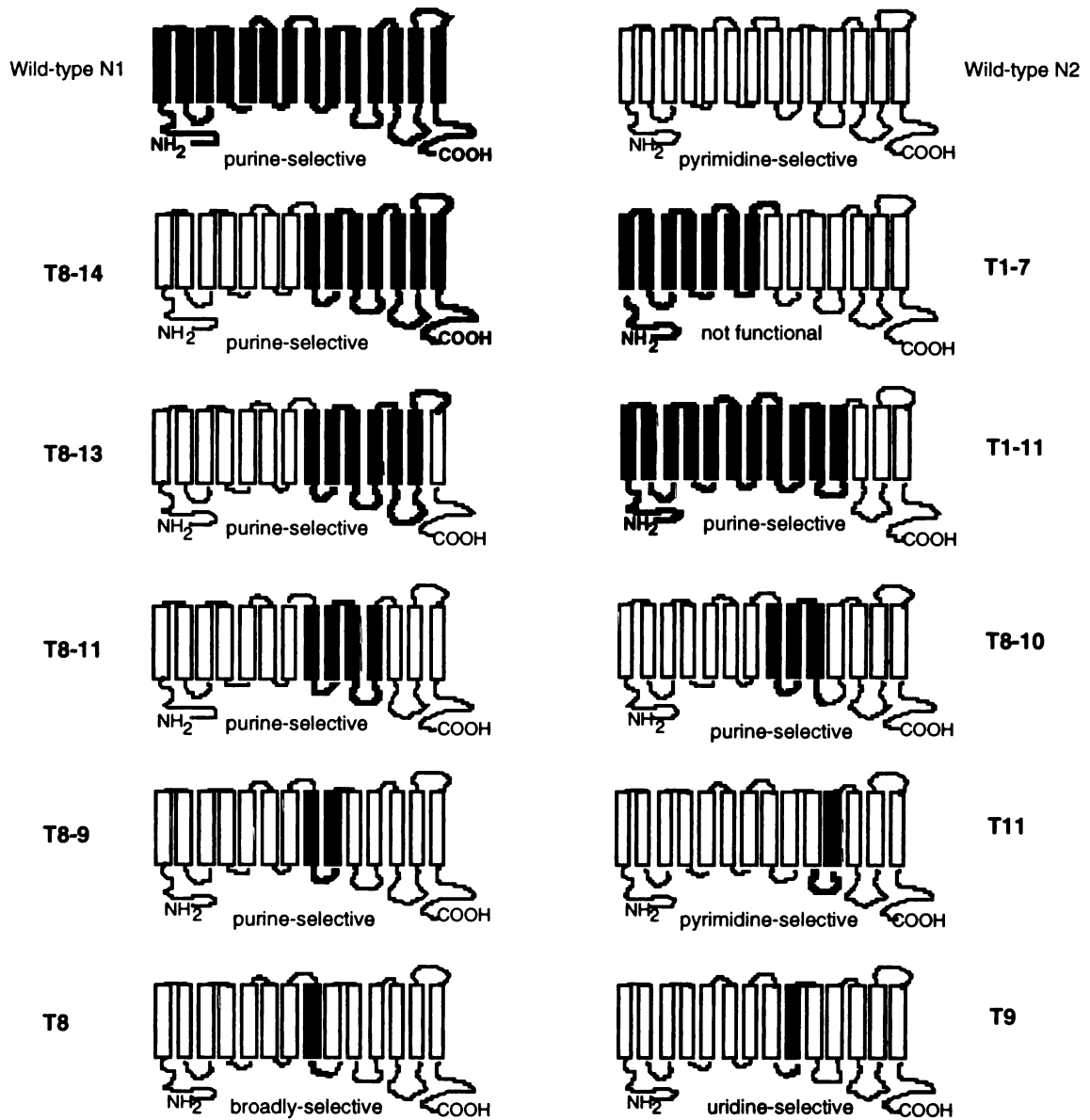


Figure 1. Structures and substrate selectivity of wild-type and chimeric transporters. Chimeras are named as the TMDs of N2 that are replaced by the corresponding TMDs of N1.

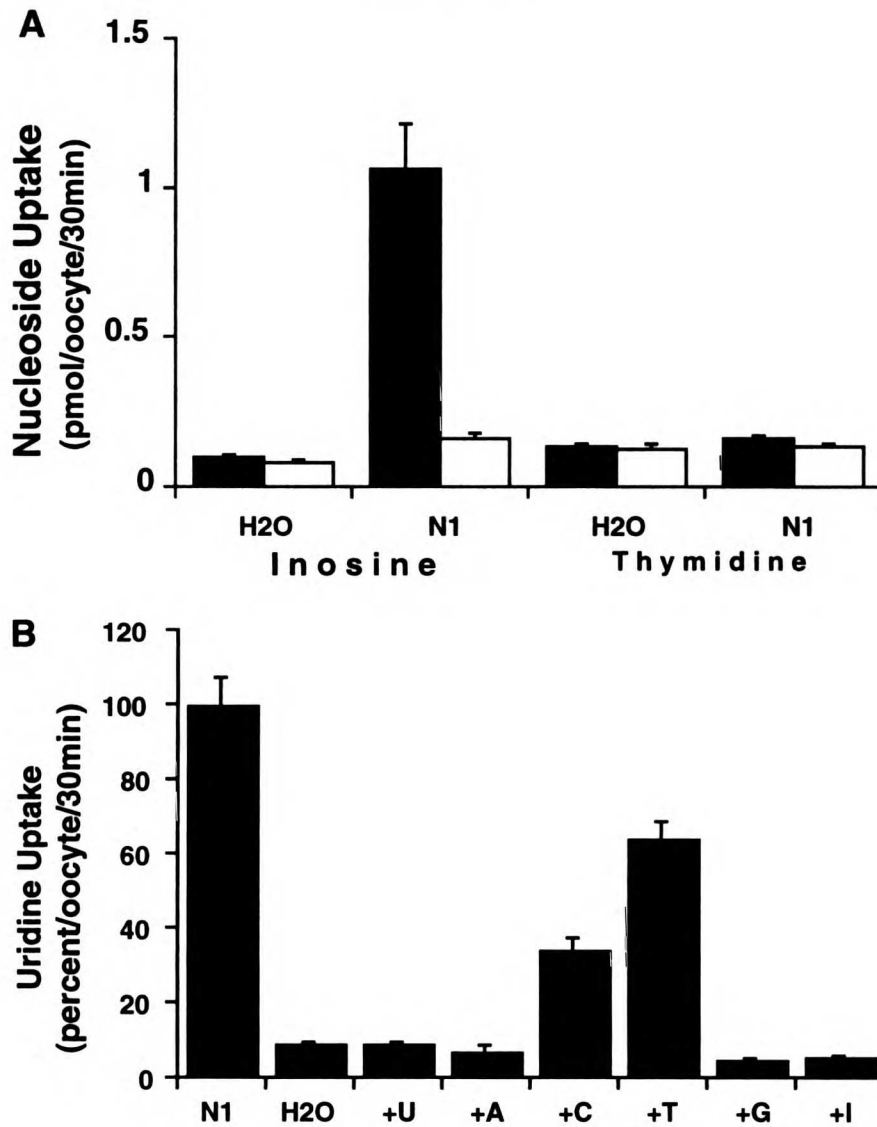


Figure 2. Uptake of <sup>3</sup>H-nucleosides by wild-type N1 (A) and effects of naturally-occurring nucleosides on <sup>3</sup>H-uridine uptake mediated by wild-type N1 (B). Each value represents the mean ± S.E. (n = 8-10). The abbreviations are: U, uridine; A, adenosine; C, cytidine; T, thymidine; G, guanosine; and I, inosine.



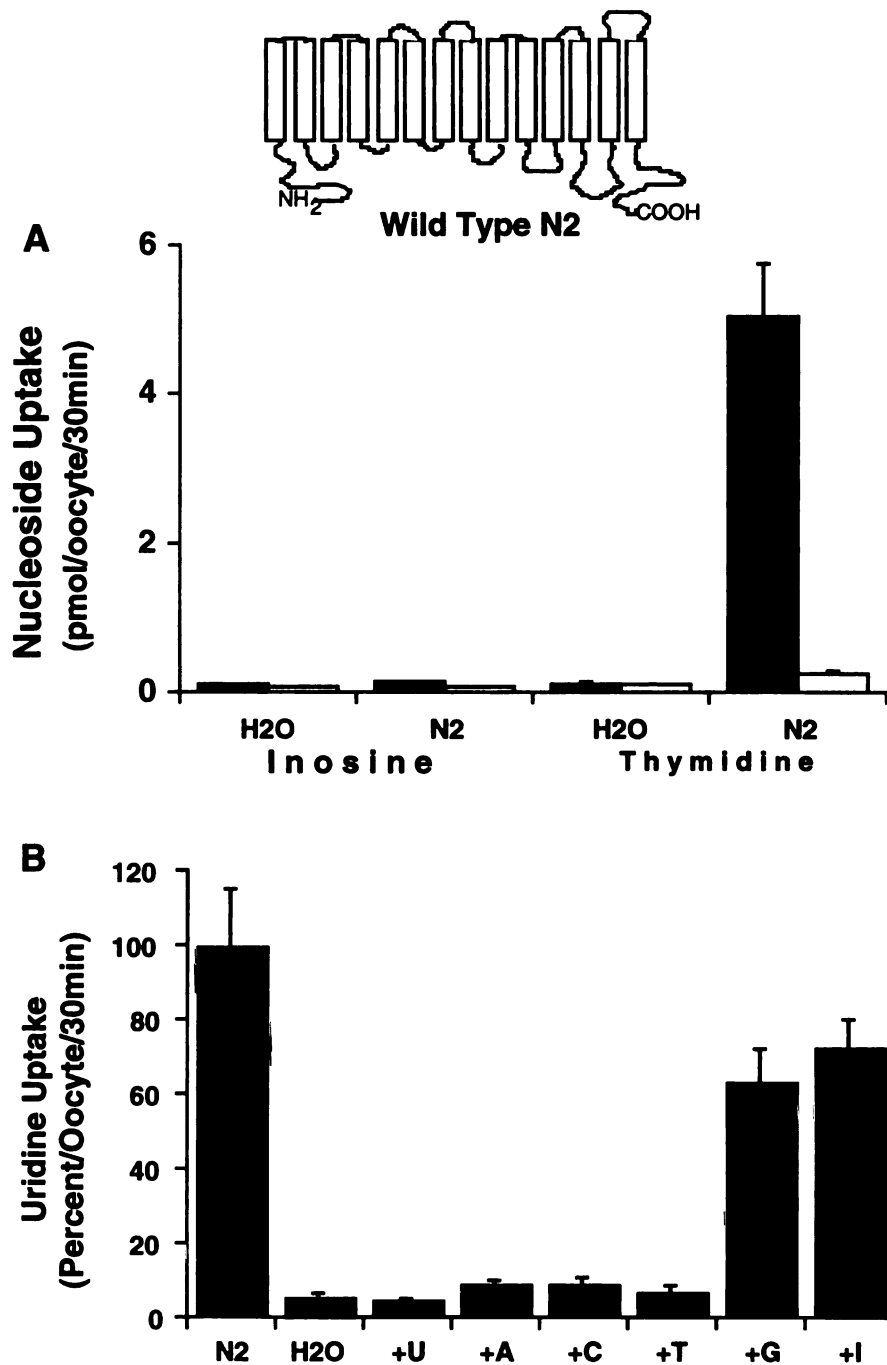


Figure 3. Uptake of  $^3\text{H}$ -nucleosides by wild-type N2 (A) and effects of naturally-occurring nucleosides on  $^3\text{H}$ -uridine uptake mediated by wild-type N2 (B). Each value represents the mean  $\pm$  S.E. ( $n = 8-10$ ). The abbreviations are: U, uridine; A, adenosine; C, cytidine; T, thymidine; G, guanosine; and I, inosine.

oocytes expressing Chimera T8-9 (Figure 4A). Replacement of Na<sup>+</sup> with choline only partially inhibited inosine uptake. The reason for this observation is unknown.

Chimera T8 exhibited a broad substrate selectivity, transporting both inosine and thymidine (Figure 5A). The transport activity was fully inhibited by all of the naturally occurring purine and pyrimidine nucleosides (Figure 5B). Broadly-selective Na<sup>+</sup>-dependent nucleoside transporters have been described and classified as N3 subtype nucleoside transporters (12, 20), but to date no typical N3 transporter has been cloned. It would be interesting to compare the sequence of Chimera T8 to that of the native N3 transporter when its sequence becomes available.

Chimera T9 was a low activity transporter with a novel substrate selectivity. When expressed in oocytes, Chimera T9 induced a 4-5 fold increase in Na<sup>+</sup>-dependent uridine uptake ( $0.72 \pm 0.11$  for cRNA-injected vs.  $0.15 \pm 0.02$  for water-injected; mean  $\pm$  SE, pmol/oocyte/ 30 min) without a significant increase in the uptake of inosine or thymidine. However, the Na<sup>+</sup>-dependent uridine uptake was inhibited to the basal level by all nucleosides at 1 mM including inosine and thymidine, suggesting that all nucleosides can serve as inhibitors to this process.

To exclude the possibility that the introduction of any N1 sequence into N2 would alter its substrate selectivity, a chimera (Chimera T11), in which the TM11 and the preceding intracellular loop of N2 were replaced with those of N1, was generated. Chimera T11 maintained the substrate selectivity of N2 (Figure 1), suggesting that replacing regions other than TM8-9 does not affect the substrate selectivity of N2.

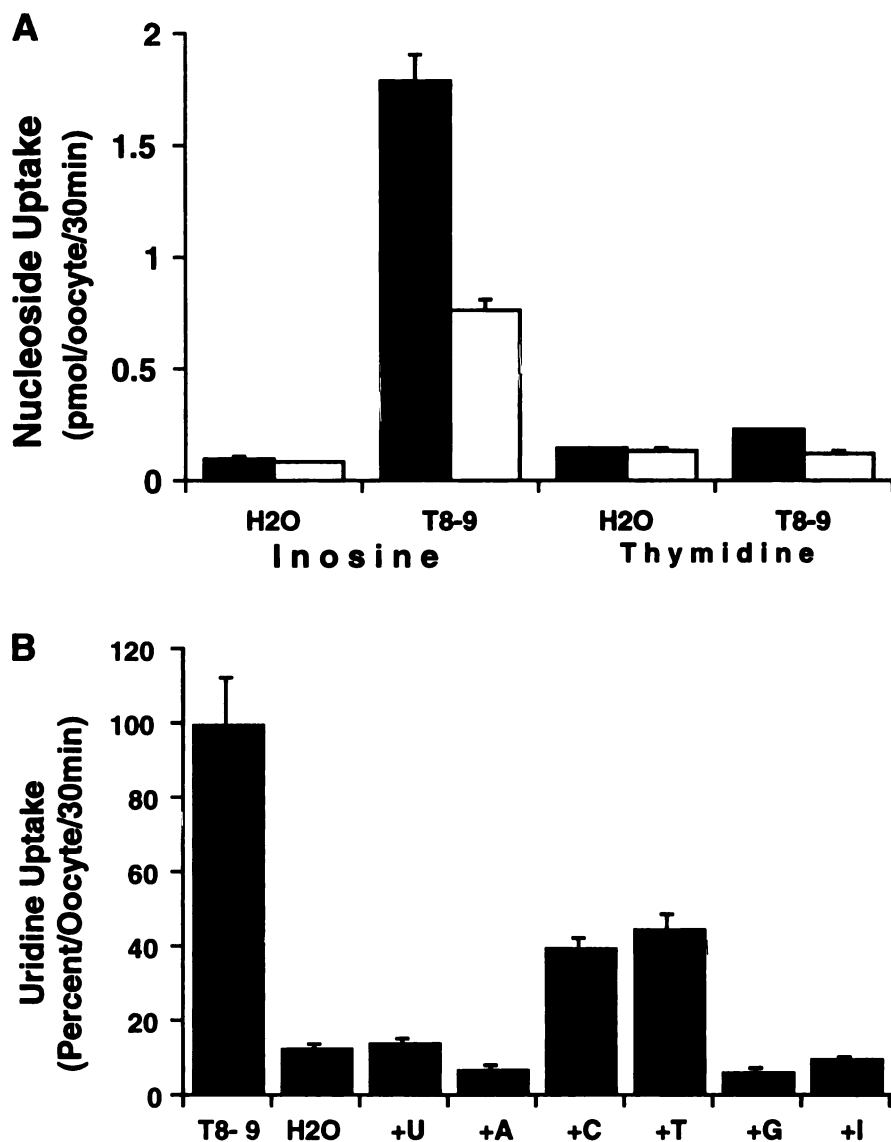
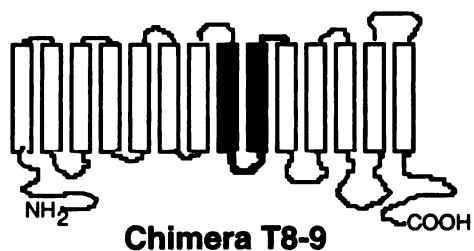


Figure 4. Uptake of  $^3\text{H}$ -nucleosides by Chimera T8-9 (A) and effects of naturally-occurring nucleosides on  $^3\text{H}$ -uridine uptake mediated by Chimera T8-9 (B). Each value represents the mean  $\pm$  S.E. ( $n = 8-10$ ). The abbreviations are: U, uridine; A, adenosine; C, cytidine; T, thymidine; G, guanosine; and I, inosine.

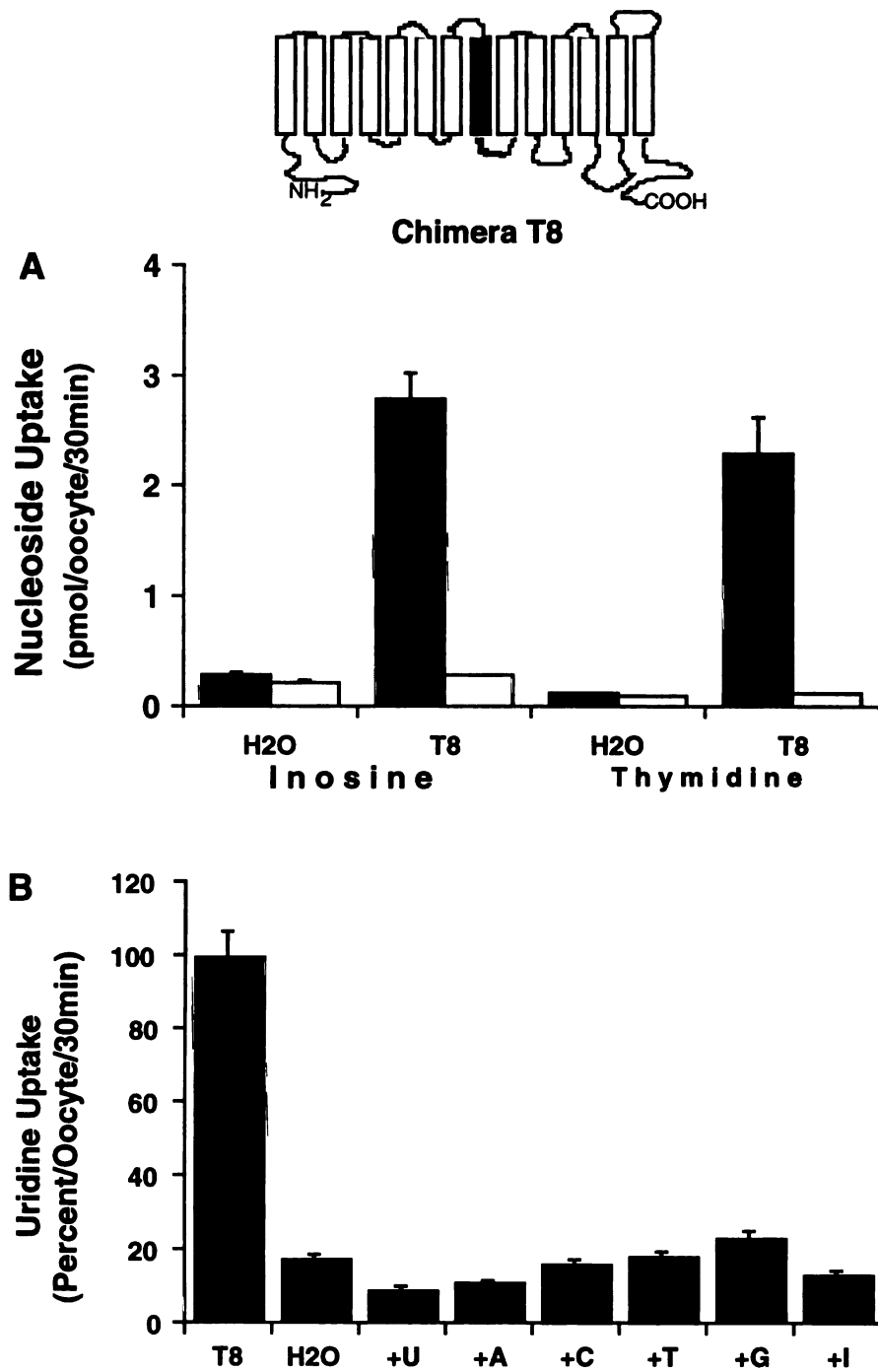


Figure 5. Uptake of  $^3\text{H}$ -nucleosides by Chimera T8 (A) and effects of naturally-occurring nucleosides on  $^3\text{H}$ -uridine uptake mediated by Chimera T8 (B). Each value represents the mean  $\pm$  S.E. ( $n = 8-10$ ). The abbreviations are: U, uridine; A, adenosine; C, cytidine; T, thymidine; G, guanosine; and I, inosine.

*Kinetic Analysis of Wild-Type and Chimeric Transporters.* The apparent transport affinities ( $K_m$ ) of wild type N1 and N2, and Chimera T8-9 and Chimera T8 towards their substrates are measured and compared (Table 1). Chimera T8, which displayed a broad N3 transport selectivity, exhibited apparent  $K_m$ 's for uridine, inosine, and thymidine similar to those of the wild-type N1 and N2 transporters (Table 1). Interestingly, Chimera T8-9, which maintained the transport selectivity of the wild-type N1, exhibited increased apparent transport affinities for both uridine ( $K_m = 3.6 \mu\text{M}$ ) and inosine ( $K_m = 6.3 \mu\text{M}$ ) as compared to those of wild type N1 (34  $\mu\text{M}$  for uridine, 15  $\mu\text{M}$  for inosine) (Table 1).

## **Discussion**

To identify structural domains involved in substrate binding and molecular determinants responsible for distinct transport selectivity, chimeric transporters were made from the cloned rat N1 and N2 transporters. Of the 14 transmembrane domains of N1 and N2, transplanting TM8-9 of N1 into N2 converted N2 from a pyrimidine- to a purine-selective transporter. Transplanting only TM8 generated a chimera with characteristics similar to the N3 transporter that has yet to be cloned. These data suggest that TM8-9 confer the minimal domain requirement for the distinct substrate selectivity of N1 and N2 nucleoside transporters, and may form at least part of a substrate binding site in these transporters. Further changes within TM8-9 may alter the fitness of the binding pocket, therefore generating nucleoside transporters with novel properties that are not observed with either wild-type transporters (e.g. Chimera T8 and Chimera T9). However, it is also possible that TM8-9 themselves may not be directly involved in the binding and/or selectivity, but may influence the transport selectivity through indirect interactions with other sites in the transporter protein. Sequence alignment revealed that eleven amino acids

**Table 1. Apparent  $K_m$  Values of Wild-type and Chimeric Transporters.**

	Apparent $K_m$ ( $\mu\text{M}$ )		
	Uridine	Inosine	Thymidine
Wild-type N1	$34 \pm 17$	$15 \pm 1.6$	-
Wild-type N2	$22 \pm 7.9$	-	$4.9 \pm 1.7$
Chimera T8-9	$3.6 \pm 0.6$	$6.3 \pm 2.4$	-
Chimera T8	$20 \pm 2.7$	$24 \pm 3.6$	$14 \pm 4.9$

The initial velocities of uptake of each nucleosides were determined at 6-8 concentration points ranging from 1  $\mu\text{M}$  to 200  $\mu\text{M}$ . The apparent  $K_m$  values were determined by fitting data to the Michaelis-Menten equation. Dashes indicate no significant uptake of the respective nucleoside and hence no available  $K_m$  values.



differ in the 63 amino acids spanning the TM8-9 of rat N1 and N2 (Figure 6). Seven of the same substitutions are also conserved among N1 and N2 transporters cloned from human, rabbit, pig, and mouse (Figure 6). The importance of these residues in determining the substrate selectivity of N1 and N2 transporters needs to be investigated by mutation studies.

The construction of functional reciprocal chimeras with regions containing TM8-9 of N2 transplanted into N1 was not successful. Two constructs exhibited no transport activity when expressed in oocytes. In structure-function studies with chimeric proteins, the function of chimeras is often lost due to reasons that may include protein misfolding, functional impairment, or improper plasma membrane targeting (21-23). Further studies are needed to investigate why these reciprocal constructs are not functional.

Chimera T8, which displayed a broad N3 transport selectivity, exhibited apparent  $K_m$ 's for uridine, inosine, and thymidine similar to those of the wild-type N1 and N2 transporters (Table 1). Interestingly, Chimera T8-9, which maintained the transport selectivity of the wild-type N1, exhibited increased apparent transport affinities for both uridine ( $K_m = 3.6 \mu\text{M}$ ) and inosine ( $K_m = 6.3 \mu\text{M}$ ) as compared to those of wild type N1 ( $34 \mu\text{M}$  for uridine,  $15 \mu\text{M}$  for inosine) (Table 1). In transport kinetic analysis, the Michaelis constant  $K_m$  reflects not only substrate affinity for the binding site, but is also influenced by rate constants of substrate translocation and dissociation which occur subsequent to recognition (22). Therefore, the observed affinity changes of Chimera T8-9 may reflect changes in any of these three processes. The apparent maximal rate of transport ( $V_{\text{max}}$ ) reflects the efficiency by which each substrate is translocated, and is greatly influenced by the expression level (22). Consequently, direct comparison of  $V_{\text{max}}$  between independent experiments is not meaningful. However, under identical expression conditions, the observed single point transport activity for uridine usually followed the order of  $\text{N2} > \text{Chimera T8} > \text{Chimera T8-9} \approx \text{N1}$ .



In this study, I identified a discrete region (TM8-9) as the structural determinant for the distinct transport selectivity of the N1 and N2 Na<sup>+</sup>-dependent nucleoside transporters. TM8-9 may form at least part of a substrate binding site in these nucleoside transporters. Furthermore, examples of engineering transporters with novel substrate selectivity from known transporters are presented (Chimera T8 and Chimera T9). As the three-dimensional structures of membrane proteins remain difficult to achieve and the structure-function relations of Na<sup>+</sup>-cotransporters are largely unknown (24-27), this study using chimeric transporters provides insight into the structure-function relationship of the Na<sup>+</sup>-dependent nucleoside transporters. Information from such studies may benefit the design of nucleoside drugs with improved membrane permeability, targeting and disposition characteristics.

## References

1. Mani, S., and M. J. Ratain. Promising new agents in oncologic treatment. *Curr Opin Oncol* **8**:525-34 (1996).
2. Morse, G. D., M. J. Shelton, and A. M. O'Donnell. Comparative pharmacokinetics of antiviral nucleoside analogues. *Clin Pharmacokinet* **24**:101-23 (1993).
3. Lerman, B. B., and L. Belardinelli. Cardiac electrophysiology of adenosine. Basic and clinical concepts. *Circulation* **83**:1499-509 (1991).
4. Belt, J. A., N. M. Marina, D. A. Phelps, and C. R. Crawford. Nucleoside transport in normal and neoplastic cells. *Adv Enzyme Regul* **33**:235-52 (1993).
5. Griffith, D. A., and S. M. Jarvis. Nucleoside and nucleobase transport systems of mammalian cells. *Biochim Biophys Acta* **1286**:153-81 (1996).
6. Cass, C. E. Nucleoside transport, in *Drug Transport in Antimicrobial and Anticancer Chemotherapy*. (N. H. Georgopapadakou, ed.) pp.403-451, Marcel Dekker, New York (1995).
7. Wiley, J. S. Seeking the nucleoside transporter [news; comment]. *Nat Med* **3**:25-6 (1997).

8. Griffiths, M., N. Beaumont, S. Y. Yao, M. Sundaram, C. E. Boumah, A. Davies, F. Y. Kwong, I. Coe, C. E. Cass, J. D. Young, and S. A. Baldwin. Cloning of a human nucleoside transporter implicated in the cellular uptake of adenosine and chemotherapeutic drugs [see comments]. *Nat Med* **3**:89-93 (1997).
9. Che, M., D. F. Ortiz, and I. M. Arias. Primary structure and functional expression of a cDNA encoding the bile canalicular, purine-specific Na(+)-nucleoside cotransporter. *J Biol Chem* **270**:13596-9 (1995).
10. Huang, Q. Q., S. Y. Yao, M. W. Ritzel, A. R. Paterson, C. E. Cass, and J. D. Young. Cloning and functional expression of a complementary DNA encoding a mammalian nucleoside transport protein. *J Biol Chem* **269**:17757-60 (1994).
11. Gutierrez, M. M., and K. M. Giacomini. Substrate selectivity, potential sensitivity and stoichiometry of Na(+)-nucleoside transport in brush border membrane vesicles from human kidney. *Biochim Biophys Acta* **1149**:202-8 (1993).
12. Wu, X., G. Yuan, C. M. Brett, A. C. Hui, and K. M. Giacomini. Sodium-dependent nucleoside transport in choroid plexus from rabbit. Evidence for a single transporter for purine and pyrimidine nucleosides. *J Biol Chem* **267**:8813-8 (1992).
13. Roovers, K. I., and G. K. Meckling. Characterization of equilibrative and concentrative Na+-dependent (cif) nucleoside transport in acute promyelocytic leukemia NB4 cells. *J Cell Physiol* **166**:593-600 (1996).

14. Borgland, S. L., and F. E. Parkinson. Uptake and release of [3H]formycin B via sodium-dependent nucleoside transporters in mouse leukemic L1210/MA27.1 cells. *J Pharmacol Exp Ther* **281**:347-53 (1997).
15. Yao, S. Y., C. E. Cass, and J. D. Young. Transport of the antiviral nucleoside analogs 3'-azido-3'-deoxythymidine and 2',3'-dideoxycytidine by a recombinant nucleoside transporter (rCNT) expressed in *Xenopus laevis* oocytes. *Mol Pharmacol* **50**:388-93 (1996).
16. Yao, S. Y., A. M. Ng, M. W. Ritzel, W. P. Gati, C. E. Cass, and J. D. Young. Transport of adenosine by recombinant purine- and pyrimidine-selective sodium/nucleoside cotransporters from rat jejunum expressed in *Xenopus laevis* oocytes. *Mol Pharmacol* **50**:1529-35 (1996).
17. Schaner, M. E., J. Wang, S. Zevin, K. M. Gerstin, and K. M. Giacomini. Transient expression of a purine-selective nucleoside transporter (SPNTint) in a human cell line (HeLa). *Pharm Res* **14**:1316-21 (1997).
18. Wang, J., S. F. Su, M. J. Dresser, M. E. Schaner, C. B. Washington, and K. M. Giacomini. Na<sup>+</sup>-dependent purine nucleoside transporter from human kidney: cloning and functional characterization. *Am J Physiol* **273**:F1058-65 (1997).
19. Ritzel, M. W., S. Y. Yao, M. Y. Huang, J. F. Elliott, C. E. Cass, and J. D. Young. Molecular cloning and functional expression of cDNAs encoding a human Na<sup>+</sup>-nucleoside cotransporter (hCNT1). *Am J Physiol* **272**:C707-14 (1997).

20. Redlak, M. J., Z. E. Zehner, and S. L. Betcher. Expression of rabbit ileal N3 Na<sup>+</sup>/nucleoside cotransport activity in *Xenopus laevis* oocytes. *Biochem Biophys Res Commun* **225**:106-11 (1996).
21. Caron, M. G. Molecular neurobiology. The chimaeras speak again [news; comment]. *Nature* **366**:409 (1993).
22. Buck, K. J., and S. G. Amara. Chimeric dopamine-norepinephrine transporters delineate structural domains influencing selectivity for catecholamines and 1-methyl-4-phenylpyridinium. *Proc Natl Acad Sci U S A* **91**:12584-8 (1994).
23. Zhang, X., K. I. Collins, and L. M. Greenberger. Functional evidence that transmembrane 12 and the loop between transmembrane 11 and 12 form part of the drug-binding domain in P-glycoprotein encoded by MDR1. *J Biol Chem* **270**:5441-8 (1995).
24. Kaplan, J. H. Molecular biology of carrier proteins. *Cell* **72**:13-8 (1993).
25. Wright, E. M., D. D. Loo, E. Turk, and B. A. Hirayama. Sodium cotransporters. *Curr Opin Cell Biol* **8**:468-73 (1996).
26. Sadee, W., V. Drubbisch, and G. L. Amidon. Biology of membrane transport proteins. *Pharm Res* **12**:1823-37 (1995).
27. Panayotova, H. M., D. D. Loo, C. T. Kong, J. E. Lever, and E. M. Wright. Sugar binding to Na<sup>+</sup>/glucose cotransporters is determined by the carboxyl-terminal half of the protein. *J Biol Chem* **271**:10029-34 (1996).

## CHAPTER 5

### CHARACTERIZATION OF A BIOENGINEERED CHIMERIC $\text{Na}^+$ - NUCLEOSIDE TRANSPORTER<sup>1</sup>

In mammalian cells, transmembrane flux of nucleosides is mediated by both equilibrative and  $\text{Na}^+$ -dependent nucleoside transporters. These processes are essential for nucleotide synthesis by salvage pathways and are the route of cellular uptake of many therapeutic nucleosides used in the treatment of cancer, viral infections, and cardiac arrhythmias (1-3).

$\text{Na}^+$ -dependent nucleoside transporters mediate the active transport of nucleosides into cells by coupling the transmembrane flux of substrates to the physiological  $\text{Na}^+$  gradient across the plasma membrane. These transporters exhibit distinct transport selectivity for purine and pyrimidine nucleosides and have been classified into several subtypes based on their substrate selectivity. The N1 system is purine-selective; the N2 system is pyrimidine-selective; and the N3 system is broadly-selective, transporting both purine and pyrimidine nucleosides. Uridine, a pyrimidine nucleoside, and adenosine, a purine nucleoside, are ubiquitously transported by all  $\text{Na}^+$ -dependent nucleoside transport systems. A  $\text{Na}^+$ :nucleoside coupling ratio of 1:1 has been reported for N1 and N2 transporters, indicating that the inward transport of each nucleoside molecule is driven by

---

<sup>1</sup> This work is accepted for publication: Wang, J. and Giacomini, K.M. *Molecular Pharmacology*, in press, 1999.

the interaction of one sodium ion (1, 2, 4). In contrast, a stoichiometry of 2:1 was observed for the N3 system, indicating two sodium ions are required for the translocation of one nucleoside molecule (5).

The N1 and N2 subtype Na<sup>+</sup>-nucleoside transporters have now been cloned from rat (rCNT1 and SPNT) and human (hCNT1 and hSPNT1) (6-9). Although the cloned N1 and N2 transporters have distinct substrate selectivity for purine and pyrimidine nucleosides, they share a high sequence homology (60-70% ) and a similar predicted membrane topology (14 putative transmembrane domains). They belong to a CNT gene family that also includes the NupC proton-nucleoside symporter of *Escherichia coli* (Che *et al.*, 1995; Huang *et al.*, 1994; (10). The broadly-selective transporter, N3, was characterized in rabbit choroid plexus, rabbit ileum and rat jejunum (5, 11-13), and was also found in cultured human promyelocytic leukemia and colorectal carcinoma cells (14). However, the molecular identity of this transporter is currently unknown.

Recently, using a chimeric transporter approach, we demonstrated that transmembrane domains (TMDs) 8 and 9 of the cloned rat N1 and N2 transporters are the major sites for substrate binding and discrimination (15, Chapter 4). While constructing and analyzing a series of N1/N2 chimeric transporters, I noticed that one chimera exhibited an unusual substrate selectivity. This chimeric transporter, termed T8, is structurally identical to N2 except that the eighth transmembrane domain was replaced by that of N1 (Figure 1). Surprisingly, unlike the wild-type N1 or N2, which are selective for either purine or pyrimidine nucleosides, T8 transports both inosine (a purine nucleoside) and thymidine (a pyrimidine nucleoside) (15). T8-mediated uptake of uridine, a common substrate of both N1 and N2, was inhibited by naturally occurring purine and pyrimidine nucleosides (15). These data suggest that T8 may be an N3-like, broadly-selective transporter which accepts both purine and pyrimidine nucleosides. However, since only one purine and one model pyrimidine nucleoside were examined, and an inhibitor of a transporter may not be a substrate, it is not known whether T8 also transports other purine

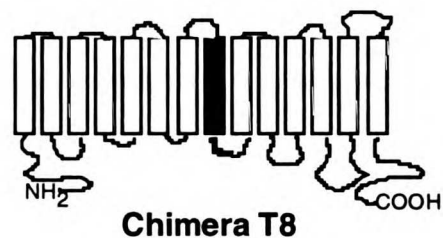
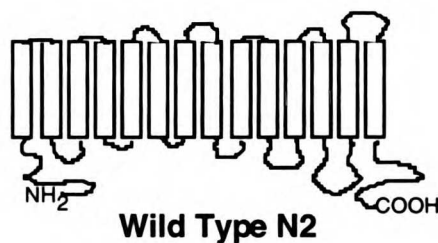


Figure 1. Secondary structures of chimera T8 and wild-type N1 and N2 transporters. Wild-type N1 represents the rat N1 clone SPNT (659 amino acids). Wild-type N2 represents the rat N2 clone rCNT1 (648 amino acids). Chimera T8 contains amino acid residues 1-300 of N2, 297-330 of N1, and 335-648 of N2.



and pyrimidine nucleosides such as guanosine and cytidine. Furthermore, if T8 is truly broadly-selective, does the enlarged substrate profile result from the combination of a distinct purine-selective site derived from N1 and a distinct pyrimidine-selective site derived from N2, i.e., the presence of two mutually exclusive recognition sites in the chimeric transporter? Alternatively, is the broad substrate selectivity of chimera T8 due to a single engineered binding site which recognizes both purine and pyrimidine nucleosides? In this study, I address these questions by determining the substrate profile, transport mechanism, and Na<sup>+</sup>-coupling stoichiometry of T8. Information from this study may help us to gain further understanding of functional properties of Na<sup>+</sup>-nucleoside transporters and may also pave the way for bioengineering nucleoside transporters for therapeutic purposes.

## **Materials and Methods**

*Chimera T8 cDNA.* The methods employed in the cDNA construction of chimeric transporters were described in Chapter 4. In brief, the cDNAs of wild-type rat N1 (SPNT) and N2 (rCNT1) were isolated by reverse transcriptase polymerase chain reaction. The Genetics Computer Group software (Wisconsin Package, Version 8 ) was used to align the nucleotides and the deduced amino acid sequences of N1 and N2. To construct chimera T8, a chimera, T8-14, consisting of TMD1-7 of N2 and TMD8-14 of N1 was first obtained by equivalent exchange at the internal *Nco I* sites. An equivalent *Afl II* site was then introduced into the N2 cDNA and chimera T8-14 cDNA at position 1158 by site-directed mutagenesis. Introducing the *Afl II* site in both clones did not change the encoded amino acids at these sites. T8 cDNA was then obtained from N2 and chimera T8-14 by equivalent exchange at the *Afl II* site. The sequence of T8 was confirmed by automated DNA sequencing in the Biochemical Resource Center at the University of California, San Francisco.

*Expression in Xenopus laevis Oocytes.* Plasmid containing chimera T8 was linearized with *XbaI*. cRNA was synthesized with T7 polymerase in the presence of

$m^7$ GpppG cap using the mCAP<sup>TM</sup> RNA Capping kit (Stratagene, La Jolla, CA). Oocytes were harvested from *Xenopus laevis* (Xenopus, Ann Arbor, MI) and defolliculated (16, 17). Healthy stage V and VI oocytes were injected with 50 nl of T8 cRNA (0.4 ng/nl) or 50 nl of water using a semi-automatic injector (PL1-188, Nikon, Melville, NY). Injected oocytes were maintained for 2-3 days at 18 °C in Barth's medium (88 mM NaCl, 1 mM KCl, 0.82 mM MgSO<sub>4</sub>, 0.4 mM CaCl<sub>2</sub>, 0.33 mM Ca(NO<sub>3</sub>)<sub>2</sub>, 2.4 mM NaHCO<sub>3</sub>, 10 mM HEPES/Tris, pH 7.4) before the assay of transport activity. Uptake experiments were carried out 48-56 hours post-injection. To minimize variability, each experiment used oocytes from a single animal.

*Transport Assays.* Uptake of nucleosides by oocytes was traced with the respective <sup>3</sup>H-labeled nucleosides (Moravek Biochemicals, Brea, CA). Assays were performed at 25°C on groups of 10 oocytes in 150 µl of transport buffer containing 100 mM NaCl or 100 mM choline chloride and 2 mM KCl, 1 mM CaCl<sub>2</sub>, 1 mM MgCl<sub>2</sub>, 10 mM HEPES, pH 7.4. At the end of the incubation, uptake was terminated by removing the incubation medium followed by six rapid washes in ice-cold choline chloride buffer. Individual oocytes were dissolved in 10% SDS and the radioactive content of each oocytes was assayed by liquid scintillation counting. For inhibition studies, nonradioactive compounds (Sigma Chemicals, St. Louis, MO) were also included in the reaction mixture at concentrations indicated in the figure legends. Chimera T8-mediated thymidine and inosine uptake was linear up to 1-3 hours, therefore initial rates of uptake in kinetic studies were measured using an incubation period of 30 min. For studies designed to determine the Na<sup>+</sup> stoichiometric coupling ratio, oocytes were preincubated in choline buffer at 25 °C for 30 min and washed three times with choline buffer before uptake to remove extracellular Na<sup>+</sup>. <sup>3</sup>H-nucleoside (10 µM) uptake was then measured in transport buffer containing 0-100 mM NaCl, using choline chloride to maintain isosmolality.

*Data Analysis.* Uptake values are presented as mean  $\pm$  standard error for 8-10 individual oocytes. The kinetic parameters were determined by fitting velocity/substrate versus velocity to the equation obtained from the Eadie-Hofstee linear transformation of the Michaelis-Menten equation. In particular, the data were fit to the equation  $V = V_{max} - K_m \cdot V/S$  where  $V$  is the initial rate of uptake,  $V_{max}$  is the maximal transport rate,  $K_m$  is the concentration of nucleoside when the initial rate is at one-half of the maximum, and  $S$  is the nucleoside concentration in the reaction mixture. Apparent  $V_{max}$  and  $K_m$  values were obtained from the slopes ( $-K_m$ ) and vertical intercepts ( $V_{max}$ ) of the Eadie-Hofstee plots. To ascertain the stoichiometric coupling ratio between  $\text{Na}^+$  and nucleoside, the data were fit to the following Hill equation:  $V = V_{max} \cdot C_{\text{Na}^+}^n / (K_d^n + C_{\text{Na}^+}^n)$  where  $V$  is the initial rate of uptake,  $V_{max}$  is the maximal rate of nucleoside transport at saturating concentrations of  $\text{Na}^+$ ,  $C_{\text{Na}^+}$  is the concentration of  $\text{Na}^+$ ,  $K_d$  is the concentration of  $\text{Na}^+$  that is able to produce one-half of the maximum rate of nucleoside transport, and  $n$  is the Hill coefficient. The fits were carried out using a nonlinear, least-squares regression fitting program of Kaleidagraph (Version 3.0, Synergy Software). Statistical analysis was carried out by comparing the tested compounds to the controls from the same experiments using an unpaired Student's  $t$ -test. Results were considered statistically different with a probability of  $p < 0.05$ .

## **Results**

*Transport of Naturally Occurring Nucleosides.* The first evidence of the broad substrate selectivity of T8 came from the observation that both inosine and thymidine are transported by this chimeric transporter (15). However, it is not known whether the transporter is truly "broadly selective". That is, are other nucleosides transported by T8. To investigate whether T8 is truly a broadly-selective transporter that also accepts other

purine and pyrimidine nucleosides as substrates, I examined the uptake of  $^3\text{H}$ -labeled naturally occurring purine (adenosine, inosine, and guanosine) and pyrimidine nucleosides (uridine, thymidine, and cytidine) by oocytes injected with T8 cRNA. Compared to water injected oocytes, a  $\text{Na}^+$ -dependent increase (3.5 to 9.6 fold) in the uptake of  $^3\text{H}$ -labeled adenosine, inosine, and guanosine was observed in T8 cRNA-injected oocytes (Figure 2). For  $^3\text{H}$ -labeled pyrimidine nucleosides (uridine, thymidine, and cytidine), a 10.6 to 18.6 fold increase was observed (Figure 3). These data suggest that T8 is a  $\text{Na}^+$ -dependent, broadly-selective nucleoside transporter which accepts both purine and pyrimidine nucleosides as substrates.

*Mechanism of Broad Selectivity.* Since T8 is derived from wild-type N1 and N2 transporters, there are two potential mechanisms for its broad substrate selectivity. It is possible that T8 possesses two binding sites, one purine-binding site obtained from N1, and one pyrimidine-binding site obtained from N2, therefore exhibiting an apparent broad selectivity for both purine and pyrimidine nucleosides. Alternatively, it is also possible that introducing TMD8 of N1 into N2 altered the binding site of N2, expanding its transport capacity to purine nucleosides. To investigate the mechanism (two mutually exclusive binding sites or one single engineered binding site ) by which T8 transports purine and pyrimidine nucleosides, I studied the effect of purine nucleosides on T8-mediated pyrimidine nucleoside uptake and the effect of pyrimidine nucleosides on T8-mediated purine nucleoside uptake using inosine as a model purine nucleoside and thymidine as a model pyrimidine nucleoside.

If T8 interacts with purine and pyrimidine nucleosides through two mutually exclusive recognition sites, inosine should not inhibit the transport of thymidine and vice versa. However, if inosine and thymidine share a common binding site, inosine should be able to inhibit the transport of thymidine and vice versa. The data show that thymidine

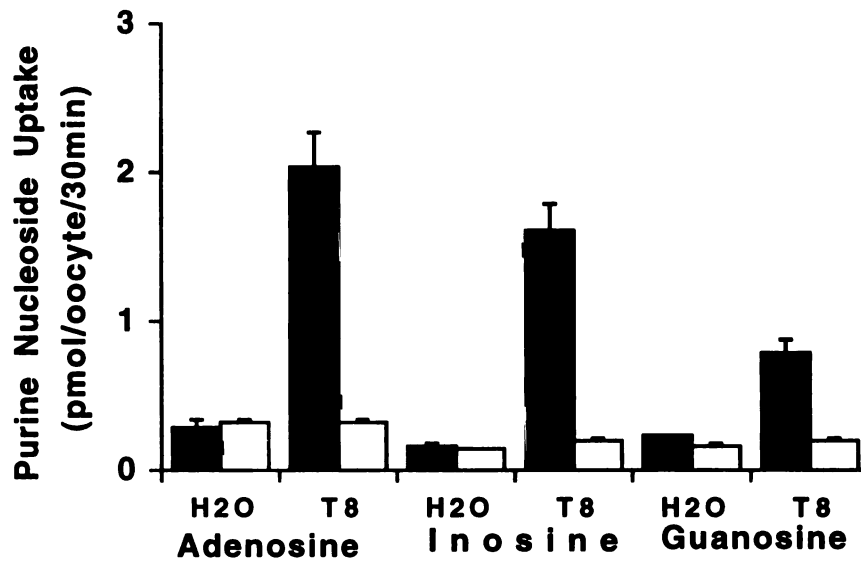


Figure 2. Uptake of  $^3\text{H}$ -labeled naturally occurring purine nucleosides by Chimera T8. Each value represents the mean  $\pm$  S.E. of data obtained from 8-10 individual oocytes from one representative experiment.

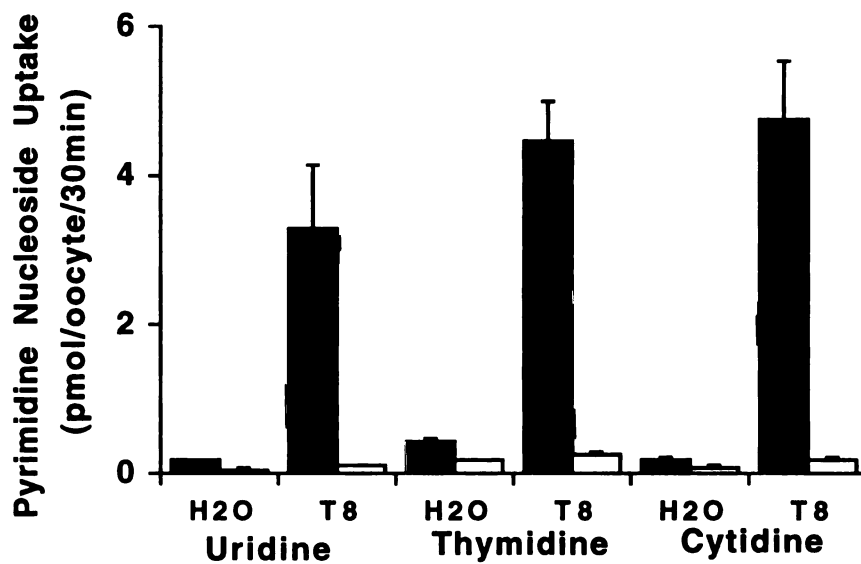


Figure 3. Uptake of  $^3\text{H}$ -labeled naturally occurring pyrimidine nucleosides by Chimera T8. Each value represents the mean  $\pm$  S.E. of data obtained from 8-10 individual oocytes from one representative experiment.

uptake was completely inhibited by (1 mM) inosine (Figure 4) and inosine uptake was completely inhibited by (1 mM) thymidine (Figure 5), suggesting that the two compounds share a single recognition site in T8.

I further determined the mechanism of interaction between inosine and thymidine. The effect of inosine at different concentrations (0, 20, and 40  $\mu\text{M}$ ) on the initial rate of thymidine uptake (Figure 6) and the effect of thymidine at different concentrations (0, 20, and 40  $\mu\text{M}$ ) on the initial rate of inosine uptake (Figure 7) were determined in the presence of  $\text{Na}^+$ . The  $\text{Na}^+$ -driven transport of thymidine was saturable ( $K_m = 41 \pm 5 \mu\text{M}$  and  $V_{max} = 7.0 \pm 0.6 \text{ pmol/oocyte/30min}$ ). In the presence of 20 and 40  $\mu\text{M}$  inosine, the apparent  $K_m$  values of thymidine ( $79 \pm 9$  and  $122 \pm 33 \mu\text{M}$ , respectively) increased significantly ( $p < 0.05$ ), whereas the apparent  $V_{max}$  values ( $8.6 \pm 0.7$  and  $9.6 \pm 2.0 \text{ pmol/oocyte/30min}$ , respectively) were not significantly different. The  $\text{Na}^+$ -driven transport of inosine was also saturable ( $K_m = 14.5 \pm 2.1 \mu\text{M}$  and  $V_{max} = 3.6 \pm 0.3 \text{ pmol/oocyte/30min}$ ). In the presence of 20 and 40  $\mu\text{M}$  thymidine, the apparent  $K_m$  values of inosine ( $34 \pm 3$  and  $36 \pm 6 \mu\text{M}$ , respectively) increased significantly ( $p < 0.05$ ), whereas the apparent  $V_{max}$  values ( $3.7 \pm 0.2$  and  $3.5 \pm 0.4 \text{ pmol/oocyte/30min}$ , respectively) were not significantly different. These data suggest that inosine competitively inhibits the transport of thymidine and thymidine competitively inhibits the transport of inosine. Eadie-Hofstee plot of these data generated inhibition patterns consistent with a competitive mechanism (Figure 6 and 7 inserts). These data further support that inosine and thymidine compete for the same substrate binding site in T8.

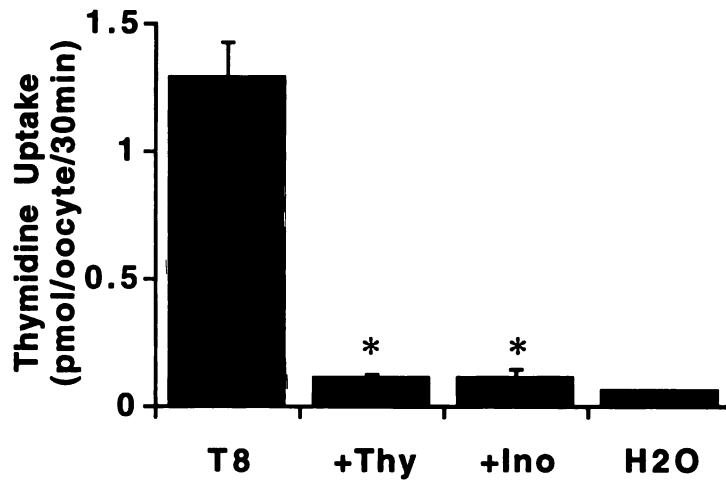


Figure 4. Effect of inosine on  $^3\text{H}$ -thymidine uptake.  $^3\text{H}$ -thymidine uptake was determined in  $\text{Na}^+$ -containing buffer in the absence or presence of 1 mM inosine (Ino) or thymidine (Thy). Each value represents the mean  $\pm$  S.E. ( $n=8-10$ ). Both inosine and thymidine significantly inhibited the uptake (\*,  $p < 0.05$ ).



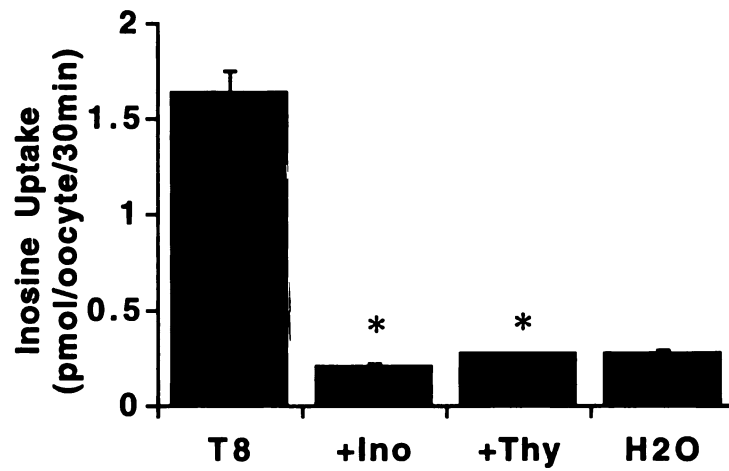


Figure 5. Effect of thymidine on  $^3\text{H}$ -inosine uptake.  $^3\text{H}$ -inosine uptake was determined in  $\text{Na}^+$ -containing buffer in the absence or presence of 1 mM inosine (Ino) or thymidine (Thy). Each value represents the mean  $\pm$  S.E. ( $n=8-10$ ). Both inosine and thymidine significantly inhibited the uptake (\*,  $p < 0.05$ ).

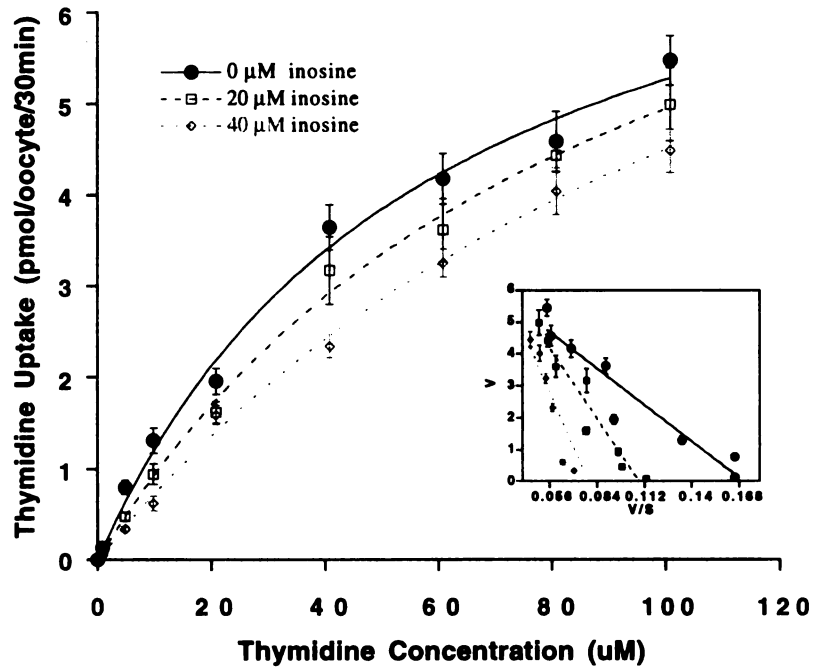


Figure 6. The inhibition mechanism of thymidine uptake by inosine. Uptake was determined in  $\text{Na}^+$ -containing buffer in the absence (solid circles) or presence of 20  $\mu\text{M}$  (squares) or 40  $\mu\text{M}$  (diamonds) of inosine. Each value represents the mean  $\pm$  S.E. ( $n = 8-10$ ). *Insert*, Eadie-Hofstee plots. V: rate of uptake. V/S: rate of uptake/substrate concentration.

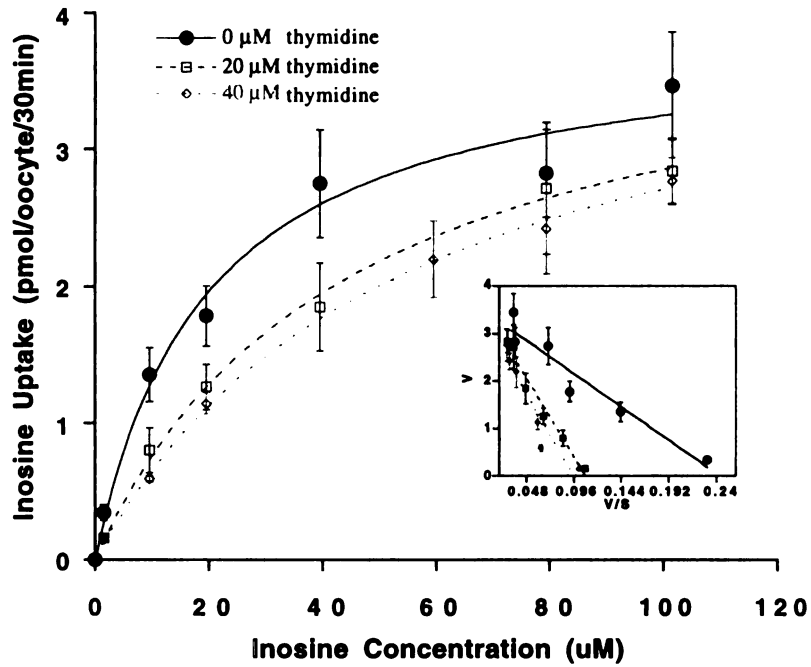


Figure 7. The inhibition mechanism of inosine uptake by thymidine. Uptake was determined in Na<sup>+</sup>-containing buffer in the absence (solid circles) or presence of 20  $\mu$ M (squares) or 40  $\mu$ M (diamonds) of thymidine. Each value represents the mean  $\pm$  S.E. (n = 8-10). *Insert*, Eadie-Hofstee plots. V: rate of uptake. V/S: rate of uptake/substrate concentration.

*Interaction with Nucleoside Analogs.* Because the data suggested that the broad substrate selectivity of T8 may result from changes within the binding site of N2, I hypothesized that T8 may possess novel selectivity for synthetic nucleoside analogs which include a wide array of therapeutic agents. The effect of various compounds on the Na<sup>+</sup>-driven transport of thymidine was studied to further define the substrate profile of T8 (Figure 8). At 1 mM, inosine, thymidine, formycin B, 2-chloro-adenosine (2CA) and 5-fluoro-uridine (5FUrd), 2-chloro-2'-deoxyadenosine (2CdA), and 5-iodo-2'-deoxyuridine (5IdUrd), significantly inhibited ( $p < 0.05$ ) Na<sup>+</sup>-driven thymidine uptake (Figure 8). At the same concentration (1 mM), ribose, thymine, xanthine, L-thymidine, 5'-thymidine monophosphate, 3'-thymidine monophosphate, 2', 3'-dideoxyinosine (ddI), 2', 3'-dideoxycytidine (ddC), 3'-azidothymidine (AZT), cytosine arabinoside (AraC), and acyclovir (Acycl) were unable to inhibit Na<sup>+</sup>-driven thymidine uptake significantly (Figure 8). Two <sup>3</sup>H-labeled compounds, 2-CdA and L-thymidine were further tested in uptake studies (Figure 9). For <sup>3</sup>H-labeled 2CdA, significantly increased uptake was observed (Figure 9) and as expected, there was no significant <sup>3</sup>H-labeled L-thymidine uptake (Figure 9). These data suggest chimera T8 is a Na<sup>+</sup>-dependent nucleoside transporter that selectively transports naturally occurring nucleosides or synthetic nucleosides that have been modified on the base or/and on the 2'-position of the ribose. Interestingly, the substrate profile of T8 is very similar to the well-characterized broadly-selective transport system N3 (5, 11). In contrast, ddI, ddC and AZT, which contain modifications on the 3'-position of the ribose and are known inhibitors of N1 or N2, did not inhibit T8-mediated uptake, further suggesting that T8 does not exhibit the combined characteristics of N1 and N2.

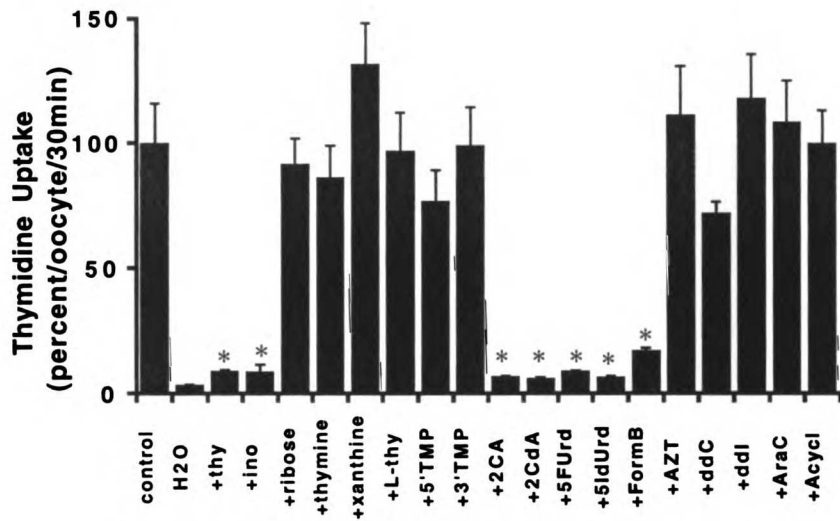


Figure 8. Effects of nucleoside and nucleoside analogs on  $^3\text{H}$ -thymidine uptake in oocytes injected with T8 cRNA. Uptake was determined in  $\text{Na}^+$ -containing buffer in the presence and absence (control) of 1 mM of various compounds. \* Significantly inhibited the T8-mediated uptake of thymidine ( $p < 0.05$ ).

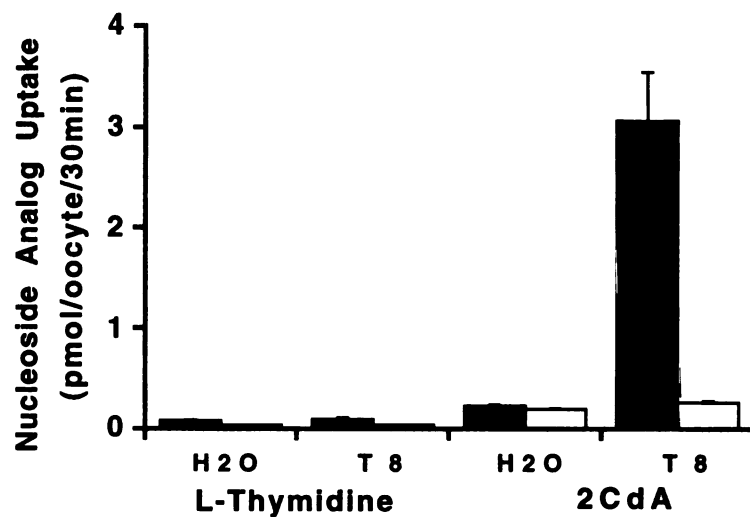


Figure 9. Uptake of <sup>3</sup>H-labeled L-thymidine and 2CdA by Chimera T8. Each value represents the mean ± S.E. (n = 8-10).

*Na<sup>+</sup> Stoichiometry.* To determine the Na<sup>+</sup> stoichiometry of T8, the effect of Na<sup>+</sup> concentrations, ranging from 0 to 100 mM, on the initial uptake of thymidine and inosine (10 μM) was examined. The uptake of thymidine (Figure 10) and inosine (Figure 11) was sensitive to Na<sup>+</sup> concentration. The data were fit to a Hill equation as described under "Materials and Methods". The predicted Na<sup>+</sup>/nucleoside coupling stoichiometry of T8, determined from Hill coefficients, was not significantly different from 1 for both thymidine and inosine (Hill coefficients,  $1.16 \pm 0.34$  and  $1.05 \pm 0.27$ , respectively). Previous studies have established a 1:1 coupling ratio for the wild-type N1 and N2 transporters (1, 2, 4). In contrast, the coupling ratios for the N3 system was determined to be 2:1 (5).

## **Discussion**

In this study, I functionally characterized a bioengineered chimeric Na<sup>+</sup>-nucleoside transporter T8. The structure of T8 is identical to the pyrimidine-selective Na<sup>+</sup>-nucleoside transporter N2 except that TMD8 was replaced by that of N1 (Figure 1). Previously using chimeric N1/N2 transporters, I demonstrated that TMD8-9 determined the substrate selectivity of N1 and N2 transporters and may constitute a major part of the substrate-binding site in these transporters (15). The integrity of TMD8-9 may be necessary for chimeric transporters to maintain the substrate selectivity of wild-type transporters since chimeras with junction sites within TMD8-9 seemed to exhibit novel properties (15). In this study, I functionally characterized chimera T8 and specifically determined its substrate profile and transport mechanism. Data from this study suggest that chimera T8 is a broadly-selective nucleoside transporter which transports both purine and pyrimidine nucleosides (Figures 2 and 3). This broad substrate selectivity may be due to structural

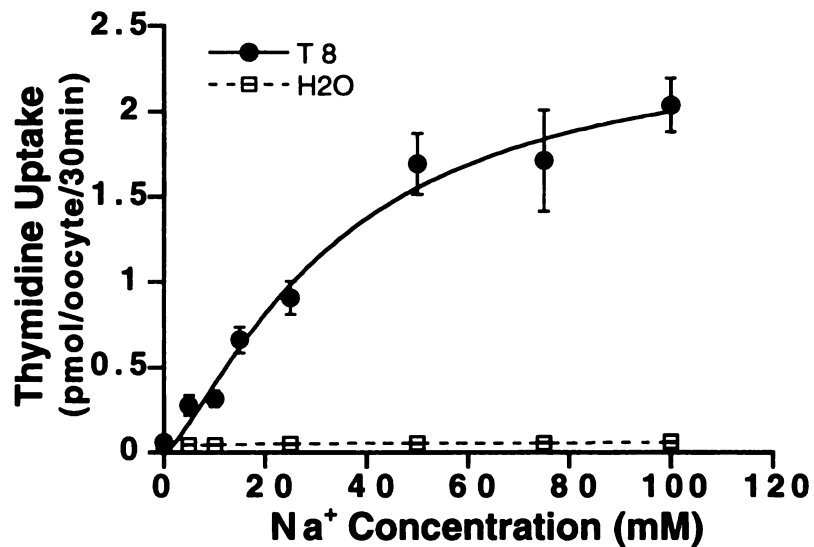


Figure 10. Sodium dependency of T8-mediated uptake of thymidine. Uptake was measured in transport buffer containing 0-100 mM NaCl, using choline chloride to maintain isosmolality. Each value represents the mean  $\pm$  S.E. (n = 8-10). Hill coefficient was determined by fitting the data to the Hill equation using non-linear regression analysis.



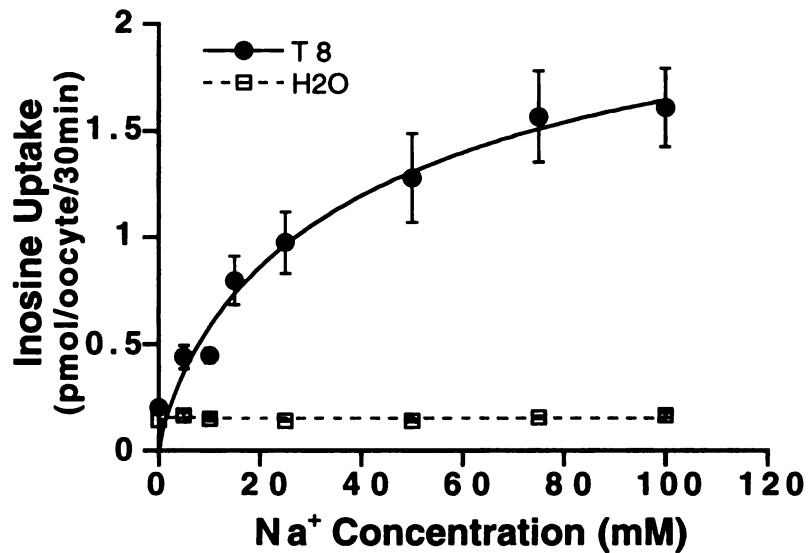


Figure 11. Sodium dependency of T8-mediated uptake of inosine. Uptake was measured in transport buffer containing 0-100 mM NaCl, using choline chloride to maintain isosmolality. Each value represents the mean  $\pm$  S.E. ( $n = 8-10$ ). Hill coefficient was determined by fitting the data to the Hill equation using non-linear regression analysis.

alterations within the binding pocket of N2, i.e. the presence of a single engineered binding site which recognizes both purine and pyrimidine nucleosides. Alternatively, the purine-selective site of N1 may be located in TMD8 and the pyrimidine-selective site of N2 may be located in TMD9; the broad substrate selectivity of T8 is simply due to the presence of these two mutually exclusive binding sites. To investigate whether T8 transports purine and pyrimidine nucleosides following interaction with one binding site or two independent binding sites, I studied the effect of inosine on T8-mediated thymidine uptake and the effect of thymidine on T8-mediated inosine uptake. The data showed that thymidine uptake was completely inhibited by inosine (Figure 4) and inosine uptake was completely inhibited by thymidine (Figure 5). Furthermore, the inhibition mechanisms were found to be competitive (Figures 6 and 7), suggesting that inosine and thymidine compete for the same substrate-binding site in T8. Collectively, these data suggest that transplanting TMD8 of N1 into N2 altered the structure of the substrate binding pocket of N2 and subsequently expanded the transport capacity of N2 to purine nucleosides.

The potential of T8 to interact with synthetic nucleoside analogs was evaluated in inhibition studies. The data in Figure 8 indicated that base-modified and 2'-ribose modified nucleosides are potent inhibitors of T8. The uptake study with <sup>3</sup>H-labeled 2-CdA (Figure 9) further demonstrated that this anticancer nucleoside is also a true permeant of T8. Previously Yao *et al.* studied the interaction of rat N2 with the antiviral drug AZT and ddC in the *Xenopus laevis* oocytes expression system (18). They found both drugs were inhibitors as well as permeants of N2 ( $K_m = 550$  and  $503 \mu\text{M}$ , respectively). Recently Schaner *et al.* demonstrated in a HeLa cell expression system that another commonly used antiviral agent, ddI, was a potent inhibitor of the wild-type rat N1 transporter ( $\text{IC}_{50} = 46 \mu\text{M}$ ) (19). In contrast, none of these compounds (AZT, ddC, and ddI) at 1 mM concentration was able to inhibit T8-mediated thymidine uptake (Figure 8). These data

further suggest that the substrate selectivity of T8 is not a simple combination of those of N2 and N1, but rather a novel property resulting from an engineered binding site.

In nature, Na<sup>+</sup>-dependent, broadly-selective nucleoside transporters have been well-documented in rabbit choroid plexus, rabbit ileum and rat jejunum (5, 11-13). These transporters, classified as N3 subtypes, were also described in cultured human promyelocytic leukemia and colorectal carcinoma cells (14). However, to date no typical N3 transporter has been cloned and the molecular identity of N3 is still unknown. Interestingly, the substrate profile of T8 is amazingly similar to that of N3. Both are broadly-selective nucleoside transporters which accept ribo- and 2'-deoxyribo- purine and pyrimidine nucleosides (Figures 2 and 3) as substrates (5, 11). Both interact with synthetic base-modified ribo- or 2'-deoxyribo- nucleosides (e.g. 2-CA, 5FUrd, and 5IdUrd) but not with ribose-modified nucleosides such as AZT and AraC and 2', 3'-dideoxynucleosides such as ddC and ddI (Figure 8 ) (5, 11). It is possible that the sequence of the uncloned N3 transporter may be very similar to the cloned N2 transporter since only a few amino acid substitutions during evolution in the TMD8 region may transform N2 into an N3 subtype transporter. Alternatively, the N2 and N1 transporters may evolve from a common N3-type ancestor and gain their substrate selectivity by a few amino acid substitutions in the TMD8-9 region. However, the Na<sup>+</sup>-coupling ratio of T8 was determined to be 1 (Figures 10 and 11), identical to the coupling ratios of N1 and N2 but different from the 2:1 ratio of N3 determined in choroid plexus. Therefore, the Na<sup>+</sup>-coupling ratio of these transporters may not be necessarily linked to their substrate selectivity, or in other words, the Na<sup>+</sup>-binding site in these transporters may be a distinct domain separated from but energetically coupled to the substrate-binding domain.

In this study, I present functional characteristics of a bioengineered chimeric Na<sup>+</sup>-nucleoside transporter. Consistent with our previous finding that TMD8-9 are the major structural components of the substrate-binding site in Na<sup>+</sup>-nucleoside transporters (15), the

unique transport characteristics of chimera T8 reflected the intrinsic changes within this binding site. The finding that chimera T8 possesses novel substrate selectivity unique to a third subtype of nucleoside transporters suggests that novel transporters can be engineered from known transporters. A thorough understanding of the molecular mechanisms governing the functional properties of the Na<sup>+</sup>-nucleoside transporters may help us to utilize these transporters or bioengineer new transporters for site-specific drug targeting and delivery.

## References

1. Cass, C. E. Nucleoside transport, in *Drug Transport in Antimicrobial and Anticancer Chemotherapy*. (N. H. Georgopapadakou, ed.) pp.403-451, Marcel Dekker, New York (1995).
2. Griffith, D. A., and S. M. Jarvis. Nucleoside and nucleobase transport systems of mammalian cells. *Biochim Biophys Acta* **1286**:153-81 (1996).
3. Wang, J., M. E. Schaner, S. Thomassen, S. F. Su, M. Piquette-Miller, and K. M. Giacomini. Functional and molecular characteristics of Na(+)-dependent nucleoside transporters. *Pharm Res* **14**:1524-32 (1997).
4. Yao, S. Y., A. M. Ng, M. W. Ritzel, W. P. Gati, C. E. Cass, and J. D. Young. Transport of adenosine by recombinant purine- and pyrimidine-selective sodium/nucleoside cotransporters from rat jejunum expressed in *Xenopus laevis* oocytes. *Mol Pharmacol* **50**:1529-35 (1996).
5. Wu, X., G. Yuan, C. M. Brett, A. C. Hui, and K. M. Giacomini. Sodium-dependent nucleoside transport in choroid plexus from rabbit. Evidence for a single transporter for purine and pyrimidine nucleosides. *J Biol Chem* **267**:8813-8 (1992).
6. Huang, Q. Q., S. Y. Yao, M. W. Ritzel, A. R. Paterson, C. E. Cass, and J. D. Young. Cloning and functional expression of a complementary DNA encoding a mammalian nucleoside transport protein. *J Biol Chem* **269**:17757-60 (1994).

7. Che, M., D. F. Ortiz, and I. M. Arias. Primary structure and functional expression of a cDNA encoding the bile canalicular, purine-specific Na(+)-nucleoside cotransporter. *J Biol Chem* **270**:13596-9 (1995).
8. Ritzel, M. W., S. Y. Yao, M. Y. Huang, J. F. Elliott, C. E. Cass, and J. D. Young. Molecular cloning and functional expression of cDNAs encoding a human Na<sup>+</sup>-nucleoside cotransporter (hCNT1). *Am J Physiol* **272**:C707-14 (1997).
9. Wang, J., S. F. Su, M. J. Dresser, M. E. Schaner, C. B. Washington, and K. M. Giacomini. Na(+)-dependent purine nucleoside transporter from human kidney: cloning and functional characterization. *Am J Physiol* **273**:F1058-65 (1997).
10. Craig, J. E., Y. Zhang, and M. P. Gallagher. Cloning of the nupC gene of *Escherichia coli* encoding a nucleoside transport system, and identification of an adjacent insertion element, IS 186. *Mol Microbiol* **11**:1159-68 (1994).
11. Wu, X., M. M. Gutierrez, and K. M. Giacomini. Further characterization of the sodium-dependent nucleoside transporter (N3) in choroid plexus from rabbit. *Biochim Biophys Acta* **1191**:190-6 (1994).
12. Huang, Q. Q., C. M. Harvey, A. R. Paterson, C. E. Cass, and J. D. Young. Functional expression of Na(+)-dependent nucleoside transport systems of rat intestine in isolated oocytes of *Xenopus laevis*. Demonstration that rat jejunum expresses the purine-selective system N1 (cif) and a second, novel system N3 having broad specificity for purine and pyrimidine nucleosides. *J Biol Chem* **268**:20613-9 (1993).

13. Redlak, M. J., Z. E. Zehner, and S. L. Betcher. Expression of rabbit ileal N3 Na<sup>+</sup>/nucleoside cotransport activity in *Xenopus laevis* oocytes. *Biochem Biophys Res Commun* **225**:106-11 (1996).
14. Belt, J. A., N. M. Marina, D. A. Phelps, and C. R. Crawford. Nucleoside transport in normal and neoplastic cells. *Adv Enzyme Regul* **33**:235-52 (1993).
15. Wang, J., and K. M. Giacomini. Molecular determinants of substrate selectivity in Na<sup>+</sup>-dependent nucleoside transporters. *J Biol Chem* **272**:28845-8 (1997).
16. Giacomini, K. M., D. Markovich, A. Werner, J. Biber, X. Wu, and H. Murer. Expression of a renal Na<sup>(+)</sup>-nucleoside cotransport system (N2) in *Xenopus laevis* oocytes. *Pflugers Arch* **427**:381-3 (1994).
17. Zhang, L., M. J. Dresser, A. T. Gray, S. C. Yost, S. Terashita, and K. M. Giacomini. Cloning and functional expression of a human liver organic cation transporter. *Mol Pharmacol* **51**:913-21 (1997).
18. Yao, S. Y., C. E. Cass, and J. D. Young. Transport of the antiviral nucleoside analogs 3'-azido-3'-deoxythymidine and 2',3'-dideoxycytidine by a recombinant nucleoside transporter (rCNT) expressed in *Xenopus laevis* oocytes. *Mol Pharmacol* **50**:388-93 (1996).
19. Schaner, M. E., J. Wang, S. Zevin, K. M. Gerstin, and K. M. Giacomini. Transient expression of a purine-selective nucleoside transporter (SPNTint) in a human cell line (HeLa). *Pharm Res* **14**:1316-21 (1997).

## CHAPTER 6

### MOLECULAR DETERMINANTS OF PYRIMIDINE SELECTIVITY IN N2 Na<sup>+</sup>-NUCLEOSIDE TRANSPORTER<sup>1</sup>

Na<sup>+</sup>-dependent nucleoside transporters play critical roles in cellular uptake of purine and pyrimidine nucleosides (1-3). These transporters are also important in the absorption and elimination of many therapeutic nucleoside analogs such as 2-chlorodeoxyadenosine, azidothymidine, and 2',3'-dideoxycytidine used in the treatment of cancer and viral infections (4-6). Na<sup>+</sup>-nucleoside transporters exhibit distinct transport selectivity for purine and pyrimidine nucleosides and have been classified into several subtypes based on their substrate selectivity (1-3). The N1 (or *cif*) system is selective for purine nucleosides; the N2 (or *cit*) system is selective for pyrimidine nucleosides; and the N3 (or *cib*) system is broadly-selective (or non-selective), transporting both purine and pyrimidine nucleosides. Uridine, a pyrimidine nucleoside, and adenosine, a purine nucleoside, are ubiquitously transported by all three systems. Recently the N1 and N2 transporters were cloned from rat and human (5, 7-9). Although the cloned N1 and N2 transporters have distinct substrate selectivity for pyrimidine and purine nucleosides, they share a high sequence homology (60-70% ) and a similar predicted membrane topology (14 putative transmembrane domains). The broadly-selective transporter, N3, was characterized in a number of tissues and cells (10-12), but the molecular identity of this transporter is currently unknown.

---

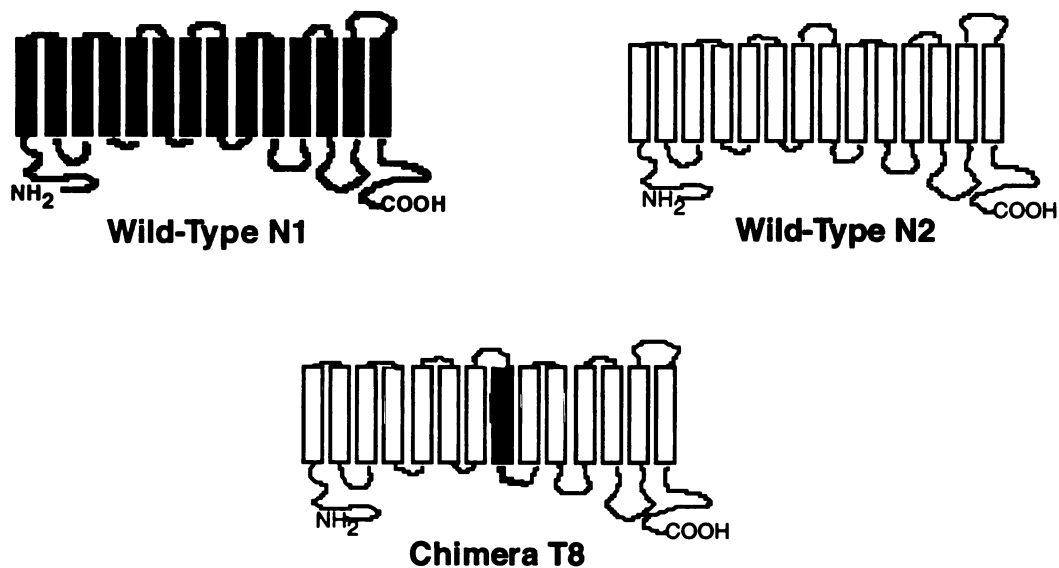
<sup>1</sup> This work is accepted for publication: Wang, J. and Giacomini, K.M. *Journal of Biological Chemistry*, in press, 1999.



To determine the structural basis for substrate recognition and discrimination in the Na<sup>+</sup>-nucleoside transporters, we previously took advantage of the high sequence similarity and yet distinct substrate selectivity of the cloned N1 and N2 transporters. By constructing and analyzing a series of chimeric rat N1/N2 transporters, I demonstrated that TMs 8 and 9 are the major sites for substrate binding and discrimination (13, Chapter 4). Interestingly, when TM8 of N2 was replaced by that of N1, the resulting transporter, chimera T8, lost pyrimidine selectivity and became a broadly-selective (or non-selective) transporter which accepts both purine and pyrimidine nucleosides as substrates (13, Chapter 4). Sequence alignment revealed that 5 amino acid residues differ between rat N2 and N1 in the TM8 region (Figure 1), suggesting that simultaneous replacement of the five divergent residues in TM8 of N2 with the corresponding residues in N1 would cause N2 to lose its selectivity for pyrimidine nucleosides. It is possible that individual residues in TM8 of N2 may gate the substrate permeation pathway which would only allow pyrimidine nucleosides and the common substrate, adenosine, to pass through. Substitution of these residues removes the gating validity, resulting in non-selective transporters (e.g. chimera T8) that also allow the passage of purine nucleosides (Chapter 5).

In this study, I focused on determining the specific residues responsible for maintaining the substrate selectivity of N2. By site-directed mutagenesis, the five residues in N2 were systematically mutated to the corresponding residues in N1 (Table 1). The substrate selectivity of each mutant was subsequently evaluated in the *Xenopus laevis* oocyte expression system. The data suggest that a single residue, serine 318, is responsible for maintaining the pyrimidine selectivity of N2. An adjacent residue, glutamine 319, was found to be important in influencing the apparent affinity for nucleosides.

A



B

		<u>TM8</u>	
<b>N2:</b>	301	MGTS <b>S</b> AT <b>E</b> T <b>L</b> SVAGNIFV <b>S</b> QTEAPLLIRPYLADMT	334
<b>N1:</b>		MG <b>T</b> <b>T</b> A <b>A</b> ET <b>L</b> AVAGNIFV <b>G</b> MTEAPLLIRPYLADMT	

Figure 1. Secondary structures of chimera T8 and wild-type N1 and N2 transporters (A). The amino acid sequences of N2 and N1 in TM8 region (B). The five residues which differ between N2 and N1 in TM8 are shown in bold. The numbers refer to the sequence of rat N2.

**Table 1. Systematic Amino Acid Substitutions in Mutants and in Chimera T8.**

<b>Construct</b>	<b>Sequence and Substitution</b>								
Wild-Type N2	MGT	<b>S</b>	<b>A</b>	TETLS	<b>S</b>	VAGNIFV	<b>S</b>	<b>Q</b>	TEAPLLIRPYLADMT
S304T		<b>T</b>							
T306A			<b>A</b>						
S310A				<b>A</b>					
S318G								<b>G</b>	
Q319M									<b>M</b>
S318G/Q319M									<b>GM</b>
T8.G318S		<b>T</b>	<b>A</b>	<b>A</b>					<b>M</b>
Chimera T8		<b>T</b>	<b>A</b>	<b>A</b>					<b>GM</b>

## Materials and Methods

*Site-directed Mutagenesis and Sequence Analysis.* The cDNAs of wild-type rat N1 (SPNT) and N2 (CNT1) transporters were obtained by reverse transcriptase polymerase chain reaction (13). The mutagenic oligonucleotides were synthesized in the Biochemical Resource Center at the University of California, San Francisco. The Stratagene's Chameleon™ and QuickChange™ site-directed mutagenesis kits (Stratagene) were used to construct mutant cDNAs following the manufacturer's protocols. Mutants with single amino acid substitutions (S304T, T306A, S310A, S318G, and Q319M) were prepared using the cDNA of wild-type rat N2 as template. The double mutant S318G/Q319M was constructed by introducing a second mutation (Q to M) at position 319 of mutant S318G. The mutant T8.G318S was constructed by changing Glycine 318 to Serine in a previously described chimeric transporter T8 (13). The sequence of each mutant was confirmed by direct DNA sequencing using an automated DNA sequencer (Applied Biosystems, Model 373A). Genetics Computer Group software package (Wisconsin Package, Version 9) was used for sequence alignment and helical wheel analysis.

*Transport Assays in Xenopus laevis Oocytes.* cRNA of each mutant was synthesized and injected into defolliculated oocytes. Uptake was measured on groups of 10 oocytes 48-56 h post-injection at 25°C in 150 µl of transport buffer (2 mM KCl, 1 mM CaCl<sub>2</sub>, 1 mM MgCl<sub>2</sub>, 10 mM HEPES, pH 7.4) containing either 100 mM NaCl or 100 mM choline chloride, and the respective <sup>3</sup>H-labeled nucleoside (Moravek Biochemicals). The kinetic parameters (apparent  $K_m$  and  $V_{max}$  values) were determined by non-linear least-squares fits of substrate/velocity profiles to the Michaelis-Menten equation using Kaleidagraph (Version 3.0, Synergy Software). Because of the intrinsic variability in the expression level of the transporters between batches of oocytes, the data are generally expressed as the mean ± S. E. from experiments performed in the same batch of oocytes.

## Results

To identify the specific residues responsible for maintaining the substrate selectivity of N2, I individually changed the five divergent residues (Table 1) in TM8 of N2 to the corresponding residues in N1. A double mutant (S318G/Q319M) and a reverse mutant (T8.G318S) were also constructed (Table 1). Mutants were first screened with the common substrate, [<sup>3</sup>H]uridine, for activity. Significant Na<sup>+</sup>-dependent uptake of uridine (10-70 fold increase) was observed for all mutants (Figure 2), suggesting that all mutants were expressed and functional.

*Substrate Selectivity of Mutants.* The substrate selectivity of each mutant was examined in uptake experiments using [<sup>3</sup>H]inosine as the model purine nucleoside and [<sup>3</sup>H]thymidine as the model pyrimidine nucleoside. The uptakes of inosine (10 μM) and thymidine (10 μM) by N2, chimera T8, mutants S304T, T306A, S310A, S318G, Q319M, and S318G/Q319M are shown in Figure 3-5. Compared to water-injected oocytes, significant Na<sup>+</sup>-dependent thymidine uptake (13-133 fold increase) was observed in oocytes expressing mutants S304T, T306A, S310A, and Q319M (Figure 4). In contrast, there was no significant inosine uptake by these mutants (Figure 4), suggesting that mutants S304T, T306A, S310A, and Q319M maintained the pyrimidine selectivity of N2. Therefore, single substitutions of these residues in N2 with the corresponding residues in N1 did not affect the substrate selectivity of N2.

In contrast, in addition to thymidine, the mutant S318G also transports inosine (Figure 5A). In oocytes expressing mutant S318G, there was a 41-fold increase in Na<sup>+</sup>-dependent inosine uptake ( $3.27 \pm 0.58$  pmol/oocyte/30min for S318G cRNA-injected oocytes vs.  $0.08 \pm 0.01$  pmol/oocyte/30min for water-injected oocytes). These data

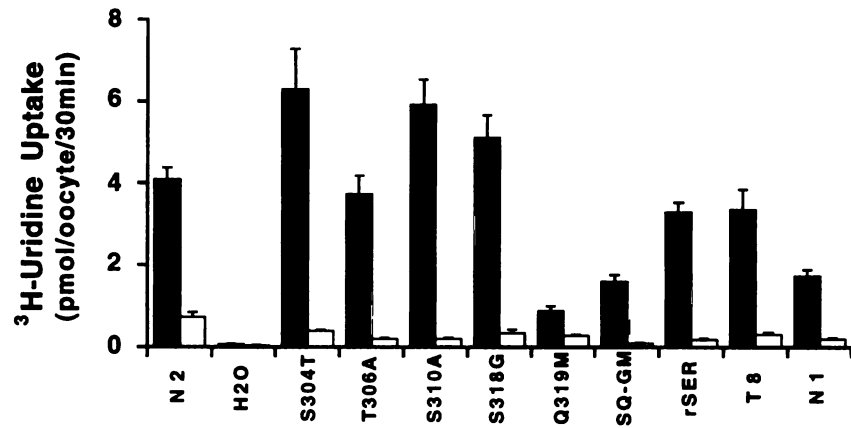


Figure 2. Uptake of <sup>3</sup>H-labeled uridine by mutants, chimera T8, and wild-type N1 and N2. Each value represents the mean  $\pm$  S.E. (n=8-10).

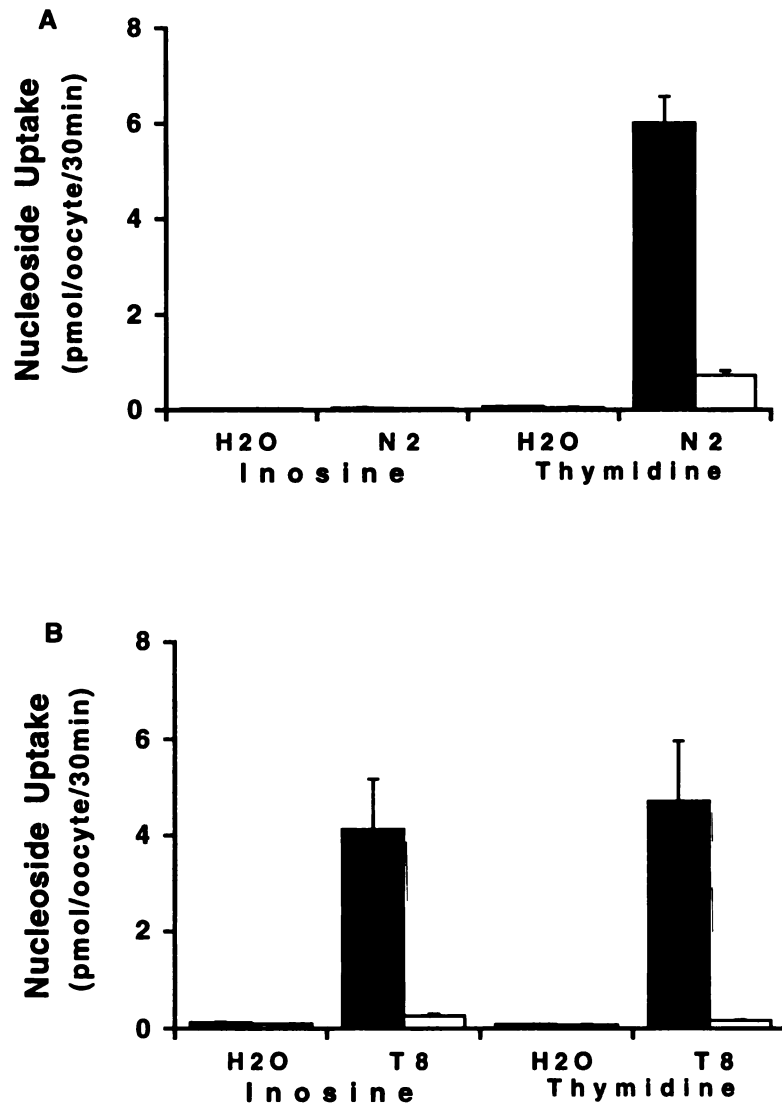


Figure 3. Uptake of  $^3\text{H}$ -labeled inosine and thymidine by wild-type N2 (A) and chimera T8 (B).

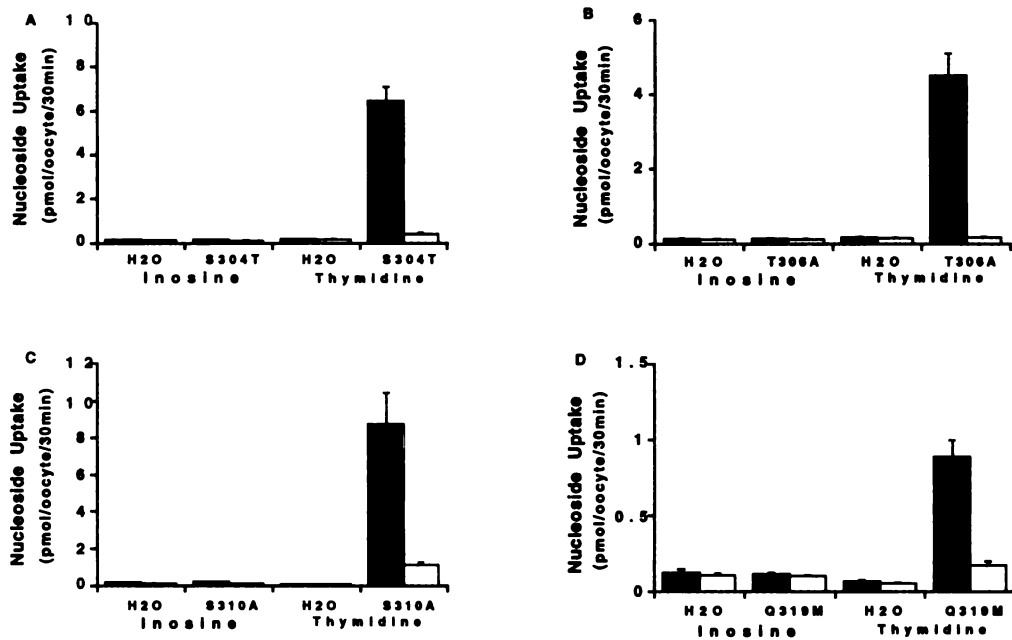


Figure 4. Uptake of <sup>3</sup>H-labeled inosine and thymidine by mutant S304T (A), mutant T306A (B), mutant S310A (C), and mutant Q319M (D).



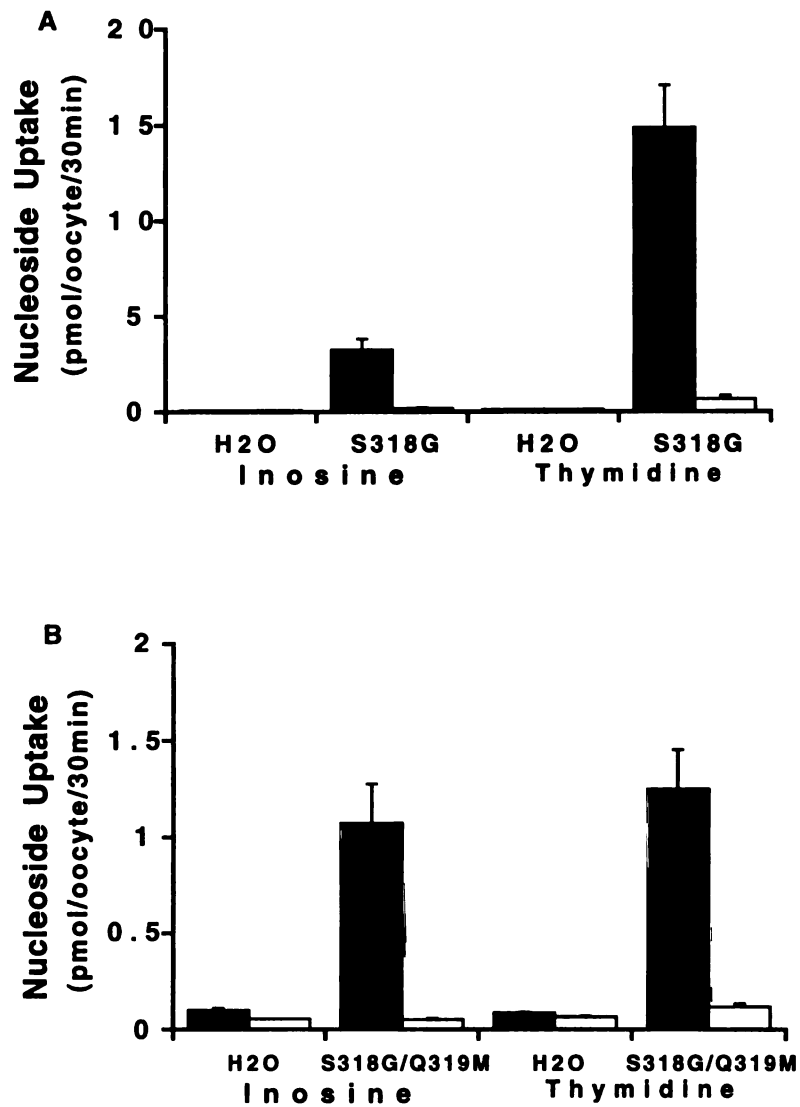


Figure 5. Uptake of  $^3\text{H}$ -labeled inosine and thymidine by mutant S318G (A) and mutant S318G/Q319M (B).

suggest that changing serine 318 in N2 to its equivalent residue in N1 (glycine) causes N2 to accept inosine as a substrate. However, compared to the transport rate of (10  $\mu$ M) thymidine ( $14.90 \pm 2.17$  pmol/oocyte/30min ), S318G transports inosine (10  $\mu$ M) at a rate 4.6 fold lower. The data shown in Figure 5A were from one representative experiment in which the same batch of oocytes was used. The experiment was performed several times. While the rate of nucleoside uptake varied among experiments (ranging from 0.71 to 3.3 for inosine and from 4.30 to 15.10 for thymidine, pmol/oocyte/30min) due to the intrinsic variability in the expression level between batches of oocytes, significant Na<sup>+</sup>-dependent inosine uptake (16- to 41-fold over water-injected oocytes) was observed in S318G cRNA-injected oocytes in all experiments. Within a single experiment, the thymidine uptake was consistently 4-6 fold higher than the inosine uptake. These data suggest that although mutant S318G accepts purine nucleosides as substrates, it still kinetically favors the transport of pyrimidine nucleosides at the tested concentration (10  $\mu$ M).

Mutant Q319M maintained the substrate selectivity of wild-type N2, however it transports thymidine with a significantly decreased rate (Figure 4D). Since glutamine 319 is also adjacent to serine 318, we suspect that this residue may play a role in substrate binding. Therefore I introduced a second Q to M mutation at position 319 of mutant S318G. This double mutant, S318G/Q319M, transports 10  $\mu$ M of inosine and thymidine at a comparable, but slow rate ( $1.07 \pm 0.20$  pmol/oocyte/30min for inosine and  $1.25 \pm 0.20$  pmol/oocyte/30min for thymidine), generating an uptake pattern similar to that of chimera T8 (Figure 5B). These data indicate that changing glutamine 319 to methionine in mutant S318G caused S318G to transport purine and pyrimidine nucleosides without much kinetic bias.

The data presented in Figures 3-5 suggested that serine 318 is important for maintaining the pyrimidine selectivity of N2. Changing this residue in N2 to glycine

causes N2 to lose its substrate selectivity. To investigate whether a reverse mutation can re-establish the pyrimidine selectivity in chimera T8, I changed the glycine 318 in chimera T8 back to the serine residue in N2. Interestingly, this mutant (termed T8.G318S), restored the pyrimidine selectivity of N2, transporting thymidine but not inosine (Figure 6). These data strongly suggest that serine 318 is essential for maintaining the pyrimidine selectivity of the N2 transporter.

*Transport Kinetics of Mutants S318G and S318G/Q319M.* To investigate why mutant S318G transports thymidine more favorably than inosine at 10  $\mu\text{M}$  (Figure 5A) and how substitution of Q319M in mutant S318G neutralized this imbalance (Figure 5B), I examined the kinetics of thymidine and inosine uptake mediated by mutant S318G and mutant S318G/Q319M (Figures 7-8). Uptake of both nucleosides via mutant S318G was saturable (Figure 7). The apparent  $K_m$  of inosine was  $273 \pm 62 \mu\text{M}$  whereas that of thymidine was  $27.5 \pm 4.3 \mu\text{M}$ . The  $V_{max}$  of inosine was  $28.8 \pm 2.5 \text{ pmol/oocyte/30min}$  whereas that of thymidine was  $24.6 \pm 0.9 \text{ pmol/oocyte/30min}$  (Figure 7). These data suggest that mutant S318G has a much lower ( $\sim 10$ -fold) apparent affinity for inosine than for thymidine, whereas the apparent maximal rate of transport,  $V_{max}$ , for inosine is close to that for thymidine. Therefore at low substrate concentrations (e.g. 10  $\mu\text{M}$ ), mutant S318G will favor the transport of thymidine over that of inosine. The uptake of inosine and thymidine mediated by mutant S318G/Q319M was also saturable (Figure 8). For this mutant, the  $K_m$  of inosine was  $54.8 \pm 14.7 \mu\text{M}$  and the  $K_m$  of thymidine was  $79.3 \pm 11.9 \mu\text{M}$ . The  $V_{max}$  of inosine was  $10.8 \pm 0.7 \text{ pmol/oocyte/30min}$  and that of thymidine was  $12.3 \pm 0.5 \text{ pmol/oocyte/30min}$  (Figure 8). These data suggest that mutant S318G/Q319M has similar apparent  $K_m$  and  $V_{max}$  values for inosine and thymidine, transporting these two compounds without much kinetic bias. Compared to the mutant S318G, the apparent affinity for inosine in the double mutant is greatly enhanced ( $K_m = 54.8$  vs.  $K_m = 273 \mu\text{M}$ ,  $p < 0.01$ ) whereas the apparent affinity for thymidine is significantly decreased ( $K_m = 79.3$  vs.  $K_m = 24.6 \mu\text{M}$ ,  $p < 0.01$ ).

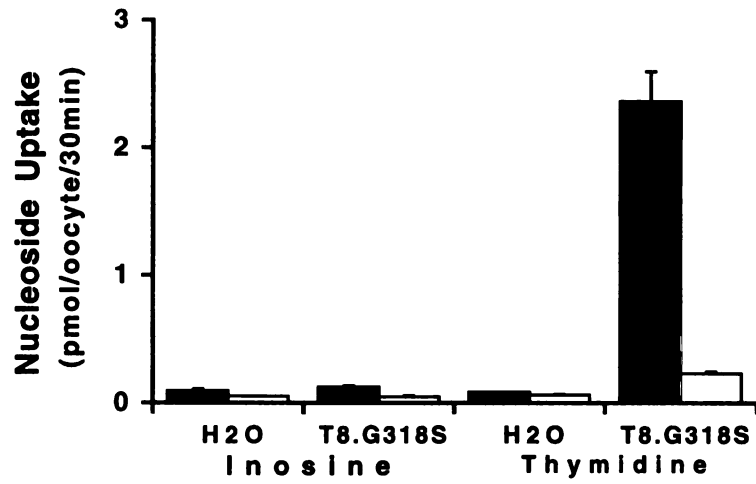


Figure 6. Uptake of <sup>3</sup>H-labeled inosine and thymidine by mutant T8.G318S.

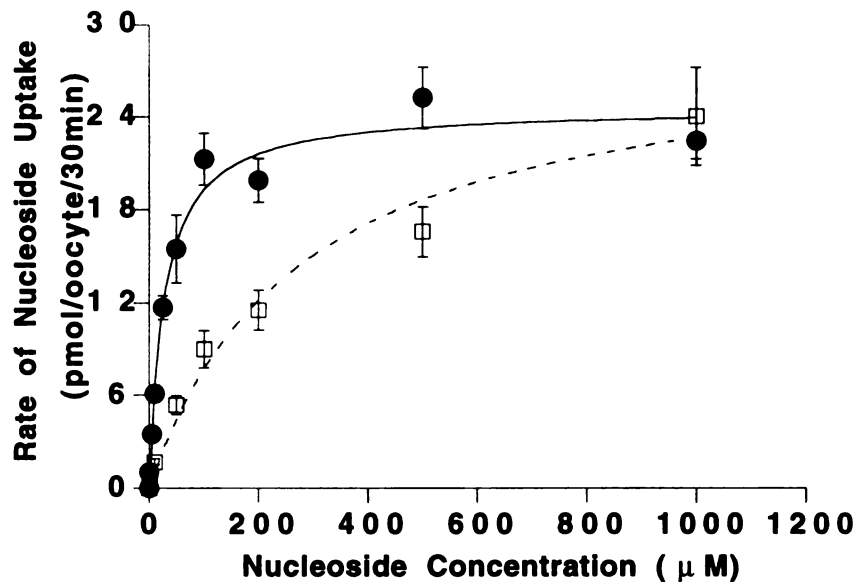


Figure 7. Michaelis-Menten studies of thymidine and inosine uptake mediated by mutant S318G. The initial velocities (30 min) of [<sup>3</sup>H]thymidine uptake (solid circles) or [<sup>3</sup>H]inosine uptake (squares) were determined in Na<sup>+</sup>-buffer containing the respective nucleoside at concentrations ranging from 1-1000 μM. Each point represents the mean ± S.E. (n=8-10).

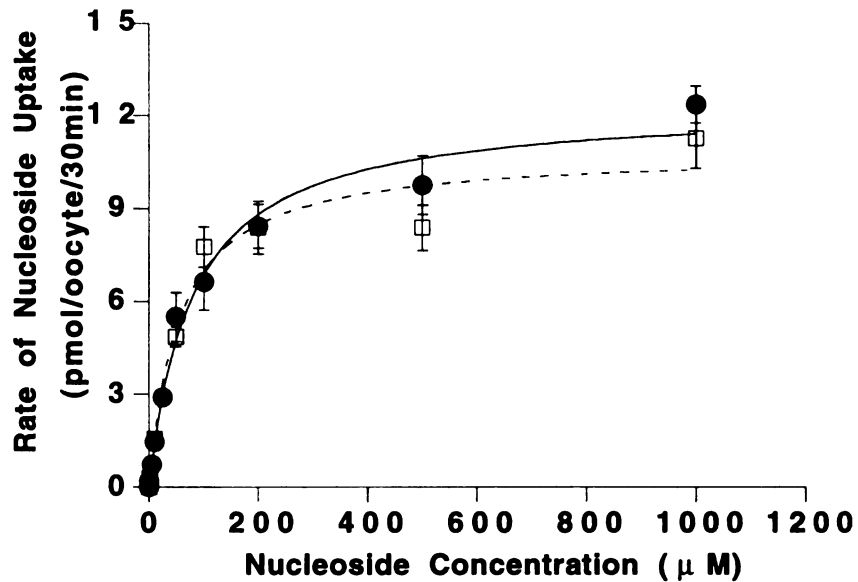


Figure 8. Michaelis-Menten studies of thymidine and inosine uptake mediated by mutant S318G/Q319M. The initial velocities (30 min) of [<sup>3</sup>H]thymidine uptake (solid circles) or [<sup>3</sup>H]inosine uptake (squares) were determined in Na<sup>+</sup>-buffer containing the respective nucleoside at concentrations ranging from 1-1000 μM. Each point represents the mean ± S.E. (n=8-10).

*Helical Wheel Analysis of TM8.* To analyze the position of serine 318 and glutamine 319 on TM8, helical wheels at a fixed angle of 100° are drawn for TM8 of N2 (Figure 9). The five substitutions in N1 are indicated by arrows. Distinct amphipathic patterns (one side of the helix being hydrophobic and the other side hydrophilic) are observed, suggesting that one side of TM8 may face an aqueous pore (e.g. the substrate binding pore) while the other side may face the hydrophobic lipid. The residue serine 318 is located in the center of hydrophilic side, suggesting its side chain may directly interact with the substrates. The residue glutamine 319 is located near the boundary of the amphipathic interface. Its side chain may interact directly with the substrates or may contribute indirectly to the conformation of the substrate recognition sites.

## **Discussion**

Our previous studies showed that replacing TM8 of N2 with that of N1 caused N2 to lose its substrate selectivity (13, Chapter 4). In this study, I focused on determining the specific residues responsible for maintaining the substrate selectivity of N2. By site-directed mutagenesis, the five divergent residues in N2 were systematically mutated to the corresponding residues in N1 (Table 1). Replacing serine 318 in N2 to its equivalent residue, glycine, resulted in a mutant (S318G) which lost the pyrimidine selectivity of N2 and began to accept purine nucleosides as substrates (Figure 5A). In contrast, replacing the other four residues with their equivalents did not alter the selectivity of N2 (Figure 4). Importantly, when the glycine residue in the broadly-selective chimera T8 was changed back to serine, the resulting transporter (T8.G318S) regained pyrimidine-selectivity (Figure 6). These data strongly suggest that serine 318 is essential for conserving the pyrimidine selectivity of wild-type N2.

Kinetic studies revealed that mutant S318G has a much lower (~ 10-fold) apparent





affinity for inosine than for thymidine (Figure 7), suggesting that although a mutant's ability to accept purine nucleosides is determined by whether a serine or a glycine residue is present at position 318, other residues may contribute to the kinetic differences in the transport of purine and pyrimidine nucleosides by mutant S318G. Indeed, a second Q to M mutation at position 319 following the S318G substitution resulted in a mutant (S318G/Q319M) which has comparable apparent  $K_m$  values for inosine and thymidine (Figure 8). These data suggest that although a single substitution of glutamine 319 with methionine would not affect the pyrimidine selectivity of N2 (Figure 4D), changing it following the serine to glycine substitution at position 318 would greatly enhance mutant S318G's apparent affinity towards purine nucleosides (Figure 5 and Figures 7-8). In transport kinetic analysis, the apparent affinity (i.e. apparent  $K_m$ ) reflects not only substrate affinity for the binding site, but is also influenced by rate constants of substrate translocation and dissociation which occur subsequent to recognition (14). Therefore, the observed changes in apparent affinity introduced by the Q to M mutation in the S318G mutant may reflect changes in any of these processes.

Studies of a number of membrane transporters suggest that the substrate permeation pathway in a transporter is a channel-like structure formed by several transmembrane helices (15-17). Charged and polar residues, often found on one side of these helices, play critical roles in interacting with the substrates (15, 18-20). Helical wheel analysis of TM8 revealed a distinct amphipathic pattern (Figure 9), suggesting that one side of TM8 may face an aqueous channel for substrate permeation. Serine 318 is located in the center of the hydrophilic side (Figure 9), suggesting that its side chain may protrude into the channel and act as a gating residue through specific interactions with the substrates. Substitution of a serine residue with a smaller residue, glycine, will result in a loss of a methylene and a hydroxyl group on the side chain. These changes may cause a gain in the size of the substrate permeation channel and a loss of some specific chemical interactions (e.g. a hydrogen bond), allowing the resulting transporter S318G to tolerate the bulkier purine

nucleosides as substrates. On the helical wheel diagram, the residue glutamine 319 is located near the boundary of the amphipathic interface (Figure 9). Its side chain may interact directly with the substrates or may affect the apparent affinity by indirect influence of the conformation of the substrate recognition site in the channel. Substitution of this residue with a methionine in mutant S318G may induce changes that make the transporter interact with purine nucleosides with an increased apparent affinity. However, it should be noted that the proposed topology of N2 consisting of 14 transmembrane domains with an internal C and N termini needs experimental validation. In addition, with the crystal structure of N2 unknown, the possibility that serine 318 may influence the selectivity of N2 through indirect interactions with other sites in the protein can not be excluded.

In summary, I identified a single residue, serine 318, which is primarily responsible for determining the substrate selectivity of the N2 Na<sup>+</sup>-nucleoside transporter. The data suggest that serine 318 may be located in the nucleoside permeation pathway and act as a gating residue that is important for the pyrimidine selectivity of N2. An adjacent residue, glutamine 319, was found to be important in influencing the transporter's apparent affinity for purine nucleosides. These studies provide important information about the molecular mechanisms that govern the functional characteristics of Na<sup>+</sup>-nucleoside transporters. Furthermore, the finding that a few residues along the solute permeation pathway are responsible for the substrate selectivity and affinity of N2 may reflect a common molecular mechanism for substrate discrimination in some membrane transporters.

## References

1. Cass, C. E. Nucleoside transport, in *Drug Transport in Antimicrobial and Anticancer Chemotherapy*. (N. H. Georgopapadakou, ed.) pp.403-451, Marcel Dekker, New York (1995).
2. Griffith, D. A., and S. M. Jarvis. Nucleoside and nucleobase transport systems of mammalian cells. *Biochim Biophys Acta* **1286**:153-81 (1996).
3. Wang, J., M. E. Schaner, S. Thomassen, S. F. Su, M. Piquette-Miller, and K. M. Giacomini. Functional and molecular characteristics of Na(+)-dependent nucleoside transporters. *Pharm Res* **14**:1524-32 (1997).
4. Yao, S. Y., C. E. Cass, and J. D. Young. Transport of the antiviral nucleoside analogs 3'-azido-3'-deoxythymidine and 2',3'-dideoxycytidine by a recombinant nucleoside transporter (rCNT) expressed in *Xenopus laevis* oocytes. *Mol Pharmacol* **50**:388-93 (1996).
5. Wang, J., S. F. Su, M. J. Dresser, M. E. Schaner, C. B. Washington, and K. M. Giacomini. Na(+)-dependent purine nucleoside transporter from human kidney: cloning and functional characterization. *Am J Physiol* **273**:F1058-65 (1997).
6. Schaner, M. E., J. Wang, S. Zevin, K. M. Gerstin, and K. M. Giacomini. Transient expression of a purine-selective nucleoside transporter (SPNTint) in a human cell line (HeLa). *Pharm Res* **14**:1316-21 (1997).

7. Huang, Q. Q., S. Y. Yao, M. W. Ritzel, A. R. Paterson, C. E. Cass, and J. D. Young. Cloning and functional expression of a complementary DNA encoding a mammalian nucleoside transport protein. *J Biol Chem* **269**:17757-60 (1994).
8. Che, M., D. F. Ortiz, and I. M. Arias. Primary structure and functional expression of a cDNA encoding the bile canalicular, purine-specific Na(+)-nucleoside cotransporter. *J Biol Chem* **270**:13596-9 (1995).
9. Ritzel, M. W., S. Y. Yao, M. Y. Huang, J. F. Elliott, C. E. Cass, and J. D. Young. Molecular cloning and functional expression of cDNAs encoding a human Na<sup>+</sup>-nucleoside cotransporter (hCNT1). *Am J Physiol* **272**:C707-14 (1997).
10. Wu, X., G. Yuan, C. M. Brett, A. C. Hui, and K. M. Giacomini. Sodium-dependent nucleoside transport in choroid plexus from rabbit. Evidence for a single transporter for purine and pyrimidine nucleosides. *J Biol Chem* **267**:8813-8 (1992).
11. Huang, Q. Q., C. M. Harvey, A. R. Paterson, C. E. Cass, and J. D. Young. Functional expression of Na(+)-dependent nucleoside transport systems of rat intestine in isolated oocytes of *Xenopus laevis*. Demonstration that rat jejunum expresses the purine-selective system N1 (cif) and a second, novel system N3 having broad specificity for purine and pyrimidine nucleosides. *J Biol Chem* **268**:20613-9 (1993).
12. Belt, J. A., N. M. Marina, D. A. Phelps, and C. R. Crawford. Nucleoside transport in normal and neoplastic cells. *Adv Enzyme Regul* **33**:235-52 (1993).
13. Wang, J., and K. M. Giacomini. Molecular determinants of substrate selectivity in Na<sup>+</sup>-dependent nucleoside transporters. *J Biol Chem* **272**:28845-8 (1997).

14. Buck, K. J., and S. G. Amara. Chimeric dopamine-norepinephrine transporters delineate structural domains influencing selectivity for catecholamines and 1-methyl-4-phenylpyridinium. *Proc Natl Acad Sci U S A* **91**:12584-8 (1994).
15. Yan, R. T., and P. C. Maloney. Residues in the pathway through a membrane transporter. *Proc Natl Acad Sci U S A* **92**:5973-6 (1995).
16. Zeng, H., R. Parthasarathy, A. L. Rampal, and C. Y. Jung. Proposed structure of putative glucose channel in GLUT1 facilitative glucose transporter. *Biophys J* **70**:14-21 (1996).
17. Jan, L. Y., and Y. N. Jan. Tracing the roots of ion channels. *Cell* **69**:715-8 (1992).
18. Kaback, H. R. A molecular mechanism for energy coupling in a membrane transport protein, the lactose permease of *Escherichia coli* [see comments]. *Proc Natl Acad Sci U S A* **94**:5539-43 (1997).
19. Merickel, A., H. R. Kaback, and R. H. Edwards. Charged residues in transmembrane domains II and XI of a vesicular monoamine transporter form a charge pair that promotes high affinity substrate recognition. *J Biol Chem* **272**:5403-8 (1997).
20. Eisenberg, D., W. Wilcox, and A. D. McLachlan. Hydrophobicity and amphiphilicity in protein structure. *J Cell Biochem* **31**:11-7 (1986).

## CHAPTER 7

### SUMMARY AND CONCLUSIONS

Nucleoside transport systems are critical in the absorption, disposition, and elimination of nucleosides and nucleoside analogs. Knowledge of nucleoside transporters is important in the evaluation and prediction of the kinetics, targeting, and toxicities of nucleosides and nucleoside analogs. Earlier work in the field of nucleoside transport documented functional and kinetic studies of nucleoside flux in isolated cells and tissue preparations (1-3). These studies established that multiple nucleoside transport systems exist in mammalian cells (1-4). Two major classes of nucleoside transporters have been identified: the equilibrative nucleoside transporters and the concentrative nucleoside transporters. The equilibrative nucleoside transporters are facilitated transport systems whereas the concentrative nucleoside transporters are Na<sup>+</sup>-dependent secondary active systems. The equilibrative nucleoside transporters have been further classified into two subtypes, *es* and *ei*., based on their sensitivities to inhibition by nitrobenzylthioinosine (NBMPR) (1-3). The Na<sup>+</sup>-dependent concentrative nucleoside transporters have been further divided into five major subtypes (N1-N5) based on their substrate selectivities for purine and pyrimidine nucleosides (1, 2, 4).

Significant progress has been made in recent years. The greatest advance is the cloning of various proteins responsible for the distinct nucleoside transport processes that have been characterized in cells or tissues in earlier functional and kinetic studies (5-12). To date, the purine (N1) and pyrimidine (N2) selective Na<sup>+</sup>-nucleoside transporters have been cloned from rat and human (5, 6, 9, 10). Studies presented in Chapter 3 described the cloning and characterization processes of the human N1 subtype transporter, hSPNT1.

Recently, the NBMPR-sensitive (*es*) and the NBMPR-insensitive (*ei*) equilibrative nucleoside transporters have also been cloned (7, 8, 11, 12).

Heterologous expression systems including *Xenopus laevis* oocytes and cultured mammalian cells, were developed to express the cloned nucleoside transporters (5, 6, 13, 14). Detailed functional and kinetic studies were carried out to determine the substrate profiles, kinetic parameters ( $K_m$  and  $V_{max}$ ), and Na<sup>+</sup>-coupling stoichiometries of the cloned or bioengineered transporters (13-16). The roles of each subtype in the absorption and disposition of specific nucleoside drugs were investigated by studying the interactions of nucleoside drugs with cloned transporters (13-16). Studies presented in Chapter 2 and 5 characterized the functional and kinetic properties of the cloned N2 transporter, rCNT1, and an unusual N3-like transporter derived from the cloned N1 and N2 transporters. Studies in Chapter 4 and 6 were focused on determining the molecular mechanisms that govern substrate recognition and discrimination in cloned Na<sup>+</sup>-nucleoside transporters.

In Chapter 2, the interaction of rCNT1 with various nucleoside drugs was determined in inhibition and uptake studies. The data showed that rCNT1 interacts with several clinically important nucleoside analogs and accepts the anticancer drugs 2CdA and AraC as permeants. This study, together with studies by Yao *et al.* and Fang *et al.* (13, 15, 16), suggest that rCNT1 plays an important role in cellular disposition of many clinically important nucleoside analogs. In the studies presented in Chapter 2, we also developed an RT-PCR method to determine the distribution of the mRNA transcript of rCNT1 along the intestine. Using this method, the transcript of rCNT1 was detected in duodenum, jejunum, ileum, but not in colon. These results suggest that rCNT1-mediated absorption occurs largely in jejunum; and to a lesser extent, in duodenum and ileum. However, the direct analysis of the regional distribution and membrane localization of the transporter protein awaits the development of rCNT1 specific antibodies.

Many purine nucleosides and their analogs are actively transported in human kidney. Studies presented in Chapter 3 focus on revealing the molecular mechanism

responsible for active purine nucleoside transport in human kidney. Using homology cloning strategies and RT-PCR, we isolated a cDNA encoding a Na<sup>+</sup>-dependent nucleoside transporter, hSPNT1, from human kidney. Functional expression in *Xenopus laevis* oocytes identified hSPNT1 as a Na<sup>+</sup>-dependent nucleoside transporter which selectively transports purine nucleosides and uridine. The  $K_m$  of uridine (80  $\mu$ M) in interacting with hSPNT1 was substantially higher than that of inosine (4.5  $\mu$ M), suggesting at low substrate concentrations, hSPNT1 prefers to transport purine nucleosides than uridine. hSPNT1 is 81% identical to the previously cloned rat Na<sup>+</sup>-nucleoside transporter, SPNT, but differs markedly from SPNT in terms of its primary structure in the N-terminus. An important difference in this region is that the rat SPNT possesses an ATP/GTP binding motif whereas hSPNT1 does not (Chapter 3 and ref. (6, 10)). These data suggest that it is possible that different mechanisms may be involved in the regulation, targeting and activation of these proteins in rats and humans. Northern analysis revealed that multiple transcripts of hSPNT1 are widely distributed in human kidney, heart, skeletal muscle, liver, intestine, and pancreas. Interestingly, the distribution of the hSPNT1 transcripts correlates well with the sites of action of purinergic effects, suggesting that hSPNT1 and related transporters may be actively involved in adenosine induced effects in humans. A possible role may be the removal of adenosine from the extracellular fluids surrounding various adenosine receptors, resulting in the attenuation of its site-specific action. Using radiation hybrid cell lines of human and hamster, the hSPNT1 gene was localized to chromosome 15q13-14.

Studies presented in Chapter 4 were designed to explore the structure-function relationship in cloned Na<sup>+</sup>-nucleoside transporters. Because the three-dimensional structures of membrane proteins are difficult to achieve, a chimeric transporter approach was used to delineate the structural domains involved in substrate binding. By constructing and analyzing a series of chimeric N1/N2 transporters, structural elements contributing to



substrate binding and selectivity were revealed. The findings are: transmembrane domain (TMD) 8-9 are the major sites for substrate binding as well as the structural determinants for substrate selectivity in the cloned N1 and N2 Na<sup>+</sup>-nucleoside transporters; transporters with novel substrate selectivities can be engineered from known transporters. These studies provide insights into the molecular mechanisms of nucleoside transport. Identification of the binding sites may also benefit the development of nucleoside drugs with improved membrane permeability and inhibitors with improved potencies and specificities.

In studies described in Chapter 4, we constructed a chimeric N1/N2 transporter, T8, which seemed to exhibit novel substrate selectivity. The structure of T8 is identical to the pyrimidine-selective N2 transporter except that TMD8 was replaced by that of N1. In Chapter 5, the substrate profile, transport mechanism, and Na<sup>+</sup>-coupling stoichiometry of T8, were described and compared with wild-type N1, N2, and N3. Data from this study suggest that transplanting TMD8 of N1 into N2 altered the structure of its binding pocket and subsequently expanded the transport capacity of N2 to both purine and pyrimidine nucleosides. The substrate profile of T8 was amazingly similar to that of N3, a broadly selective transporter that has been characterized but not yet cloned. It is possible that the sequence of the uncloned N3 transporter may be very similar to the cloned N2 transporter because only a few amino acid substitutions during evolution in the TMD8 region will transform N2 into an N3 transporter subtype. Alternatively, the N2 and N1 transporters may both evolve from a common N3-type ancestor and gain their substrate selectivity by a few amino acid substitutions in the TMD8-9 region. The Na<sup>+</sup>-coupling ratio of T8 was determined to be 1, identical to the coupling ratios of N1 and N2 but different from the 2:1 ratio of N3 determined in choroid plexus. Therefore, the Na<sup>+</sup>-coupling ratios of these transporters are not necessarily linked to their substrate selectivity; or in other words, the Na<sup>+</sup>-binding site in these transporters may be a distinct domain separated from, but

energetically coupled to the substrate-binding domain. Information from this study helps us to gain a further understanding of the structure and function of Na<sup>+</sup>-nucleoside transporters, and also paves the way for bioengineering nucleoside transporters for site-specific drug targeting and delivery.

The studies in Chapter 5 confirmed the finding that replacing TMD 8 of N2 with that of N1 would cause N2 to lose its pyrimidine selectivity. Five residues differ between rat N2 and N1 in TMD8. The studies presented in Chapter 6 were designed to identify the critical residues responsible for the transport selectivity of N2. Using site-directed mutagenesis, the five residues in N2 were systematically changed to their equivalents in N1. Replacing the serine residue at position 318 to its equivalent N1 residue, glycine, caused N2 to lose its selectivity for pyrimidine nucleosides and accept purine nucleosides as substrates. In contrast, replacing the other four residues did not change the pyrimidine selectivity of N2. Furthermore, when glycine 318 in chimera T8 was changed back to serine, this non-selective transporter regained the pyrimidine-selectivity of N2. These data suggest that serine 318 may be located in the nucleoside permeation pathway and act as a gating residue responsible for the pyrimidine selectivity of N2. An adjacent residue, glutamine 319, was found to be important in influencing the transporter's apparent affinity for purine nucleosides. These studies provide important information about the molecular mechanisms that govern the substrate selectivity of Na<sup>+</sup>-nucleoside transporters. Furthermore, the finding that a few residues along the solute permeation pathway are responsible for the substrate selectivity and affinity may reflect a common molecular mechanism for substrate discrimination in some membrane transporters.

In summary, studies on nucleoside transporters have progressed significantly in recent years. The cloning of various nucleoside transporters has opened the door for the study of structure, function, regulation, targeting, localization, and energy-coupling of nucleoside transporters. Research presented in this dissertation contributes significantly to the cloning and structure-function analysis of Na<sup>+</sup>-nucleoside transporters. However, areas

including the regulation, targeting, Na<sup>+</sup>-coupling, and genetic variations of nucleoside transporter are least understood. Development of specific antibodies are necessary for the study of regulation and targeting. Further structure-function analysis are needed to identify the Na<sup>+</sup>-binding domains in the cloned Na<sup>+</sup>-nucleoside transporters. Pharmacogenetic studies on nucleoside transporters may help us to understand the contribution of nucleoside transporter polymorphisms to inter-individual variation in drug efficacy and toxicity that has been observed in clinical therapy. Further studies are needed to identify the key elements important for the purine-selectivity of N1 transporters. A number of broadly selective Na<sup>+</sup>-nucleoside transporters (i.e., N3, N4 and N5) have been characterized in various tissues (1, 17-19). More recently, a novel Na<sup>+</sup>-dependent, guanosine-specific, NBMPR-sensitive transporter was characterized in acute promyelocytic leukemia cells (20). However, these transporters have not been cloned and there is currently no information on the molecular structure of the transporters. Further molecular cloning studies are needed to elucidate the molecular identities of these transporters. The role of the cloned transporters in the absorption and disposition of nucleoside analogs in the intact animal has not been elucidated. Development of a knockout mouse models for nucleoside transporters may lead to an enhanced understanding of the physiologic and pharmacologic role of nucleoside transporters in *vivo*.

## References

1. Cass, C. E. Nucleoside transport, in *Drug Transport in Antimicrobial and Anticancer Chemotherapy*. (N. H. Georgopapadakou, ed.) pp.403-451, Marcel Dekker, New York (1995).
2. Griffith, D. A., and S. M. Jarvis. Nucleoside and nucleobase transport systems of mammalian cells. *Biochim Biophys Acta* **1286**:153-81 (1996).
3. Belt, J. A., N. M. Marina, D. A. Phelps, and C. R. Crawford. Nucleoside transport in normal and neoplastic cells. *Adv Enzyme Regul* **33**:235-52 (1993).
4. Wang, J., M. E. Schaner, S. Thomassen, S. F. Su, M. Piquette-Miller, and K. M. Giacomini. Functional and molecular characteristics of Na(+)-dependent nucleoside transporters. *Pharm Res* **14**:1524-32 (1997).
5. Huang, Q. Q., S. Y. Yao, M. W. Ritzel, A. R. Paterson, C. E. Cass, and J. D. Young. Cloning and functional expression of a complementary DNA encoding a mammalian nucleoside transport protein. *J Biol Chem* **269**:17757-60 (1994).
6. Che, M., D. F. Ortiz, and I. M. Arias. Primary structure and functional expression of a cDNA encoding the bile canalicular, purine-specific Na(+)-nucleoside cotransporter. *J Biol Chem* **270**:13596-9 (1995).
7. Griffiths, M., N. Beaumont, S. Y. Yao, M. Sundaram, C. E. Boumah, A. Davies, F. Y. Kwong, I. Coe, C. E. Cass, J. D. Young, and S. A. Baldwin. Cloning of a human

nucleoside transporter implicated in the cellular uptake of adenosine and chemotherapeutic drugs [see comments]. *Nat Med* **3**:89-93 (1997).

8. Griffiths, M., S. Y. Yao, F. Abidi, S. E. Phillips, C. E. Cass, J. D. Young, and S. A. Baldwin. Molecular cloning and characterization of a nitrobenzylthioinosine-insensitive (ei) equilibrative nucleoside transporter from human placenta. *Biochem J* **328**:739-43 (1997).

9. Ritzel, M. W., S. Y. Yao, M. Y. Huang, J. F. Elliott, C. E. Cass, and J. D. Young. Molecular cloning and functional expression of cDNAs encoding a human Na<sup>+</sup>-nucleoside cotransporter (hCNT1). *Am J Physiol* **272**:C707-14 (1997).

10. Wang, J., S. F. Su, M. J. Dresser, M. E. Schaner, C. B. Washington, and K. M. Giacomini. Na<sup>(+)</sup>-dependent purine nucleoside transporter from human kidney: cloning and functional characterization. *Am J Physiol* **273**:F1058-65 (1997).

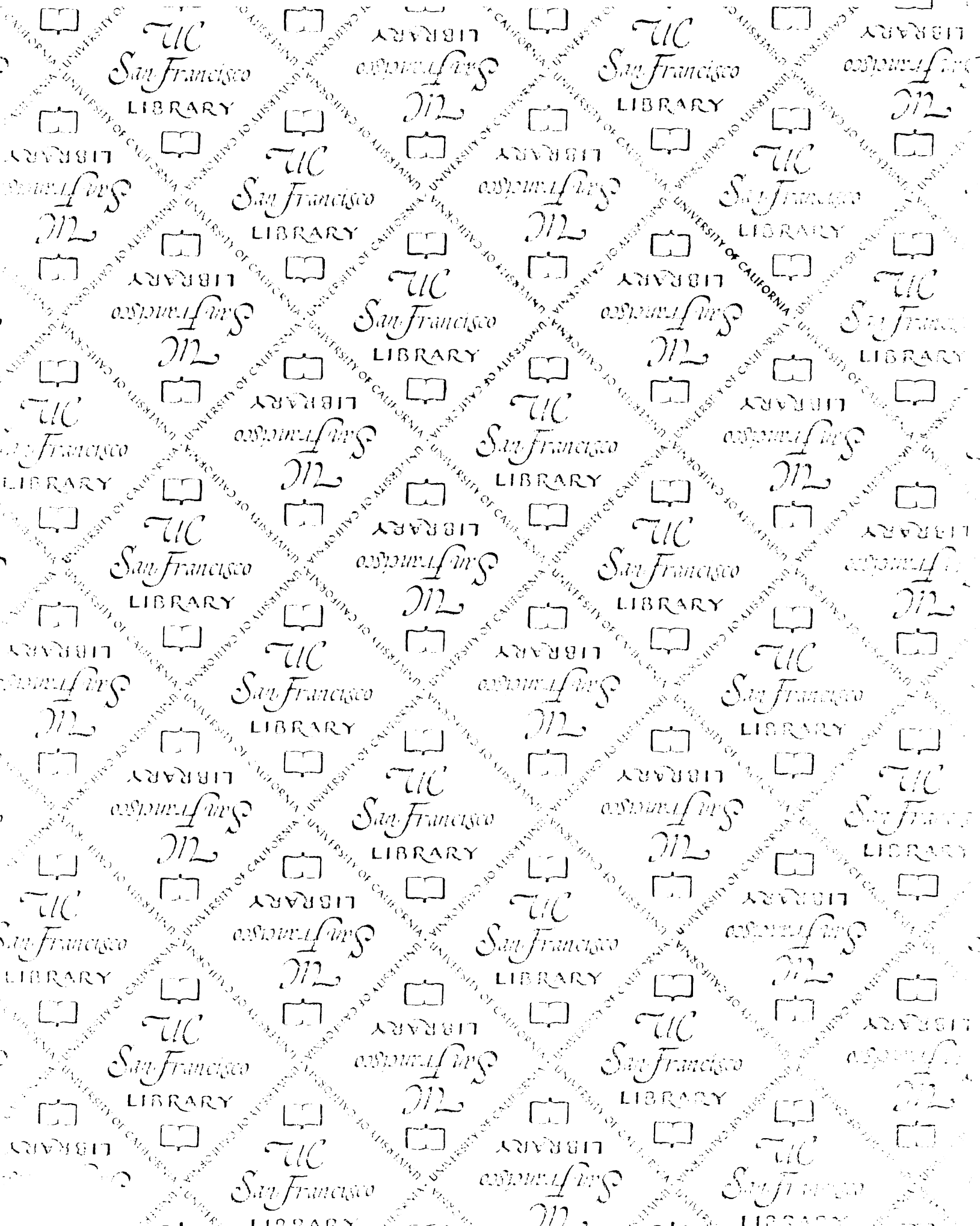
11. Yao, S. Y., A. M. Ng, W. R. Muzyka, M. Griffiths, C. E. Cass, S. A. Baldwin, and J. D. Young. Molecular cloning and functional characterization of nitrobenzylthioinosine (NBMPR)-sensitive (es) and NBMPR-insensitive (ei) equilibrative nucleoside transporter proteins (rENT1 and rENT2) from rat tissues. *J Biol Chem* **272**:28423-30 (1997).

12. Crawford, C. R., D. H. Patel, C. Naeve, and J. A. Belt. Cloning of the human equilibrative, nitrobenzylmercaptapurine riboside (NBMPR)-insensitive nucleoside transporter ei by functional expression in a transport-deficient cell line. *J Biol Chem* **273**:5288-93 (1998).

13. Fang, X., F. E. Parkinson, D. A. Mowles, J. D. Young, and C. E. Cass. Functional characterization of a recombinant sodium-dependent nucleoside transporter with selectivity for pyrimidine nucleosides (cNT1rat) by transient expression in cultured mammalian cells. *Biochem J* **317**:457-65 (1996).
14. Schaner, M. E., J. Wang, S. Zevin, K. M. Gerstin, and K. M. Giacomini. Transient expression of a purine-selective nucleoside transporter (SPNTint) in a human cell line (HeLa). *Pharm Res* **14**:1316-21 (1997).
15. Yao, S. Y., C. E. Cass, and J. D. Young. Transport of the antiviral nucleoside analogs 3'-azido-3'-deoxythymidine and 2',3'-dideoxycytidine by a recombinant nucleoside transporter (rCNT) expressed in *Xenopus laevis* oocytes. *Mol Pharmacol* **50**:388-93 (1996).
16. Yao, S. Y., A. M. Ng, M. W. Ritzel, W. P. Gati, C. E. Cass, and J. D. Young. Transport of adenosine by recombinant purine- and pyrimidine-selective sodium/nucleoside cotransporters from rat jejunum expressed in *Xenopus laevis* oocytes. *Mol Pharmacol* **50**:1529-35 (1996).
17. Wu, X., G. Yuan, C. M. Brett, A. C. Hui, and K. M. Giacomini. Sodium-dependent nucleoside transport in choroid plexus from rabbit. Evidence for a single transporter for purine and pyrimidine nucleosides. *J Biol Chem* **267**:8813-8 (1992).
18. Wu, X., M. M. Gutierrez, and K. M. Giacomini. Further characterization of the sodium-dependent nucleoside transporter (N3) in choroid plexus from rabbit. *Biochim Biophys Acta* **1191**:190-6 (1994).

19. Gutierrez, M. M., and K. M. Giacomini. Substrate selectivity, potential sensitivity and stoichiometry of Na(+)-nucleoside transport in brush border membrane vesicles from human kidney. *Biochim Biophys Acta* **1149**:202-8 (1993).

20. Flanagan, S. A., and K. A. Meckling-Gill. Characterization of a novel Na+-dependent, guanosine-specific, nitrobenzylthioinosine-sensitive transporter in acute promyelocytic leukemia cells. *J Biol Chem* **272**:18026-32 (1997).





# For reference

Not to be taken  
from the room.

